

**University of Alberta**

Effects of Illite Clays, Divalent Cations and Temperature on Bitumen Recovery

by

Xinlin Ding



A thesis submitted to the Faculty of Graduate Studies and Research in partial fulfillment  
of the requirements for the degree of Master of Science

in

Chemical Engineering

Department of Chemical & Materials Engineering

Edmonton, Alberta

Fall 2006



Library and  
Archives Canada

Bibliothèque et  
Archives Canada

Published Heritage  
Branch

Direction du  
Patrimoine de l'édition

395 Wellington Street  
Ottawa ON K1A 0N4  
Canada

395, rue Wellington  
Ottawa ON K1A 0N4  
Canada

*Your file* *Votre référence*  
*ISBN: 978-0-494-22252-2*  
*Our file* *Notre référence*  
*ISBN: 978-0-494-22252-2*

#### NOTICE:

The author has granted a non-exclusive license allowing Library and Archives Canada to reproduce, publish, archive, preserve, conserve, communicate to the public by telecommunication or on the Internet, loan, distribute and sell theses worldwide, for commercial or non-commercial purposes, in microform, paper, electronic and/or any other formats.

The author retains copyright ownership and moral rights in this thesis. Neither the thesis nor substantial extracts from it may be printed or otherwise reproduced without the author's permission.

#### AVIS:

L'auteur a accordé une licence non exclusive permettant à la Bibliothèque et Archives Canada de reproduire, publier, archiver, sauvegarder, conserver, transmettre au public par télécommunication ou par l'Internet, prêter, distribuer et vendre des thèses partout dans le monde, à des fins commerciales ou autres, sur support microforme, papier, électronique et/ou autres formats.

L'auteur conserve la propriété du droit d'auteur et des droits moraux qui protègent cette thèse. Ni la thèse ni des extraits substantiels de celle-ci ne doivent être imprimés ou autrement reproduits sans son autorisation.

---

In compliance with the Canadian Privacy Act some supporting forms may have been removed from this thesis.

Conformément à la loi canadienne sur la protection de la vie privée, quelques formulaires secondaires ont été enlevés de cette thèse.

While these forms may be included in the document page count, their removal does not represent any loss of content from the thesis.

Bien que ces formulaires aient inclus dans la pagination, il n'y aura aucun contenu manquant.

  
**Canada**

## ABSTRACT

The negative effects of two types of illite clays, designated as illite P and W, respectively, on bitumen recovery were found to be related to their acidity. In de-ionized water the presence of divalent cations significantly increased the detrimental effect of illite P on bitumen recovery. The effect was found to be compounded at a lower process temperature and low pH values. Zeta potential distribution measurements were conducted to investigate the effects of water chemistry and temperature on the interactions between bitumen and illite clays. The results correlated well with the flotation data. XRD analysis showed that illite P contained smectite type clays. In addition, illite P was found to have higher surface area, cation exchange capacity and cation adsorption rate than illite W. It appears that the smectite nature of illite P in the presence of a sufficient level of divalent cations and low pHs are key factors in the depression of bitumen recovery.

## **ACKNOWLEDGEMENTS**

I am full of gratitude to both my supervisors, Dr. Jacob Masliyah and Dr. Zhenghe Xu, for their thoughtful guidance, support and encouragement throughout the course of this thesis.

I would also like to thank Dr. Oladipo Omotoso and Ms. Heather for their valuable discussion and suggestion on clay characterization.

My thanks also goes to all the members of the Oil sands group at the University of Alberta who helped me keep moving forward.

My eternal gratitude goes to my loving wife, Ms Lihua Guo, for her support and encouragement, and for all the experience we shared in the tough time of our family life.

Finally, I would like to thank the NSERC Industrial Chair in Oil Sands Engineering for the financial support.

To my loving wife, Ms. Lihua Guo

## TABLE OF CONTENTS

1.0 INTRODUCTION	1
2.0 LITERATURE REVIEW	5
2.1 Effect of fines (clay minerals)	5
2.2 Effect of water chemistry	10
2.2.1 Added inorganic bases/ pH	10
2.2.2 Surfactants	12
2.2.3 Divalent cations	13
2.3 Effect of temperature	17
3.0 BITUMEN FLOTATION TESTS	21
3.1 Introduction	21
3.2 Experimental	22
3.2.1 Materials	22
3.2.2 Experimental set-up	24
3.2.3 Procedures	25
3.3 Results and discussion	27
3.3.1 Effects of divalent cations and illite clays	27
3.3.2 Effect of temperature	35
3.3.3 Effect of process aids	38
3.3.4 Effect of process water	40
3.4 Conclusions	42
4.0 ZETA POTENTIAL DISTRIBUTION MEASUREMENTS	44
4.1 Zeta potential ( $\zeta$ )	44
4.2 Zeta potential distribution measurements	45
4.3 Materials and Experimental Procedures	48
4.4 Results and discussion	51
4.4.1 Effects of divalent cations	51
4.4.2 Effect of temperature	60

4.4.3 Effect of process aids	63
4.5 Conclusions	70
5.0 CHARACTERIZATION OF CLAYS	71
5.1 Fourier transform infra-red (FTIR)	71
5.2 X-ray diffraction (XRD)	72
5.3 Cation exchange capacity (CEC)	75
5.4 Specific surface area	77
5.5 Cation adsorption kinetics test	79
5.6 Conclusions	80
6.0 CONCLUSIONS	81
7.0 RECOMMENDATIONS	82
REFERENCES	83
APPENDIX A	90
Dean Stark Method	90
APPENDIX B	94
Effect of Calcium Ions on Bitumen Flotation Tests	94
APPENDIX C	98
Effect of Calcium Ions on Zeta Potential Measurements	98
APPENDIX D	105
Ethylene Glycol Monoethyl Ether (EGME) Method for Specific Surface Area (SA)	105

## LIST OF TABLES

Table 3.1.	Composition of F11B oil sand ore (mass %)	22
Table 5.1.	Mineral composition by XRD	73

## LIST OF FIGURES

Figure 2.1.	Synergetic effect of calcium ions and clays on bitumen flotation recovery (high grade oil sands, de-ionized water, and flotation at 80°C) (Kasongo et al., 2004).	16
Figure 2.2.	Effect of temperature on bitumen recovery (Bichard, 1987).	18
Figure 3.1.	Particle size distributions of two illite clays.	23
Figure 3.2.	(a) Schematic diagram of the flotation process, and (b) photograph of the Denver flotation cell.	24
Figure 3.3.	Effect of magnesium ions and illite P on bitumen flotation kinetics using de-ionized water initially adjusted to pH 8.5 at 25°C.	27
Figure 3.4.	Effect of increasing illite P on bitumen flotation recovery using de-ionized water initially adjusted to pH 8.5.	28
Figure 3.5.	Effect of illite P on pH of the tailings water from the flotation systems without addition of divalent cations.	29
Figure 3.6.	Synergetic effect of divalent cations and illite P on bitumen recovery at 25°C using de-ionized water initially adjusted to pH 8.5.	29
Figure 3.7.	Effect of illite P on the pH of the tailing water from the flotation systems with 1 mM magnesium ions addition at 25°C using de-ionized water initially adjusted to pH 8.5.	30
Figure 3.8.	Comparison of the synergetic effects of divalent cations and illite clays on bitumen recovery at 25°C using de-ionized water initially adjusted to pH 8.5.	31

Figure 3.9.	Comparison of the synergetic effects of divalent cations and illite clays on bitumen recovery at 35°C using de-ionized water initially adjusted to pH 8.5.	31
Figure 3.10.	Effect of pH on bitumen recovery using de-ionized water at 25°C.	33
Figure 3.11.	Effect of pH on bitumen recovery using de-ionized water at 35°C.	34
Figure 3.12.	Divalent cation concentrations of tailing water as a function of the amount of illite P addition in the flotation systems with the co-addition of 1mM MgCl <sub>2</sub> at 25°C.	34
Figure 3.13.	Effect of temperature on bitumen flotation kinetics using de-ionized water initially adjusted to pH 8.5.	35
Figure 3.14.	Effect of temperature on bitumen recovery using de-ionized water with an initially adjusted pH of 8.5	36
Figure 3.15.	Effect of illite P addition on the pH of the tailing water from the flotation systems with the addition of 1 mM magnesium ions at 25°C and 35°C using de-ionized water initially adjusted to pH 8.5.	37
Figure 3.16.	Divalent cation concentrations of tailing water as a function of the amount of illite P addition to the flotation systems with the co-addition of 1mM MgCl <sub>2</sub> .	38
Figure 3.17.	Effect of NaOH addition on bitumen recovery for the flotation systems with the co-addition of 1mM MgCl <sub>2</sub> and 5 wt% illite P using de-ionized water at 35°C.	39
Figure 3.18.	Effect of NaOH (0.03wt% of oil sands) and NaHCO <sub>3</sub> (0.33wt% of oil sands or 1000ppm based on water) addition on bitumen recovery for the	

	flotation systems with the co-addition of 1mM MgCl <sub>2</sub> and 5 wt% illite P using de-ionized water.	40
Figure 3.19.	Comparison of bitumen recovery in Aurora process water with that in de-ionized water.	41
Figure 3.20.	Bitumen recovery versus pH of tailing water	42
Figure 4.1.	Schematic representation of the electric double layer according to Stern's model.	45
Figure 4.2.	Schematic zeta potential distributions for a binary colloidal system that can be interpreted for particle interactions.	47
Figure 4.3.	Schematic of zeta potential measurements.	49
Figure 4.4.	Photograph of Zetaphoremeter IV <sup>TM</sup> (CAD).	50
Figure 4.5.	Effect of magnesium ions on the average zeta potentials of illite clays at 25°C.	52
Figure 4.6.	Effect of magnesium ions on the average zeta potential of bitumen in 1mM KCl solutions at 25°C.	53
Figure 4.7.	Zeta potential distributions for (a) individual bitumen emulsion and illite W suspension and (b) their mixture at pH 8.5 and 25°C in 1mM KCl solutions.	54
Figure 4.8.	Zeta potential distributions for (a) individual bitumen emulsion and illite P suspensions and (b) their mixture at pH 8.5 and 25°C in 1mM KCl solutions.	55

- Figure 4.9. Zeta potential distributions for (a) bitumen emulsion and illite W suspensions and (b) their mixture at pH 8.5 and 25°C in 1mM KCl solutions containing 24ppm magnesium ions. 56
- Figure 4.10. Effect of bitumen to illite W ratio on zeta potential distributions measured at pH 8.5 and 25°C in 1mM KCl solutions containing 24ppm magnesium ions. 57
- Figure 4.11. Zeta potential distributions for (a) bitumen emulsion and illite P suspensions and (b) their mixture at pH 8.5 and 25°C in 1mM KCl solutions containing 24ppm magnesium ions. 58
- Figure 4.12. Effect of bitumen to illite P ratio on the zeta potential distributions measured at pH 8.5 and 25°C in 1mM KCl solutions containing 24ppm magnesium ions. 59
- Figure 4.13. Effect of temperature on the average zeta potential of bitumen in 1mM KCl solutions. 60
- Figure 4.14. Effect of temperature on the average zeta potentials of illite clays in 1mM KCl solutions. 61
- Figure 4.15. Zeta potential distributions for (a) bitumen emulsion and illite P suspensions and (b) their mixture at pH 8.5 and 35°C in 1mM KCl solutions containing 24ppm magnesium ions. 61
- Figure 4.16. Effect of bitumen to illite P ratio on the zeta potential distributions measured at pH 8.5 and 35°C in 1mM KCl solutions containing 24ppm magnesium ions. 63

- Figure 4.17. Zeta potential distributions for (a) individual bitumen emulsion and illite P suspension and (b) their mixture at pH 4.9 and 25°C in 1mM KCl solutions containing 24ppm magnesium ions. 64
- Figure 4.18. Zeta potential distributions for (a) individual bitumen emulsion and illite W suspensions and (b) their mixture at pH 4.9 and 25°C in 1mM KCl solutions containing 24ppm magnesium ions. 65
- Figure 4.19. Zeta potential distributions for (a) bitumen emulsion and illite P clay suspensions and (b) their mixture at 25°C in the supernatant of the produced tailings water (pH 8.5) (from the flotation test with pH controlled at 8.5) with the addition of 24ppm magnesium ions. 66
- Figure 4.20. Zeta potential distributions for (a) bitumen emulsion and illite P suspensions and (b) their mixture at 25°C in the supernatant of the produced tailings water (pH 4.9) (from the flotation test without pH control) with the addition of 24ppm magnesium ions. 67
- Figure 4.21. Zeta potential distributions for (a) individual bitumen emulsion and illite P suspensions and (b) their mixture at pH 8.6 and 25°C in 1mM KCl solutions with the addition of 24ppm magnesium and 1000ppm NaHCO<sub>3</sub> based on water. 68
- Figure 4.22. Zeta potential distributions for (a) individual bitumen emulsion and illite P suspensions and (b) their mixture at pH 8.6 and 35°C in 1mM KCl solutions with the addition of 24ppm magnesium and 1000ppm NaHCO<sub>3</sub>. 69
- Figure 5.1. FTIR spectra of two illite clays. 72

Figure 5.2.	Oriented XRD Patterns of illite W.	74
Figure 5.3.	Oriented XRD Patterns of illite P	75
Figure 5.4.	Calcium adsorption on the two illite clays as a function of time in solutions containing initially 1mM calcium ions at a solid to liquid ratio of 1 g/L.	79
Figure 5.5.	Magnesium adsorption on two illite clays as a function of time in solutions	80
Figure B.1.	Effect of calcium ions and illite P on bitumen flotation kinetics at 25°C using de-ionized water initially adjusted to pH 8.5.	94
Figure B.2.	Effect of illite P on pH of the tailings water from the flotation systems with the addition of 1 mM calcium ions.	95
Figure B.3.	Divalent cation concentrations of tailing water as a function of the amount of illite P addition in the flotation systems with the co-addition of 1mM CaCl <sub>2</sub> .	95
Figure B.4.	Effect of NaOH addition on bitumen recovery P for the flotation systems with the co-addition of 40ppm calcium ions and 5 wt% illite P at 35°C.	96
Figure B.5.	Effect of NaOH (0.03wt% of oil sands) and NaHCO <sub>3</sub> (0.33wt% of oil sands or 1000ppm based on water) addition on bitumen recovery for the flotation systems with the co-addition of 1mM CaCl <sub>2</sub> and 5 wt% illite P using de-ionized water.	96
Figure B.6.	Effect on bitumen recovery of Aurora process water compared with de-ionized water.	97

Figure C.1.	Effect of calcium ions on the zeta potentials of illite clays in 1 mM KCl solution at 25°C.	98
Figure C.2.	Effect of calcium ions on zeta potential of bitumen in 1 mM KCl solution at 25°C.	98
Figure C.3.	Zeta potential distributions for (a) bitumen emulsion and illite W suspensions and (b) their mixture at pH 8.5 and 25°C in 1mM KCl solutions containing 40ppm calcium ions.	99
Figure C.4.	Effect of bitumen to illite W ratio on the zeta potential distributions measured at pH 8.5 and 25°C in 1mM KCl solutions containing 40ppm calcium ions.	99
Figure C.5.	Zeta potential distributions for (a) bitumen emulsion and illite P suspensions and (b) their mixture at pH 8.5 and 25°C in 1mM KCl solutions containing 40ppm calcium ions.	100
Figure C.6.	Effect of bitumen to illite P ratio on the zeta potential distributions measured at pH 8.5 and 25°C in 1mM KCl solutions containing 40ppm calcium ions.	100
Figure C.7.	Zeta potential distributions for (a) bitumen emulsion and illite P suspensions and (b) their mixture at pH 8.5 and 35°C in 1mM KCl solutions containing 40ppm calcium ions.	101
Figure C.8.	Effect of bitumen to illite P ratio on the zeta potential distributions measured at pH 8.5 and 35°C in 1mM KCl solutions containing 40ppm calcium ions.	101

- Figure C.9. Zeta potential distributions for (a) individual bitumen emulsion and illite P suspension and (b) their mixture at pH 4.9 and 25°C in 1mM KCl solutions containing 40ppm calcium ions. 102
- Figure C.10. Zeta potential distributions for (a) individual bitumen emulsion and illite W suspensions and (b) their mixture at pH 4.9 and 25°C in 1mM KCl solutions containing 40ppm calcium ions. 102
- Figure C.11. Zeta potential distributions for (a) bitumen emulsion and illite P suspensions and (b) their mixture at 25°C in the supernatant of the produced tailings water (pH 8.5) (from the flotation test with pH controlled at 8.5) with the addition of 40ppm calcium ions. 103
- Figure C.12. Zeta potential distributions for (a) bitumen emulsion and illite P suspensions and (b) their mixture at 25°C in the supernatant of the produced tailings water (pH 4.9) (from the flotation test without pH control) with the addition of 40ppm calcium ions. 103
- Figure C.13. Zeta potential distributions for (a) individual bitumen emulsion and illite P suspensions and (b) their mixture at pH 8.6 and 25°C in 1mM KCl solutions with addition of 40ppm calcium ions and 1000ppm NaHCO<sub>3</sub>. 104
- Figure C.14. Zeta potential distributions for (a) individual bitumen emulsion and illite P suspensions and (b) their mixture at pH 8.6 and 35°C in 1mM KCl solutions with the addition of 40ppm calcium ions and 1000ppm NaHCO<sub>3</sub>.

## LIST OF NOMENCLATURE

a	spherical particle radius, m
d	inter-plane distance, m
n	order of diffraction
$U_E$	velocity per unit field strength or electrophoretic mobility, (m/s)/(V/m)

### Greek Letters

$\theta$	scattering angle, degree
$\lambda$	wavelength of the x-ray, m
$\epsilon_0$	permittivity of vacuum, $C^2/N\ m^2$ or $C/Vm$
$\epsilon$	dielectric constant, dimensionless
$\zeta$	zeta potential, V
$\kappa$	inverse Debye length, $m^{-1}$
$\kappa^{-1}$	Debye length, m
$\mu$	fluid viscosity, Pa s

## 1.0 INTRODUCTION

Oil sands (formerly called tar sands) are aggregates of coarse sand, fines ( $-44\ \mu\text{m}$  particles including silt, very fine quartz and clay minerals), water and bitumen (high molar mass viscous petroleum). The largest deposit of oil sands in the world is located in northern Alberta, Canada. The deposit contains about 300 million barrels of bitumen that can be recovered using current in-situ and open pit mining technologies (Mathieson and Stenason, 2001, cited in Masliyah, 2004). It can potentially secure the energy supply for Canada in the next 200-300 years. The oil sands in Athabasca typically contain 10% bitumen, 86% sand and fines, and 4% water. Oil sand ores containing less than 6% bitumen are not economical to process and are rejected with the overburden at a current technology level (Bichard, 1987).

There are two types of technologies for recovering bitumen from oil sands: in-situ and open pit mining methods. Currently, about one quarter of bitumen is produced from in-situ recovery and the rest is from the open pit mining method (Alberta Department of Energy, 2004). In-situ technology is usually used for bitumen deposits buried too deeply (more than 75 metres) for mining to be practical. It is mostly used for deposits buried more than 400 metres below the surface. The Alberta Energy and Utilities Board (AEUB) estimates that 80 percent of the total oil sands can only be recovered by in-situ techniques (Alberta Department of Energy, 2004). Steam Assisted Gravity Drainage (SAGD) is a dominant in-situ technique that is currently used in the oil sands industry. The basic idea of this method is to reduce the bitumen viscosity by injecting steam into

reservoirs through vertical or horizontal wells. Bitumen can flow out easily through the well under pressure because of the reduced viscosity. So far the largest in-situ bitumen recovery project in Canada has been conducted at Cold Lake. Among the other in-situ technologies under development are Cyclic Steam Stimulation (CSS), Pressure Cyclic Steam Drive (PSCD), pulse technology and Vapor Extraction (VAPEX) (Alberta Department of Energy, 2004). Open pit mining method remains the main technology used to recover bitumen from the Athabasca oil sands. Mining involves massive excavation to remove the overburden and reach the oil sand formation. To date the maximum overburden thickness that can be removed economically is about 70 metres and only the more favorable sites have been developed. The present commercial processes are a lower temperature version of the well known Clark Hot Water Process (CHWP). A typical bitumen extraction process involves the following essential steps: first, oil sand lumps are crushed and the crushed oil sands are transported to slurry preparation where hot water is mixed with the ore. The resulting slurry is pumped into a hydrotransport slurry pipeline where slurry conditioning takes place. During the slurry transport, bitumen is liberated from the sand grains and the liberated bitumen becomes aerated. A gravity separator is then used to recover the aerated bitumen as bitumen froth. After removing the water and solids from the bitumen froth, the bitumen is ready for upgrading.

It is well known that the mining extraction methods require large volumes of water. It has been reported that it may require 2.5 to 4.0 barrels of imported fresh water to produce one barrel of bitumen (National Energy Board, 2004). With the increasing need to produce bitumen but with an increasingly limited water supply, operators have to reclaim water

from mature fine tailings for their process to maintain operation. For this purpose, gypsum is added into the tailings to accelerate the coagulation and setting of mature fine solids and the release of water. However, the use of gypsum is anticipated to increase the concentration of calcium cations in the reclaimed water. Magnesium is also a divalent ion and it is usually present in bitumen extraction slurries. Their presence is also harmful to bitumen recovery. A number of researchers (Sanford, 1983; Takamura and Wallace, 1988; Smith and Schramm, 1992; Zhou et al., 1999; Kasongo et al., 2000) reported that in industrial and laboratory tests, the levels of ions and clay minerals present in the slurry have a significant impact on bitumen recovery. The primary clay minerals observed in the various extraction process streams were kaolinite and illite (Bichard, 1987; Budziak et al., 1988; Omotoso and Mikula, 2004). To our best knowledge, most of the research has been focused on montmorillonite and kaolinite clays and only few studies (Kasongo, 2000; Wallace, 2004) were conducted to study the effect of illite on bitumen recovery. Further exploration on illite clay is necessary to gain a better understanding of its effect on bitumen recovery. Many studies show that temperature has a great effect on bitumen recovery from oil sand ores. Whether temperature can mitigate slime-coating remains to be further explored. In addition, the effect of magnesium ions has not been systematically studied.

The main objective of this study is to obtain a better understanding of the bitumen extraction mechanism using water-based bitumen extraction technology, thus helping improve the bitumen recovery efficiency. To investigate the effects of divalent cations (calcium and magnesium), illite clay, process aids (NaOH and NaHCO<sub>3</sub>) and temperature

on bitumen recovery, both electrokinetic studies and flotation tests were conducted. In addition, two sources of illite clays were used and characterized to explain their effect on bitumen recovery. The findings through these investigations provided more insights into oil sands ore processing in aqueous environments.

The organization of the thesis is as follows:

In chapter one, a brief introduction to the bitumen extraction, the objectives and organization of the thesis are given.

Chapter two reviews the literature of water-based bitumen extraction including effects of fines, water chemistry and temperature.

Chapter three demonstrates the effects of temperature, divalent cations, illite clays and process aids on bitumen recovery by flotation tests.

Chapter four presents the results of the interaction between bitumen and illite clays by zeta potential distribution measurements. The effect of temperature, divalent cations and process aids is qualitatively reported.

Chapter five is concerned about the characterization of two kinds of illite clays. The X-ray diffraction (XRD), cation exchange capacity (CEC), specific surface area (SSA), etc. are reported.

The general conclusions are given in chapter six.

## **2.0 LITERATURE REVIEW**

Many factors such as oil sands ore type (e.g., grade, fines content and aging time), operating conditions (e.g., temperature, shear rate, air flow rate and cell design), and water chemistry have been identified to influence bitumen recovery efficiency from the Athabasca oil sands using aqueous extraction methods (Sanford and Seyer, 1979; Sanford, 1983; Takamura and Wallace, 1988; Kasongo et al., 2000; Schramm et al., 2001 and 2003). Kasperski (2001) and Masliyah (2004) both have given an excellent overview on current knowledge of water-based bitumen extraction from Athabasca oil sands. This chapter aims to give a brief literature review of the studies that were focused on the effects of fines, water chemistry and temperature on bitumen recovery.

### **2.1 Effect of fines (clay minerals)**

It has been widely recognized that bitumen-fines interactions have a significant impact on bitumen recovery. Much research has been carried out to investigate the effect of fines on bitumen recovery from oil sands. Hepler and Smith (1994) reported that in both laboratory tests and commercial production the presence of fines in the original feed greatly affects bitumen recovery from the Athabasca oil sands. The pioneering research of Clark and Pasternack (1949) studied the effect of clay in the hot water separation process as applied to Athabasca oil sands. They found evidence showing that clays naturally present in oil sands played a key role in the recovery process. The presence of a small amount of clay helped the bitumen to disperse into flecks lying unattached among the sand grains, which would benefit bitumen recovery from the oil sands. But with an

increase of the amount of clay, the clay content in the bitumen flecks increased and the flecks became dispersed in water. Such dispersion would be harmful to bitumen recovery. No clay property was provided in the study. Sanford (1983) found that bitumen recovery was strongly correlated with the fines content of the oil sands. Under the same operating conditions, more fines gave less bitumen recovery. Schramm et al. (1985) studied the processability of mixtures of oil sands and also suggested that clays present in the oil sands were detrimental to bitumen recovery. The work of Smith and Schramm (1992) showed that mineral components in oil sands could reduce carboxylate surfactant concentrations either by consuming NaOH or by precipitating surfactants, thus impacting bitumen recovery in the hot water process. In commercial plants, high fine ores were also found to be more difficult to process. The existence of high fines content increased the middlings density and the water content in the bitumen froth and reduced bitumen recoveries (Cuddy, 2000; Cox, 2000; Tipman, 2000).

To gain a better understanding of the interactions between bitumen and fines (in an attempt to further improve bitumen recovery), a great deal of research efforts has been made to explore the interactions between bitumen and fines (different clay minerals). Due to the complexity of oil sands and bitumen systems, a well-designed simulation environment was usually employed. Dai and Chung (1995) used a coker feed bitumen and various sized silica to perform bitumen pickup tests. They found a relationship between bitumen-silica interactions, solution pH, and particle sizes. At  $\text{pH} > 6$ , sands could be easily detached from the bitumen surface while at  $\text{pH} < 6$ , strong attachment between bitumen and silica was observed. The interaction was also particle-size

dependent and they found that the finer the particles are, the stronger is the attachment. To simulate the coagulation behavior of complex bitumen systems, a simple model system was created by Zhou et al. (1999) to investigate the effects of pH, calcium ion concentrations and surfactants on the coagulation behavior between bitumen and fine silica (-5  $\mu\text{m}$ ). They made very similar observations on the pH dependent coagulation behavior between bitumen and silica as reported by Dai and Chung (1995). Chong et al. (2002) investigated the impact of fines content on bitumen recovery by using model oil sands and found that the fines content was one of the key factors affecting bitumen recovery and that in the absence of NaOH, a small amount of fines was beneficial to bitumen recovery, which was in line with the observations by Clark and Pasternack (1949).

To further study the effect of fines, a commercial clay mineral (instead of silica) was used in various studies. Basu et al. (2004) studied the effect of calcium ions and montmorillonite clay on bitumen displacement by water on a model glass surface. Their results suggest that the presence of calcium ions and montmorillonite clay has a negative impact on bitumen liberation from sand grains in the commercial production. A novel technique was developed by Liu et al. (2002) to investigate the interactions between bitumen and clays in an aqueous solution from zeta potential distribution measurements. For a single component suspension, a single modal zeta potential distribution peak was obtained under a given solution condition. In the case of a two-component mixture, the measured zeta potential distributions showed either one or two distribution peaks, depending on the chemical make-up of the aqueous solution and the type/amount of clays

present. Using this method, Liu et al. (2002) found a stronger attraction between bitumen and montmorillonite clay than that between bitumen and kaolinite clay when 40ppm of calcium ions was present. This was in an excellent agreement with the flotation results reported by Kasongo et al. (2000). Fong et al. (2004) carried out a series of systematic screening experiments with model oil sands and found that coarse solids with size above 106  $\mu\text{m}$  had no effect on bitumen recovery. However, the presence of fine silica (up to 15~40 wt %) and commercial illite, kaolinite and montmorillonite (up to 1~5 wt %) reduced bitumen recovery. For fine silica and illite clay, the bitumen recovery could be restored by a higher dosage of NaOH, while for montmorillonite and kaolinite, the bitumen recovery loss was permanent. They concluded that magnesium ions had a more pronounced negative effect on bitumen recovery than calcium ions based on their mass concentration.

Most of the aforementioned research regarding the effect of fines was based on model oil sand systems. However, due to differences in activities between model oil sand systems and real oil sand ores, it was necessary to confirm the effect of fines on bitumen recovery using natural Athabasca oil sands. To achieve this purpose, Kasongo et al. (2000) developed a novel “doping” method that involved the addition of a prescribed amount of calcium and/or clays into a good processing estuarine oil sand ore in batch flotation tests. They found that the addition of calcium ions (up to 40 ppm) or clay (kaolinite, illite or montmorillonite) at 1 wt% of processed oil sands had a marginal effect on bitumen recovery. However, a sharp reduction in bitumen recovery was observed when both calcium ions and montmorillonite clay were added together while using de-ionized water

for bitumen extraction. Solution analysis of the tailing water revealed that the adverse impact of calcium ions and montmorillonite clay on bitumen recovery was associated with a stronger affinity of calcium for montmorillonite clays than for kaolinite or illite clay.

Recently, Liu et al. (2003 and 2004) quantitatively measured the colloidal forces between bitumen and silica, montmorillonite and kaolinite clays by using atomic force microscope (AFM). The implication of the interaction forces measured by AFM was confirmed by zeta potential distribution measurements and flotation test results by Kasongo et al. (2000).

Wallace et al. (2004) found a relationship between the poor processing behavior of oil sands ore and soluble potassium in the slurry. They hypothesized that elevated soluble potassium was due to the degraded illite that had swelling properties similar to montmorillonite. In the Athabasca oil sands, the major clay minerals were found to be illite and kaolinite (Bichard, 1987; Budziak et al. 1988; Omotoso and Mikula, 2004). Thus, a better understanding of the effect of illite clays on bitumen recovery would be helpful to understand poor processability of certain oil sands ore and improve bitumen recovery. To our best knowledge, however, only few studies to date (Kasongo, 2000; Wallace, 2004) have been carried out on the effect of illite clay on bitumen recovery. In this study, further investigation such as electrokinetic studies, flotation tests and clay characterizations was conducted on two different sources of commercial illite clays to explore their effects on bitumen extraction.

## 2.2 Effect of water chemistry

The bitumen extraction process includes the following sub-processes: liberation of bitumen from the sand grains; attachment of the liberated bitumen to air bubbles; and flotation of aerated bitumen (Hepler and Hsi, 1989; Hepler and Smith, 1994). Interactions between bitumen and clay minerals or air bubbles play a key role in bitumen recovery as they dictate these sub-processes. Water chemistry has a significant effect on the interactions, and extensive research has been performed to evaluate its impact.

### 2.2.1 Added inorganic bases/ pH

A known fact is that water extraction processes work better at an alkaline pH. This pH is usually obtained by adding process aids. Inorganic bases (such as  $\text{Na}_2\text{SiO}_3$ ,  $\text{Na}_5\text{P}_3\text{O}_{10}$ ,  $\text{NaHCO}_3$ ,  $\text{Na}_2\text{CO}_3$ ,  $\text{NH}_4\text{OH}$ , and trona (mineral grade sodium carbonate), etc) have been tested as process aids in the hot water extraction process (Clark, 1929; Sanford, 1983; Bichard, 1987; Dai and Chung, 1996a). Their effects on bitumen recovery were comparable to NaOH, although their optimum dosages were higher than that of NaOH. Research and industrial interests have been mainly focused on NaOH and it has been recognized that the key role of NaOH in the process is to react with some acidic components in bitumen to generate natural surfactants (Sanford and Seyer, 1979; Schramm and Smith, 1989).

In 1932, Clark and Pasternack (1932) reported the important role of alkaline additives in maximizing bitumen recovery. Sanford and Seyer (1979) found that the role of NaOH was to neutralize the organic acids and generate surfactants that are believed to facilitate

the flotation recovery of bitumen. Sanford (1983) indicated that NaOH was only effective when present in the conditioning step and that the optimum dosage of NaOH required for maximum bitumen recovery was a function of the amount of fine solids in the oil sands ore. The work of Schramm et al. (1985) showed that the role of NaOH was to generate natural carboxylate surfactants. Smith and Schramm (1992) showed that only a small fraction of the added NaOH was needed to produce natural surfactants, and the bulk of NaOH reacted with polyvalent metal carbonates, sulfates, and clays in the oil sand. Dai and Chung (1996b) studied the role of NaOH on both the liberation of bitumen from sands and bitumen emulsification using model oil sands. It was identified that a critical NaOH amount was needed to achieve optimal effect, and bitumen recovery loss was either due to incomplete bitumen/sand separation or due to oil-in-water emulsification resulting from deficiency or over-dosage of NaOH, respectively.

The pH of oil sands slurry is considered to be an important parameter in oil sands processing (Clark and Pasternack, 1932). Sanford (1983) studied the effect of pH on bitumen recovery and found that there was no general relationship between the pH of oil sands slurry and bitumen recovery, either with or without NaOH addition. However, Bichard (1987) stated that for a system without caustic addition, the bitumen recovery in hot water flotation was a function of the “naturally occurring pH” of the oil sands. For instance, neutral to alkaline oil sands exhibit high bitumen recovery and neutral to acidic oil sands exhibit poorer bitumen recovery. With caustic addition, the optimum pH for bitumen recovery was found to be around 9 and varied slightly ( $\pm 1$  pH) with different oil sands. Many approaches have been tried to understand the effect of pH on bitumen

recovery. Using the so-called pickup tests using model oil sands, Dai and Chung (1995) observed that increasing pH always favored bitumen liberation. By studying bitumen displacement on a model glass plate, Basu et al. (1996) found that at higher pH, the bitumen displacement rate was lower (the lower the rate, the longer the time required to attain complete displacement) and the corresponding equilibrium contact angle was higher (the higher the angle, the easier the detachment of bitumen from the sand grains), illustrating that the use of a high pH to achieve a large bitumen contact angle (easy detachment of bitumen from the sand grains) was essential even though the rate of displacement was lower at the higher pH. To gain a fundamental understanding of the effect of pH, Liu et al. (2004, 2005) quantitatively measured the colloidal forces between bitumen and silica, and between bitumen surfaces in aqueous solutions by using an atomic force microscope (AFM). Their study showed that the solution pH was a critical factor in controlling the bitumen/silica and bitumen/bitumen interactions. At a lower pH, there was a weaker repulsive force and a stronger adhesion forces between bitumen surfaces, which was favorable for bitumen droplet coagulation. At a higher pH, there was a stronger repulsive force and a weaker adhesive force between bitumen and silica, which was favorable for mitigation of slime coating. Therefore, they suggested that choosing an appropriate solution pH was important for bitumen extraction.

### 2.2.2 Surfactants

In the pioneering work of Clark (1944), it was speculated that water-soluble surfactants generated by the addition of NaOH played a key role in the bitumen separation process. Sanford and Seyer (1979) proved the speculation by confirming the existence of organic

carbon in the tailings and their effect on bitumen recovery. Their studies showed the connection between surfactants in the tailings and NaOH used in the hot water extraction process. All the tailings had similar titration end points as the commercial surfactant sodium oleate, which was ascribed to the existence of sodium carboxylates. The concentrated solids-free tailing water from one run was used in a second run flotation test without NaOH addition, and the same bitumen recovery as that with NaOH addition was obtained. This work provided the evidence that surfactants were indeed an active process aid. Moreover, the work by Baptista and Bowman (1969) and Schramm and Smith (1987) showed that the surfactants produced in the process were primarily carboxylates of naphthentic acids and sulfonates. Sanford (1983) found that non-ionic surfactants had no beneficial effect on bitumen recovery and commercial anionic surfactants were as effective as strong inorganic bases. Whether the surfactants employed in the process were natural or commercial, a critical free surfactant concentration for optimal bitumen recovery was observed (Schramm et al., 1984, 1985). Schramm et al. (1984, 1985, 1987) reported that the essential roles of surfactants were to alter surface charges and interfacial tensions due to their adsorption at surfaces and interfaces.

### 2.2.3 Divalent cations

The negative impact of divalent cations on oil sands processability has been observed in both commercial operations and laboratory tests (Sanford, 1983; Bichard 1987; Baptista, 1989a, b; Schramm and Smith, 1989; Kasongo et al., 2000; Mikula et al., 2004). In general, the effect of divalent cations is very much dependent on ore properties and ion concentrations in solution.

Sanford (1983) investigated the relationship between bitumen recovery and the divalent cation (calcium and magnesium) concentration using distilled water and found that there was no general correlation between these two. He carried out the experiments in two ways. First, he conducted flotation tests on two batches of oil sands which had quite similar bitumen and fines contents but were very different with respect to  $\text{Ca}^{2+}$  and  $\text{Mg}^{2+}$  concentrations (40 and 21ppm for one ore, in comparison to 4.2 and 3.2ppm for the other). He observed very little difference in bitumen recovery for these two ores. Second, he collected bitumen recovery data (without NaOH addition) and  $\text{Ca}^{2+}$  and  $\text{Mg}^{2+}$  concentrations in aqueous tailings from a variety of freshly mined oil sand samples and he could not find any correlation between bitumen recovery and divalent cations concentrations (up to 14ppm). However, Bichard (1987) obtained quite different conclusions than Sanford's work. He studied the effects of  $\text{Ca}^{2+}$  and  $\text{Mg}^{2+}$  on oil sands ore processability using distilled water and found that  $\text{Ca}^{2+}$  and  $\text{Mg}^{2+}$  had a very similar detrimental effect on oil sand processability even in alkaline solution and that the poorer processability was related to large amount of these soluble ions in the water phase ( $\text{Ca}^{2+}$  ions up to 60ppm). The discrepancy between Sanford's and Bichard's conclusions may be due to the difference in fines content of the oil sands and the divalent cations concentration range they studied. Baptista (1989b) found that in both the continuous pilot unit and the commercial plant, bitumen recoveries were inversely related to the concentration of exchangeable cations from the oil sands, instead of the total fines content in the oil sands. Therefore, he believed that the cation exchange capacity (CEC) of oil sands, expressed either as calcium or calcium and magnesium, could be used as a "marker" for oil sand processability. The concentration range of calcium ions was

between 6 and 12meq/kg total oil sand solids (40-80ppm based on a normal ore to water ratio). Mikula et al. (2004) found that the effect of divalent cations was dependent on various ore properties. For high-grade ores, the bitumen recovery changed little with the concentration increase of calcium and magnesium ions. However, for medium and low-grade ores, up to a 3 mM divalent cations could be tolerated in the small-scale batch extraction process. This observation was verified by their commercial implementation. Schramm and Smith (1989) investigated the processability of mined oil sands contaminated with overburden material using distilled water and found that the poor processability was due to the polyvalent metal ions from the overburden material. They showed that the metal ions could affect processability in two ways: one was through reacting with NaOH, thus preventing NaOH from reacting with bitumen to generate carboxylate surfactants. The other was based on the fact that free metal ions or precipitated metal hydroxides could reduce the free carboxylate surfactants by adsorption or reaction. Kasongo et al. (2000) found that when both calcium ions (up to 40ppm) and montmorillonite clay at 1 wt% of processed oil sands were added together, a sharp reduction in bitumen recovery was observed using de-ionized water (Figure 2.1). They also analyzed the tailing water and found that calcium ion concentration in this case was much lower than other cases. They proposed that montmorillonite clay slime-coated on bitumen surfaces due to the presence of calcium ions. Using zeta potential distribution measurements, Liu et al. (2002) observed that calcium ions induced montmorillonite clay to slime-coat on bitumen droplet surface in certain aqueous solutions.

By using a model system to simulate the coagulation behavior of complex bitumen systems, Zhou et al. (1999) explained that the coagulation of bitumen with silica at a low pH was due to the interaction of cationic surfactants present in bitumen with silica, and that the presence of calcium ions in this pH range reduced the coagulation efficiency by

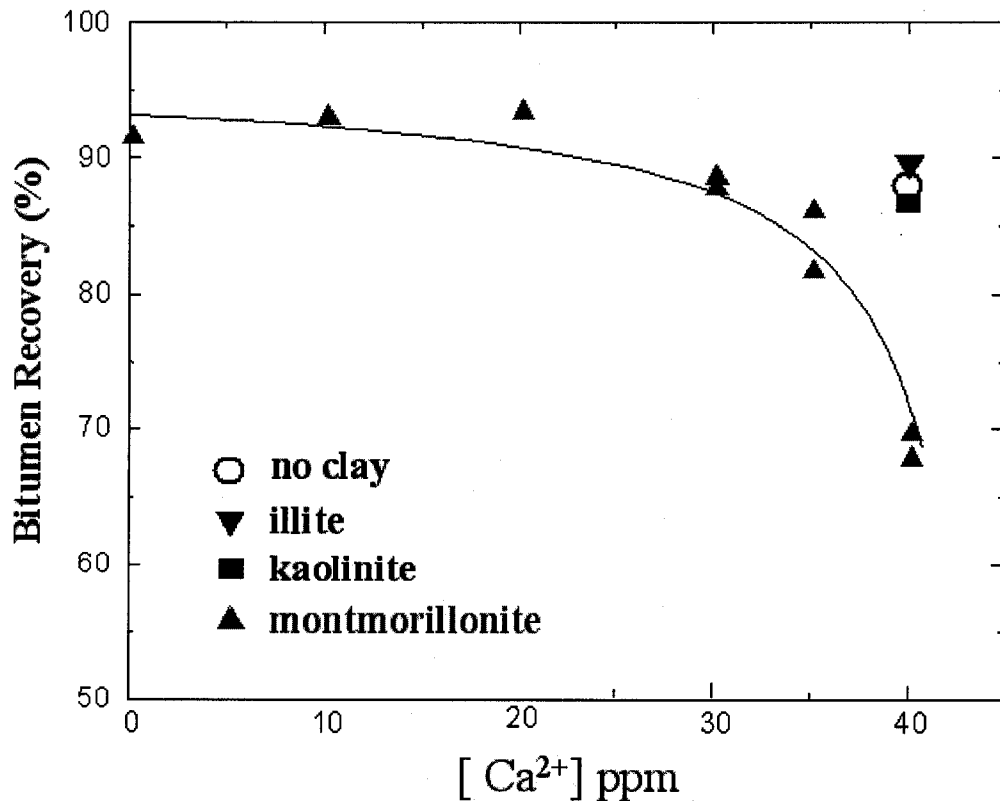


Figure 2.1. Synergetic effect of calcium ions and clays on bitumen flotation recovery (high grade oil sands, de-ionized water, and flotation at 80°C) (Kasongo et al., 2004).

acting as a barrier for cationic surfactant to adsorption on silica surfaces. At a high pH, calcium ions induced bitumen coagulation with silica by acting as a bridge between bitumen and silica via chemisorbed  $\text{CaOH}^+$  ions on silica surfaces that interacted with anionic surfactants in the solution or on the bitumen surface.

A series of studies were carried out by Liu et al. (2003; 2004 and 2005) to gain a fundamental understanding of the effect of calcium ions on bitumen recovery. By measuring the forces between bitumen and silica or clay using an atomic force microscope, they found that the presence of calcium ions decreased the repulsive forces and increased the adhesion forces, which was interpreted to be harmful to bitumen recovery.

### 2.3 Effect of temperature

Since the Clark hot water extraction method was first used commercially to extract bitumen from Athabasca oil sands in 1960s, the operating temperatures in the commercial plants were decreased to reduce thermal energy consumption. In recent years, several industrial extraction processes have been successfully operated at about 40-50°C. In particular, an even lower temperature extraction process (at around 25°C) was initialized at the Aurora plant of Syncrude Canada Ltd.

In literature, a large quantity of studies was aimed at exploring the effect of temperature on bitumen recovery. It is claimed that temperature in the range of 50-93°C had no significant effect on bitumen recovery (Bichard, 1987; Schramm et al. 2003; Zhou et al., 2004). However, in the range of 25-50°C, temperature has been found to have a great effect on bitumen recovery (Bichard, 1987; Schramm et al. 2003; Ding et al., 2004; Luthra et al., 2004; Zhou et al., 2004). The early study by Bichard (1987) showed that for different types of oil sand ores, temperature in the range of 49-93 °C (120-200 °F) had no significant effect on bitumen recovery. Figure 2.2 shows the effect of temperature on

bitumen recovery with Area D, Hole 11 oil sand. The author observed that good bitumen recoveries were obtained at temperatures above a critical value from a given ore. For instance, when the temperature was above the critical value, the density of bitumen was less than that of water and the bitumen floated out easily. As seen in Figure 2.2, the critical temperature is around 32°C (90°F). From BEU tests, Schramm et al. (2003)

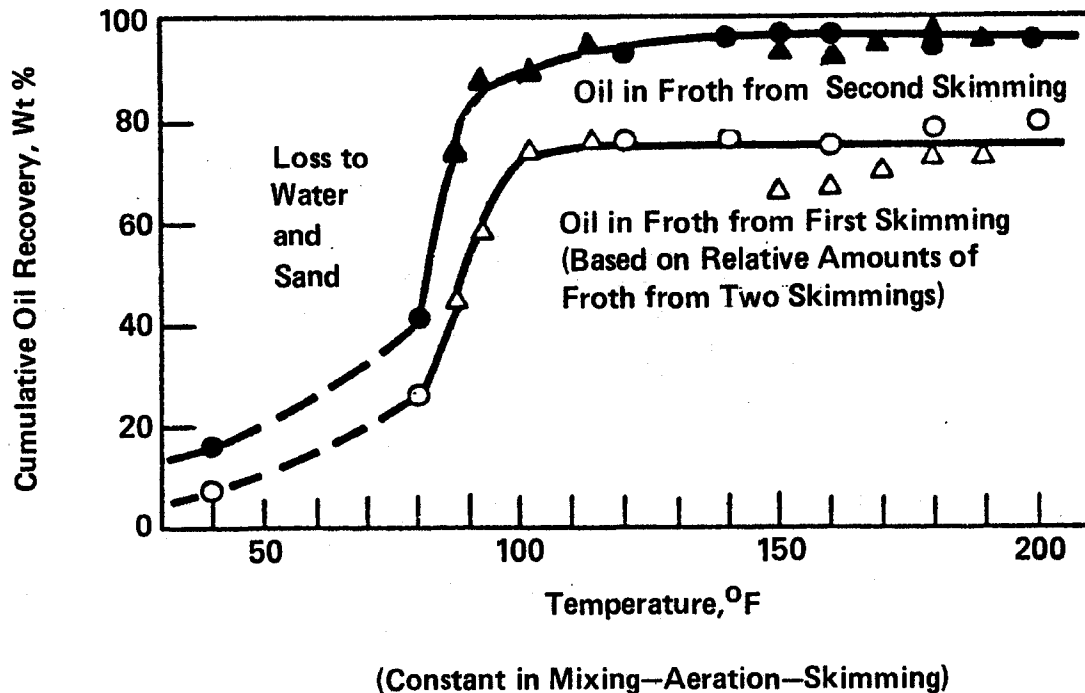


Figure 2.2. Effect of temperature on bitumen recovery (Bichard, 1987).

found a similar trend in terms of the effect of temperature on bitumen recovery. They concluded that the change in viscosity, rather than the change in density, played a key role in determining bitumen recovery. Zhou et al. (2004) also studied the effect of temperature on bitumen recovery by using a laboratory Denver flotation cell. Both good and poor processing ores were used in the flotation tests. Their findings were in line with the reports by Bichard (1987) and Schramm et al. (2003). Luthra et al. (2004) developed

a new imaging technique to estimate bitumen liberation and reported that the observed effect of temperature on bitumen recovery using the imaging technique was also in accordance with the findings by Zhou et al. (2004).

Meanwhile, many mechanistic studies have been conducted to further explore how temperature affects bitumen recovery. Dai and Chung (1995) conducted bitumen pickup tests by using model oil sand systems. By performing the tests on pure bitumen, separately at 22°C and 60°C, they found that the bitumen coverage was higher at 60°C than at 22°C. To check whether the bitumen viscosity change was the only factor, they conducted pickup tests for pure bitumen at 60°C and naphtha-diluted bitumen (N/B = 1/9) at 22°C (which had the same viscosity as pure bitumen at 60°C). They still observed different bitumen coverage; i.e. the bitumen viscosity alone could not explain the temperature effect. Then they checked the physicochemical properties of the silica-water-bitumen system and found that the negative zeta potential of silica increased significantly as the temperature increased. They also calculated the total inter-particle forces by using the classical DLVO theory and found that at pH<9 the energy barrier for silica - bitumen at 60°C was higher than that for silica-bitumen and silica-diluted bitumen at 22°C. They concluded that higher temperatures had at least two effects: a reduction in the viscosity and an increase in the electrostatic repulsion between sand and bitumen. By using confocal microscopic methods, Munoz and Mikula (1997) proposed a mechanism of bitumen-air attachment for a high-grade oil sands ore. At a higher temperature, bitumen droplets and air bubbles formed an intimate bitumen-air association, resulting in good bitumen flotation. At a lower temperature, the bitumen tended to behave like a particle

where the bitumen had much less chance to contact air and form easily floatable bitumen-air aggregates. Recently, Long et al. (2004) quantitatively measured the interaction and adhesion forces between bitumen and fines/clay in water as a function of temperature using an atomic force microscope. They found that the adhesion forces between fines/clay and bitumen decreased with decreasing temperature and totally disappeared at a critical value of about 32-35°C. The depressed adhesion forces were favorable for bitumen aeration. This observation can explain why bitumen recovery experiences a sharp increase with increasing temperature from room temperature to around 40 °C. They also investigated the effect of a chemical additive, methylisobutyl carbinol (MIBC) on the colloidal forces and answered the question of how MIBC influences bitumen recovery without affecting bitumen viscosity as proposed by Schramm et al. (2003). They reported that the MIBC addition reduces the adhesion force between clay and bitumen, which would be beneficial to bitumen aeration due to reduced slime coating of fines on bitumen.

## 3.0 BITUMEN FLOTATION TESTS

### 3.1 Introduction

Flotation is a surface wettability-based separation technology. During flotation, hydrophobic particles are aerated and carried to the surface for collection. Flotation has been extensively used in mineral processing and has also been successfully used in bitumen extraction from oil sands (Sanford and Seyer, 1979; Helper and Hsi, 1989; Helper and Smith, 1994; Kasongo et al., 2000; Zhou et al., 2004). A few techniques for laboratory testing of oil sands processability have been developed over the past decades. Bichard (1987) used beaker or jar tests to conduct his research on oil sands processability. To simulate the commercially used Clark Hot Water Extraction (CHWE) process, Sanford and Seyer (1979) developed a Batch Extraction Unit (BEU). It has been extensively used to conduct research on oil sands processability. Recently, Kasongo et al. (2000) and Zhou et al. (2004) used a modified Denver flotation cell to conduct their flotation tests, which could more sensitively detect the effect of operating parameters on bitumen recovery than BEU tests at temperatures below 50°C.

The main objective of this chapter is to document the investigation on the effects of illite clays and divalent cations alone or in combination on bitumen recovery from Athabasca oil sands by carrying out flotation tests in a modified Denver flotation cell. To achieve this purpose, a doping method developed by Kasongo et al. (2000) was used. A high grade oil sands ore, designated as F11B from Syncrude Canada Ltd., was used as an oil sands sample in this study. To aid the interpretation of results, de-ionized water, rather

than process water, was used in most tests. Use of de-ionized water in these tests avoids complications caused by various species in process water when interpreting the test results. In addition, the effects of temperature and process aids such as NaOH and NaHCO<sub>3</sub> on bitumen recovery were also investigated. The effect on bitumen recovery of using process water instead of de-ionized water in flotation tests is also reported in this chapter.

## 3.2 Experimental

### 3.2.1 Materials

The high-grade oil sands ore F11B was homogenized and stored in a refrigerator maintained at -29°C to minimize oxidation. Prior to the flotation tests, the ore was allowed to thaw for approximately one hour at room temperature. The average composition of the oil sands ore was analyzed by the Dean Stark method (details were included in Appendix A), as shown in Table 3-1. It was based on the analyses of 10 small, randomly picked bags of F11B ore. The error was less than 0.5 %.

Table 3.1. Composition of F11B oil sand ore (mass %)

Bitumen	Water	Solids	Fines <sup>a</sup>
14.5	3.2	82.3	9.5

<sup>a</sup> The fines level is defined as the mass fraction of solids smaller than 44µm and is expressed as a percentage of total solids.

Two batches of illite clays were separately purchased from Ward's Minerals and the Clay Minerals Society at the Purdue University. These illites were designated as illite W and P, respectively. To ensure a fair comparison, each batch of clays was ground in a porcelain

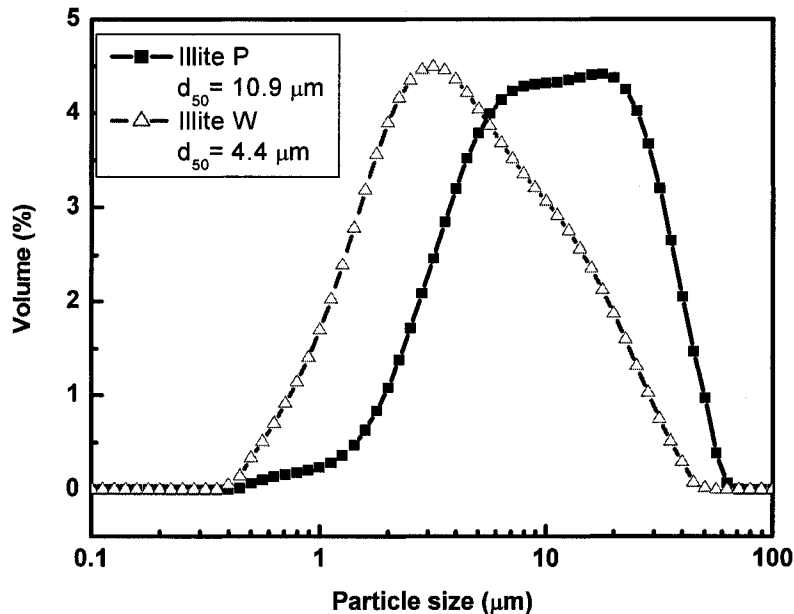


Figure 3.1. Particle size distributions of two illite clays.

ball mill for five hours and a 44μm sieve was used to remove the coarse solids. The fine solids were used for all the tests and characterizations in this study. The particle size distributions of these fines were measured by a Mastersizer 2000 and the results are shown in Figure 3.1. Reagent grade  $\text{CaCl}_2 \cdot 2\text{H}_2\text{O}$  (Fisher) and  $\text{MgCl}_2 \cdot 6\text{H}_2\text{O}$  (BDH) were used as the source of calcium and magnesium ions and reagent grade NaOH (Fisher) was used as pH modifier. De-ionized water with a resistivity of 18.2 MΩ cm, prepared with Elix 5 followed by a Millipore ultra pure water system, was used in all the experiments unless otherwise specified. The Aurora process water contained 28ppm  $\text{Ca}^{2+}$  and 16ppm  $\text{Mg}^{2+}$  and its pH was about 8.2.

### 3.2.2 Experimental set-up

A modified Denver flotation cell was used in the bitumen flotation tests. In order to control the temperature, a water jacket connected to a thermal-controlled water bath was attached to a 1 litre stainless steel flotation cell (Figure 3.2a). Air was introduced into the oil sands slurry through the hollow shaft. A bench valve was used to adjust the flow rate. The rotating shaft could be controlled between 0 to 3000 rpm. A photograph of the Denver flotation cell is shown in Figure 3.2b.

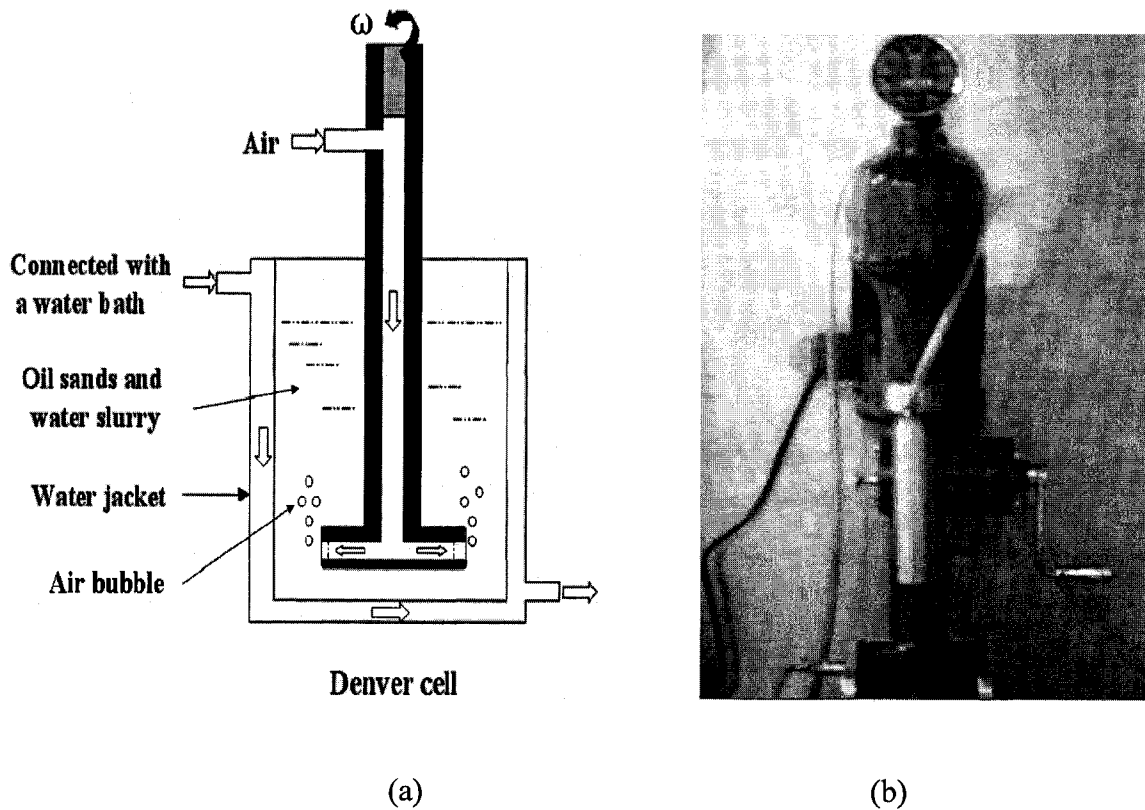


Figure 3.2. (a) Schematic diagram of the flotation process, and (b) photograph of the Denver flotation cell.

### 3.2.3 Procedures

#### *Bitumen flotation tests*

For baseline tests, 300 gram of F11B oil sands ore and 950 mL of de-ionized water whose pH was adjusted to about 8.5 at a given temperature were placed in the cell. Temperature of the cell was maintained at the given value. After the slurry was conditioned at 1500 rpm for 5 minutes, air was introduced at a rate of 150 mL/min. Bitumen froth was collected as a function of time for a period of 18 minutes. For the first minute, the froth was collected in a jar. Froth collected between 1 and 3 minutes was placed in separate jar. Similarly, froth collection continued over specified period intervals into separate jars. All the jars were put aside for assay. The final temperature and pH of the tailings were recorded. Four 50 mL centrifuge tubes were filled with the tailings slurry and centrifuged at 15,000g for 30 minutes in an Allegra 64 Centrifuge. The supernatants were set aside for water analysis and zeta potential measurement. All the other flotation tests were performed using a similar procedure with the exception that clays and/or magnesium or calcium ions were added into the slurry prior to conditioning. Each test was repeated several times and the average are reported. The operation error was within 4%. Unless otherwise specified, de-ionized water was used in all the flotation tests.

#### *Bitumen-water-solid analysis*

A Dean Stark method (Bulmer and Star, 1979) was used to obtain the content of bitumen, solids and water in the oil sands ore sample and the froth. The method is based on: (1)

high vapor pressure of water and toluene relative to bitumen; (2) solubility of bitumen in toluene; and (3) insolubility of water in toluene to separate bitumen, solids and water.

Details on the Dean Stark method are included in Appendix A. By separating bitumen and water from the solids, the mass percent of each component was determined by:

$$\% \text{ bitumen} = \frac{\text{bitumen collected}}{\text{sample weight}} \times 100$$

$$\% \text{ solids} = \frac{\text{solids collected}}{\text{sample weight}} \times 100$$

$$\% \text{ water} = \frac{\text{water collected}}{\text{sample weight}} \times 100$$

The bitumen recovery was defined as the mass ratio of bitumen in total froth to bitumen in oil sands ore feed sample, i.e.

$$\text{Bitumen recovery (\%)} = \frac{\text{bitumen in froth}}{\text{bitumen in oil sands ore feed sample}} \times 100$$

#### *Tailings water analysis*

SpectrAA (250F) was used to analyze the divalent cation concentrations in the aqueous tailings of all the flotation tests. The detection limit of SpectrAA was 0.1ppm for divalent cations. The AA analysis on the baseline tests showed that the concentrations of calcium and magnesium ions were 0.2 and 0.4ppm, respectively, confirming that the F11B oil sands sample contained a negligible amount of soluble divalent cations.

### 3.3 Results and discussion

#### 3.3.1 Effects of divalent cations and illite clays

Figure 3.3 shows bitumen flotation recovery at 25°C as a function of flotation time. The addition of 24ppm (equivalent to 1 mM) magnesium ions and/or illite P clay at 0.5% by weight of total oil sands ore had little effect on bitumen flotation kinetics or recovery.

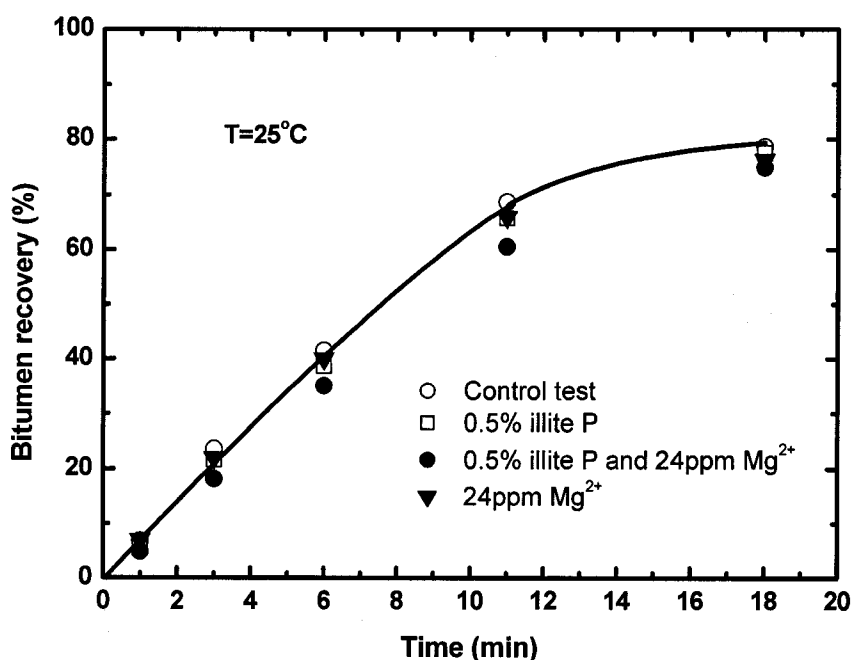


Figure 3.3. Effect of magnesium ions and illite P on bitumen flotation kinetics using de-ionized water initially adjusted to pH 8.5 at 25°C.

(Since the effects of calcium and magnesium ions were very similar, only one set of data (magnesium) was plotted to preserve data clarity. The corresponding plot for calcium ions is presented in Appendix B, see Figure B.1).

To explore whether the amount of illite P clay is a factor affecting bitumen recovery, flotation tests were performed with an increased amount up to 5%. The results summarized in Figure 3.4 show that for the system without divalent cations addition, total bitumen recovery decreased with an increased amount of illite P for both extraction temperatures.

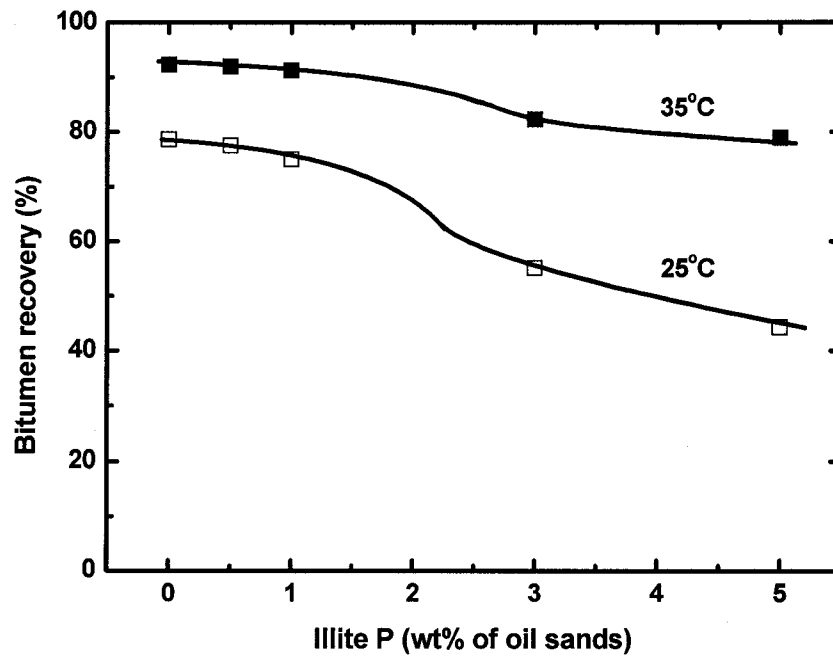


Figure 3.4. Effect of increasing illite P on bitumen flotation recovery using de-ionized water initially adjusted to pH 8.5.

The pH of the produced tailings water as a function of the amount of illite P is plotted in Figure 3.5. The results in this figure show that the pH also decreased with an increased amount of added illite P. This is due to the acidity of illite clay (Bichard, 1987; Du et al., 1996). For the flotation systems containing 1mM calcium or magnesium ions, the bitumen recoveries experienced a sharp reduction when the clay level exceeded a certain amount at room temperature, as shown in Figure 3.6. It is evident that calcium and

magnesium ions had the same effect on depressing bitumen recovery based on molar equivalent when they were co-presented with a certain amount of illite P.

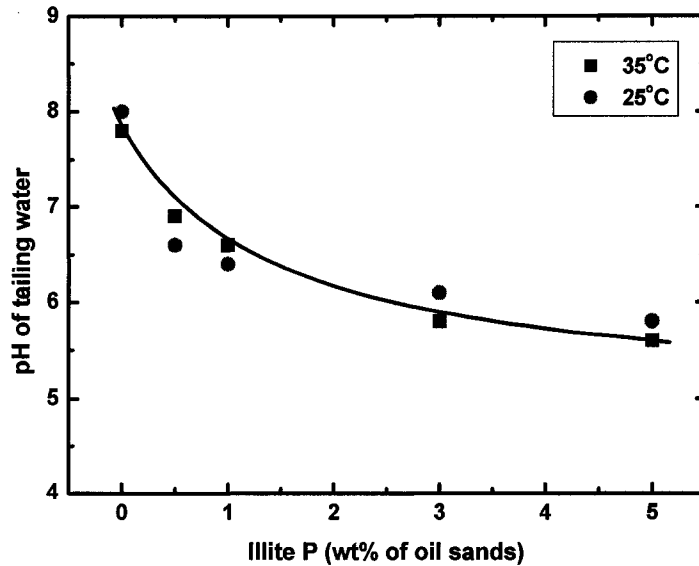


Figure 3.5. Effect of illite P on pH of the tailings water from the flotation systems without addition of divalent cations.

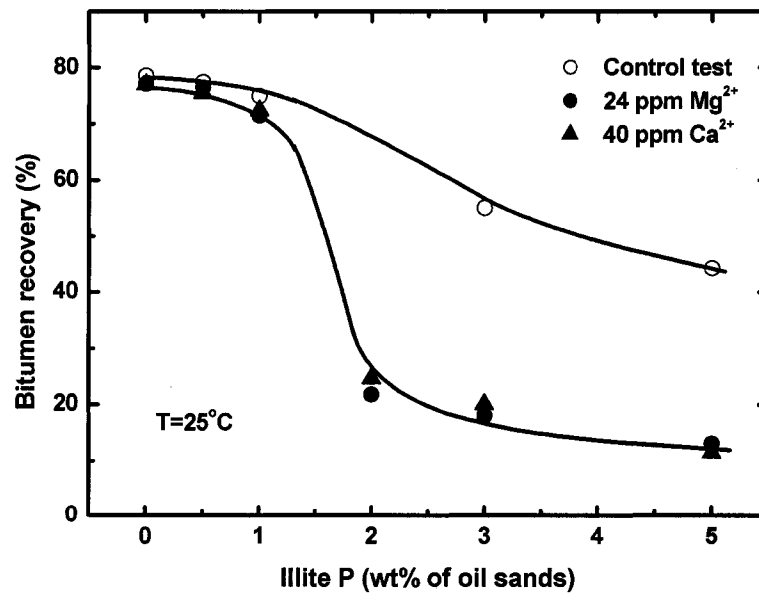


Figure 3.6. Synergetic effect of divalent cations and illite P on bitumen recovery at 25°C using de-ionized water initially adjusted to pH 8.5.

The pH of the produced tailings water was also plotted as a function of the amount of illite P (Figure 3.7). It shows a larger pH drop than that for flotation systems without the addition of magnesium ions.

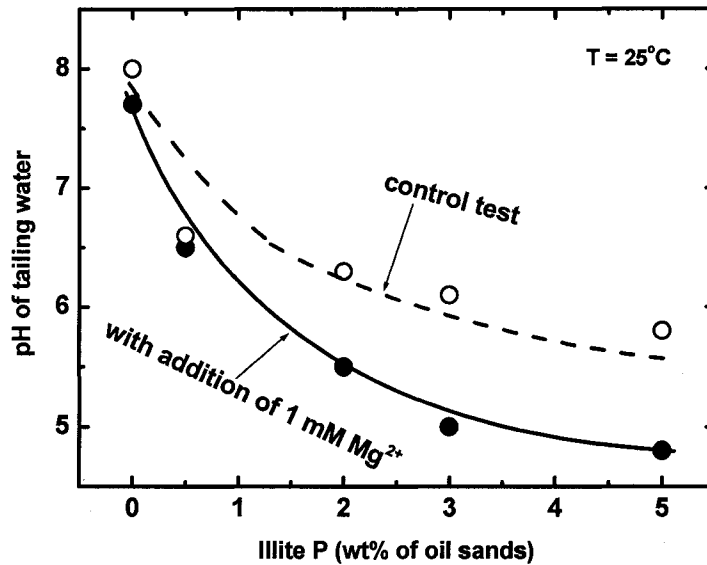


Figure 3.7. Effect of illite P on the pH of the tailing water from the flotation systems with 1 mM magnesium ions addition at 25°C using de-ionized water initially adjusted to pH 8.5.

(The corresponding plot for calcium ions is included in Appendix B, see Figure B.2).

Compared with illite P, the combination of 5% of illite W and 1mM calcium or magnesium ions interfered with the bitumen recovery to a much less extent for both temperatures as shown in Figures 3.8 and 3.9. For illite W, similar pH changes were observed as with illite P for both processing temperatures. For example, at room temperature the pH of the tailing water was about 6.0 for the flotation system with the addition of 5% illite W only and the pH was 5.0 for the system with the co-addition of

5% illite W and 24ppm magnesium ions. For the case of illite P, the corresponding pHs were about 5.8 and 4.8, respectively.

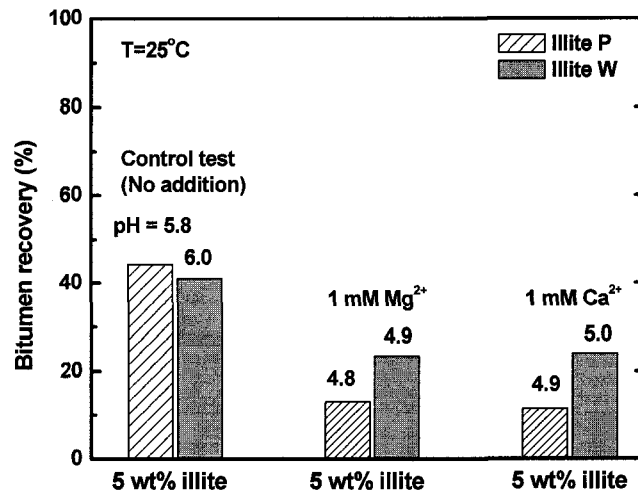


Figure 3.8. Comparison of the synergetic effects of divalent cations and illite clays on bitumen recovery at 25°C using de-ionized water initially adjusted to pH 8.5.

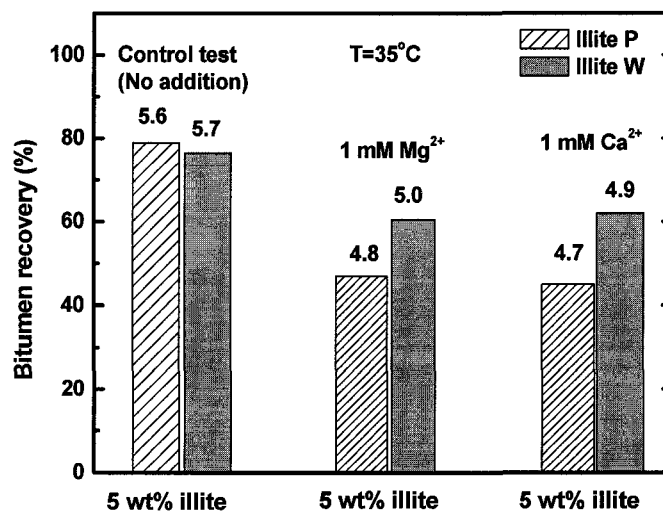


Figure 3.9. Comparison of the synergetic effects of divalent cations and illite clays on bitumen recovery at 35°C using de-ionized water initially adjusted to pH 8.5.

It is well known that water based extraction processes work better in an alkaline aqueous medium (Clark and Pasternack, 1932; Sanford, 1983; Bichard, 1987; Liu et al., 2004, 2005). In acidic aqueous medium, bitumen liberation from the sand grains is difficult and low bitumen recovery would be expected (Dai and Chung, 1995). As a result, the negative effect of illite clays on bitumen recovery might arise from the acidity of process medium impacted by the addition of these clays. The more detrimental synergetic effect of illite clay and magnesium ions on bitumen recovery is attributed to incomplete bitumen liberation and slime coating of illite on the liberated bitumen. To confirm whether pH is a key factor in bitumen recovery, flotation tests were conducted at a controlled pH of 8.5 by adding NaOH solution into the flotation slurry. Since the adverse effect on bitumen recovery was much evident for illite P than that for illite W, the tests were performed using illite P. As shown in Figures 3.10 and 3.11, for the flotation slurry containing illite P and/or magnesium ions, the bitumen recovery at pH 8.5 was increased greatly for both extraction temperatures. This observation on the effect of NaOH is in line with previous studies (Clark, 1929; Sanford, 1983; Bichard, 1987; Dai and Chung, 1996b).

To detect changes in the concentration of divalent cations in the flotation systems, AA analyses were conducted on the produced solid-free tailings water. The measured divalent cation concentrations were plotted as a function of the amount of illite P under different conditions (Figure 3.12). The figure shows that divalent cation concentrations first experienced a sharp decrease and then decreased more slowly with an increased amount of illite P addition to flotation tests without pH control. For pH controlled flotation tests,

the divalent cation concentrations were close to zero. At pH 8.5, the calcium and magnesium ions could not be precipitated as hydroxide salts (Dai and Chung, 1992). Therefore, the decrease of divalent cations concentration might be due to the reaction or adsorption with surfactants and illite clays at pH 8.5 (Smith and Schramm, 1992).

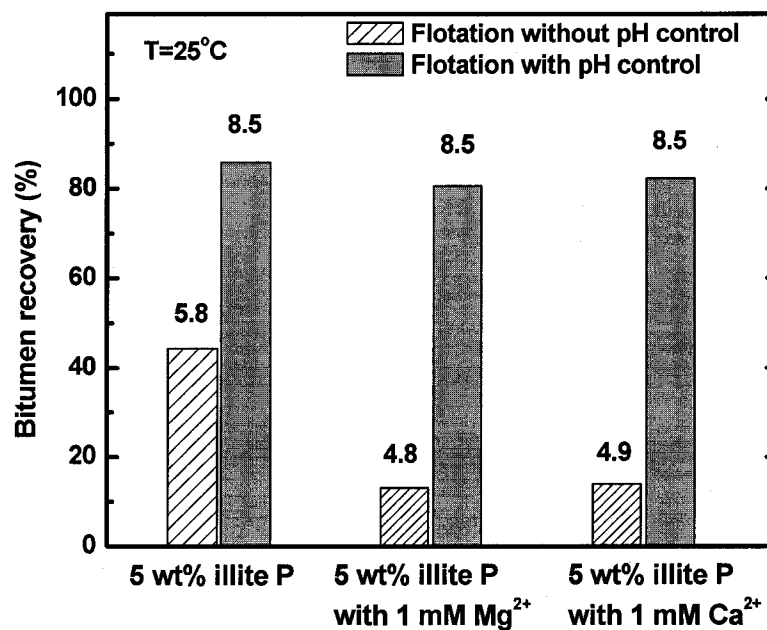


Figure 3.10. Effect of pH on bitumen recovery using de-ionized water at 25°C.

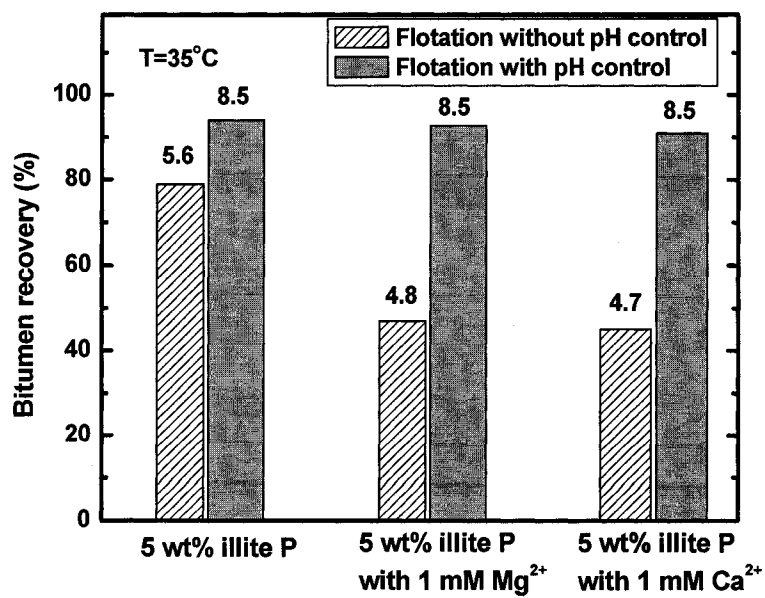


Figure 3.11. Effect of pH on bitumen recovery using de-ionized water at 35°C.

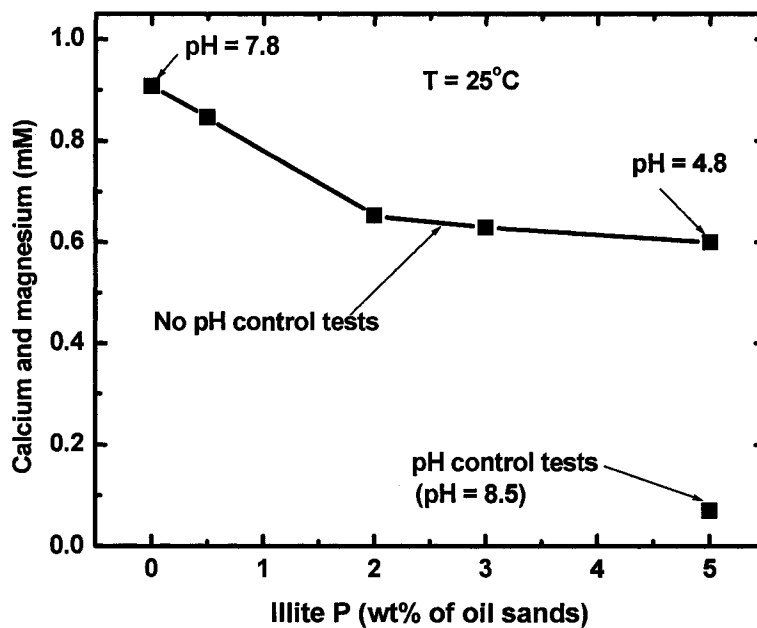


Figure 3.12. Divalent cation concentrations of tailing water as a function of the amount of illite P addition in the flotation systems with the co-addition of 1mM MgCl<sub>2</sub> at 25°C.

### 3.3.2 Effect of temperature

It has been found that in the range of 25-50°C, temperature has great effect on bitumen recovery (Bichard, 1987; Dai and Chung, 1995; Schramm et al. 2003; Ding et al., 2004; Zhou et al., 2004; Long et al., 2004). As shown in Figure 3.13, flotation kinetics was greatly improved with increasing temperature, i.e. a higher bitumen recovery rate at high flotation temperature. For example, in the absence of added clay, an increase in processing temperature from 25 to 35°C caused a recovery increase from about 80% to 90%.

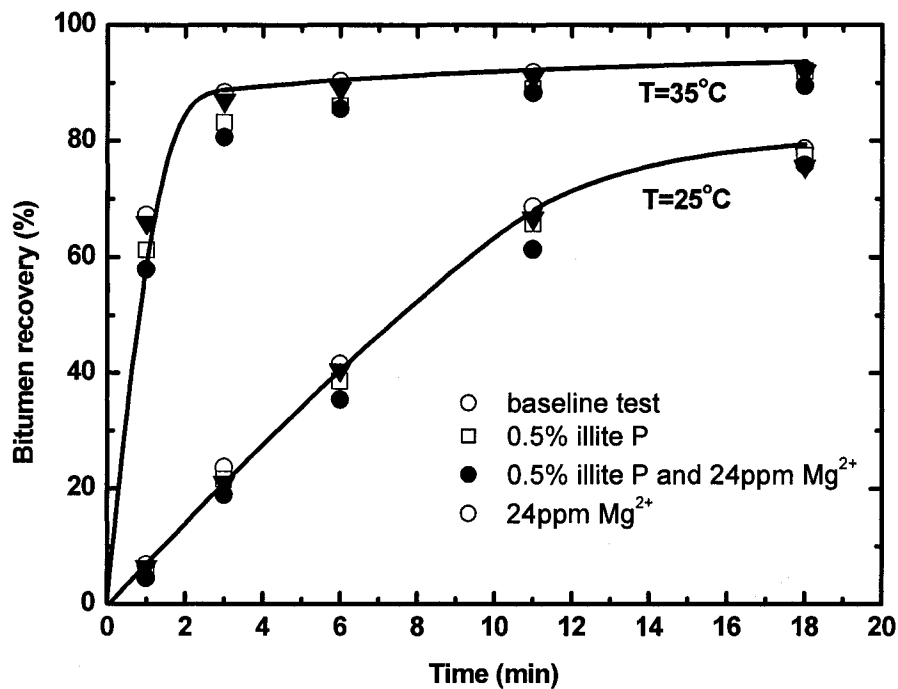


Figure 3.13. Effect of temperature on bitumen flotation kinetics using de-ionized water initially adjusted to pH 8.5.

To further explore the effect of temperature on bitumen recovery, flotation tests were conducted with increased amount of clay addition at 35°C. The results are shown in Figure 3.14 together with the corresponding data at 25°C. It is evident that increasing temperature did increase the bitumen recovery greatly even at the worst condition, i.e. co-addition of 5% illite P and 1 mM divalent cations. When the temperature was further increased to 50°C, only a marginal further improvement in bitumen recovery was observed for a flotation system with co-addition of 5% illite P and 1mM MgCl<sub>2</sub>. This observation is consistent with Bichard's work dealing with the effect of temperature on bitumen recovery (1987).

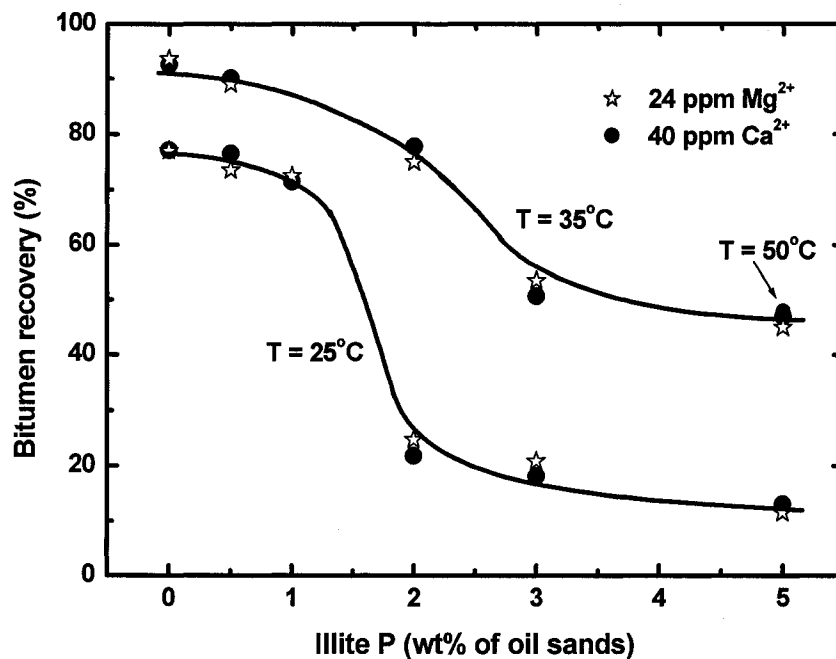


Figure 3.14. Effect of temperature on bitumen recovery using de-ionized water with an initially adjusted pH of 8.5

The pHs of the tailing water are plotted as a function of the amount of illite P as shown in Figure 3.15. It shows that pHs changed little when temperature was increased from 25 to 35°C. As shown in Figure 3.16, divalent cations concentration in the tailing water also changed little with temperature.

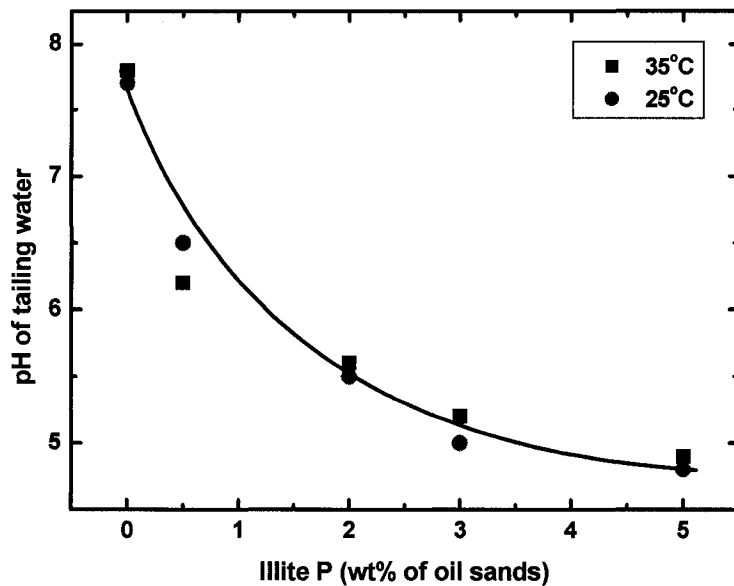


Figure 3.15. Effect of illite P addition on the pH of the tailing water from the flotation systems with the addition of 1 mM magnesium ions at 25°C and 35°C using de-ionized water initially adjusted to pH 8.5. (The corresponding plot for calcium ions is included in Appendix B, see Figure B.2).

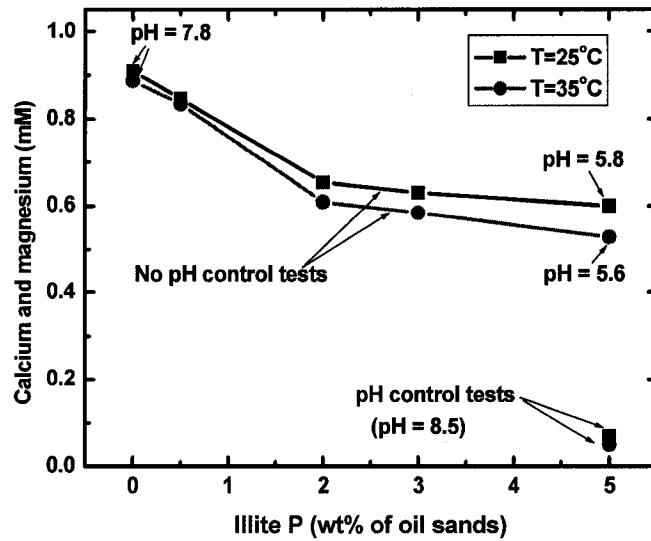


Figure 3.16. Divalent cation concentrations of tailing water as a function of the amount of illite P addition to the flotation systems with the co-addition of 1mM  $MgCl_2$ .  
(The corresponding plot for calcium ions is included in Appendix B, see Figure B.3).

### 3.3.3 Effect of process aids

Clark (1932) reported that strong inorganic bases were good process aids in the hot water extraction process. Sanford and Seyer (1979) further explored the effect of NaOH and demonstrated that NaOH can neutralize organic acids in bitumen to generate surfactants, which have been proven to be active species during processing. To investigate whether the commonly used process aids such as NaOH and  $NaHCO_3$  can resolve the slime coating problem and improve bitumen recovery, some flotation tests were repeated with the addition of a given amount of NaOH or  $NaHCO_3$  to the slurry water. As shown in Figure 3.17, for systems containing oil sand only, the bitumen recovery experienced a maximum at about 0.03wt % of NaOH addition (based on total oil sands feed sample)

and then decreased. This decrease was likely due to bitumen emulsification. For systems containing oil sands, 5wt% illite P and 24ppm of magnesium ions, the bitumen recovery increased sharply and then decreased slightly after experiencing a maximum at about 0.06wt % addition of NaOH. Sanford (1983) made the similar observation on the effect of NaOH on bitumen recovery, i.e. there is an optimum dosage of NaOH for maximum bitumen recovery and the optimum dosage increases with an increased fines content in the oil sands ore. The effect of  $\text{NaHCO}_3$  on bitumen recovery is shown in Figure 3.18. At room temperature, the addition of 1000ppm  $\text{NaHCO}_3$  with respect to water (0.33wt% of total oil sands feed sample) oil increased bitumen recovery from 13.1% to 64.4%. The pH of the tailings water was also increased from 4.9 to 8.6.

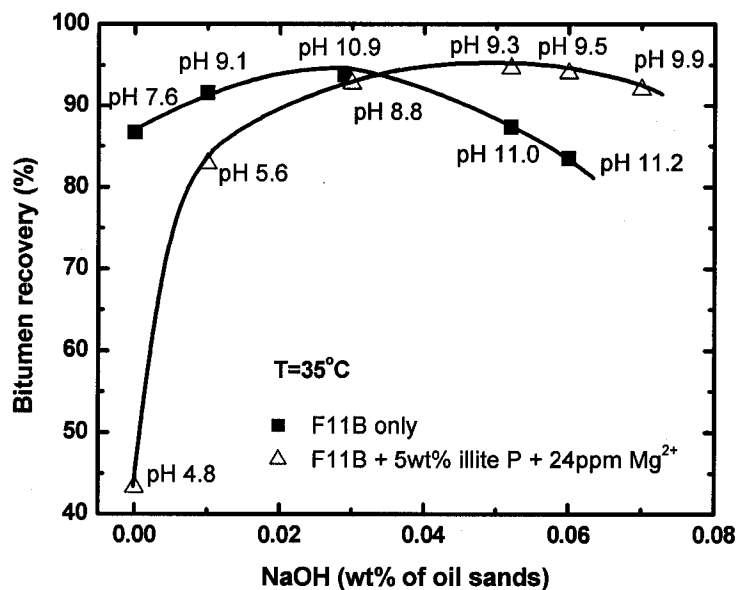


Figure 3.17. Effect of NaOH addition on bitumen recovery for the flotation systems with the co-addition of 1mM  $\text{MgCl}_2$  and 5 wt% illite P using de-ionized water at 35°C.

(The corresponding plot for calcium ions is included in Appendix B, see Figure B.4).

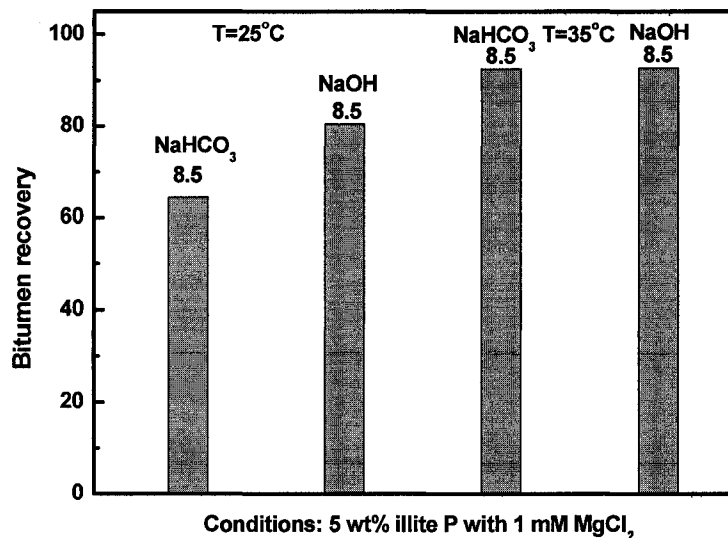


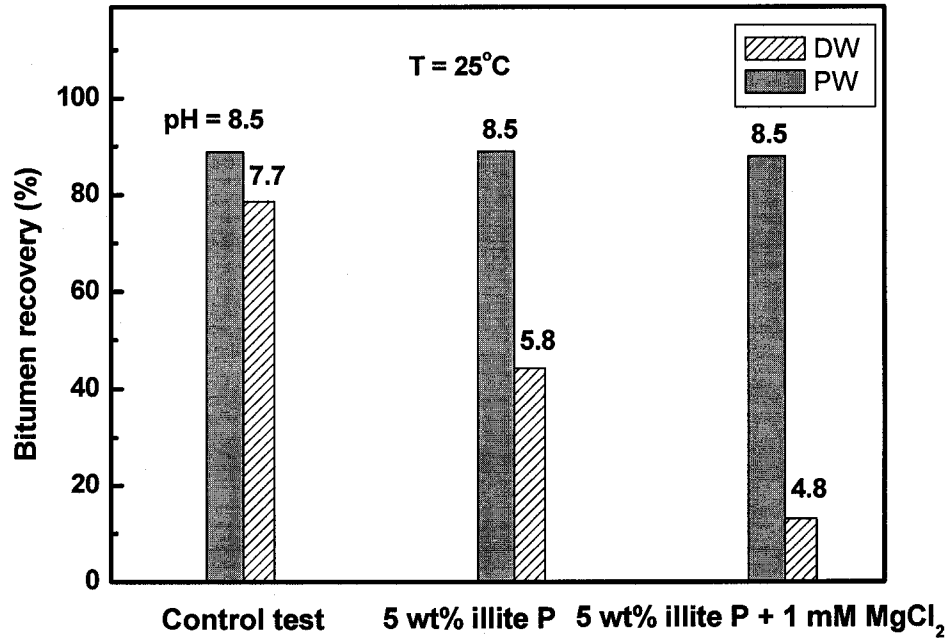
Figure 3.18. Effect of NaOH (0.03wt% of oil sands) and NaHCO<sub>3</sub> (0.33wt% of oil sands or 1000ppm based on water) addition on bitumen recovery for the flotation systems with the co-addition of 1mM MgCl<sub>2</sub> and 5 wt% illite P using de-ionized water.

(The corresponding plot for calcium ions is included in Appendix B, see Figure B.5).

### 3.3.4 Effect of process water

As mentioned above, all the flotation tests were performed using de-ionized water to avoid any complications in interpreting the results due to the presence of chemical species in the process water. To link the study using the model systems with the real world practice, Aurora process water was also used in a set of flotation tests at room temperature. The control test was the test for a system containing oil sands only (i.e. no addition of clay or divalent cations). As shown in Figure 3.19, the bitumen recovery was

78.6% for baseline test in de-ionized water, in contrast to 89% in Aurora process water.



Control test: F11B oil sands only; DW: de-ionized water; PW: process water

Figure 3.19. Comparison of bitumen recovery in Aurora process water with that in de-ionized water.

(The corresponding plot for calcium ions is included in Appendix B, see Figure B.6).

With the addition of 5 wt% illite P, the bitumen recovery dropped to 44.3%. When 24ppm magnesium was added together with 5 wt% illite P, the bitumen recovery dropped drastically to 13.1%. In contrast, the bitumen recoveries in process water remained unchanged for the above-mentioned three conditions and the pHs of tailing water also had little change. In other words, with the use of process water, no negative effects on bitumen recovery due to the addition of 5 wt% illite P and 24ppm magnesium ions were

found, clearly illustrating the role of chemical species in process water in eliminating negative impact of clays and fines.

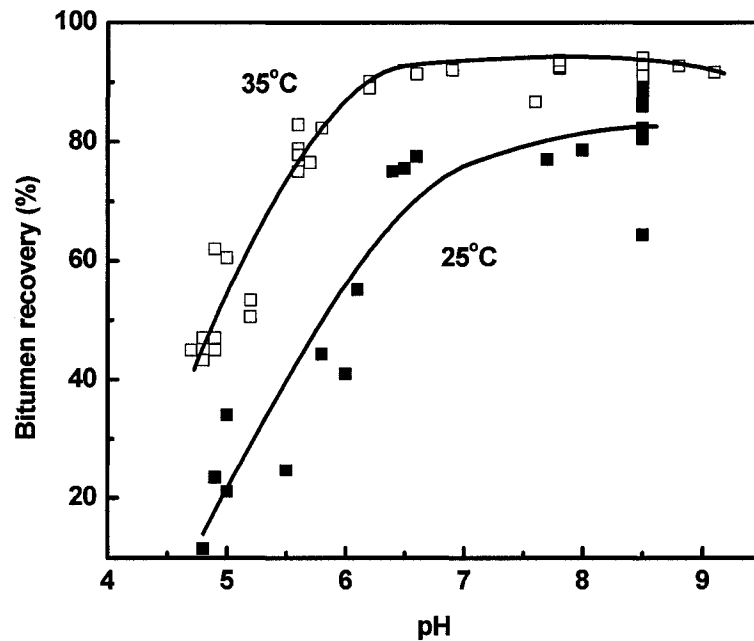


Figure 3.20 Bitumen recovery versus pH of tailing water.

Summarizing all the results in a single graph, Figure 3.20 shows that for a given temperature, the bitumen recovery correlates well with processing pH.

### 3.4 Conclusions

1. Using de-ionized water the detrimental effects of illite clays on bitumen recovery was due to the clays' acidity, and the adverse effects could be reconciled by the addition of process aids such NaOH and NaHCO<sub>3</sub>.

2. The presence of 1mM calcium or magnesium ions alone had little effect on bitumen recovery. But when co-added with illite clays, both had the same adverse effect on molar equivalent when tests were performed in de-ionized water.
3. The synergetic effect of divalent cations and illite P was worse than that with illite W.
4. Temperature mitigated the adverse effect on bitumen recovery due to the addition of illite clays and divalent cations.
5. Process aids such as NaOH and NaHCO<sub>3</sub> had a great effect on bitumen recovery while using de-ionized water.
6. Co-addition of divalent cations and illite clays did not have any negative impact on bitumen recovery when tests were performed in Aurora process water rather than in de-ionized water.

## 4.0 ZETA POTENTIAL DISTRIBUTION MEASUREMENTS

The main objective of this chapter is to investigate the mechanisms on the observed effect of divalent cations, temperature and process aids on bitumen recovery. Zeta potential distribution measurements were performed to investigate the interactions between bitumen and illite clays.

### 4.1 Zeta potential ( $\zeta$ )

When a colloidal particle is immersed in an aqueous solution, a net charge is usually developed at the interface by any of several mechanisms. These mechanisms include the dissociation of ionogenic groups on the particle surface, the differential adsorption from solution of ions of different charges into the surface region, and for clays, ion exchange mechanisms (Hunter, 2001). The development of the net charge at the particle surface affects the distribution of ions in the neighboring interfacial region and an electrical double layer is formed in the region of the particle-liquid interface. When subjected to an electric field as in electrophoresis, each particle and its most closely associated ions move through the solution as a unit. There is an imaginary surface between the unit and the surrounding medium at which the non-slip fluid flow boundary condition breaks. This surface is called the shear plane (or slipping plane), as shown in Figure 4.1 (Masliyah, 1994). The zeta potential is the electric potential at the shear plane with the potential of the bulk solution as a reference (usually assumed to be zero). Almost all particles in contact with a liquid acquire an electric charge on their surfaces. The zeta potential is an important and useful indicator of this charge and can be used to predict the stability of

colloidal suspensions or emulsions. For hydrophobic colloids, the greater is the zeta potential, the more likely the suspension is to be stable due to mutual electrostatic repulsion that overcomes the natural tendency to aggregate or coagulate. Therefore, the zeta potential is an important parameter characterizing colloidal dispersions and aggregation processes. The zeta potential of a particle is usually determined by electrophoretic mobility measurements.

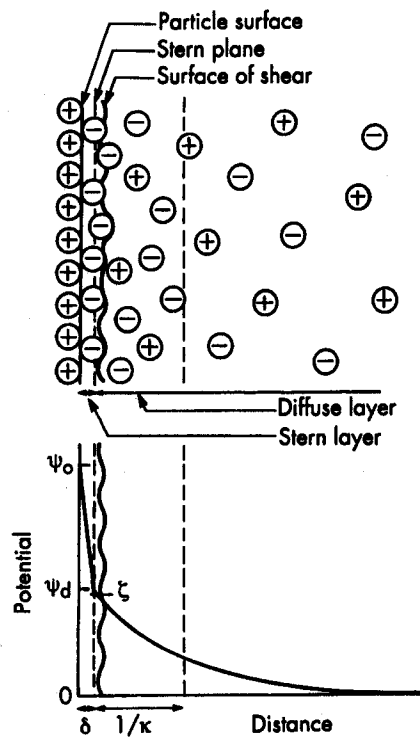


Figure 4.1. Schematic representation of the electric double layer according to Stern's model.

#### 4.2 Zeta potential distribution measurements

This novel technique was developed by Liu et al. (2002) to investigate the interactions between bitumen and clay in an aqueous solution. For a single component suspension, a single peak zeta potential distribution was obtained under a given solution condition. In the case of a two-component mixture, the measured zeta potential distributions showed either one or two distribution peaks, depending on the chemical make-up of the aqueous solution and the type/amount of clays present. The interpretation of the results from zeta potential distribution measurements is illustrated in Figure 4.2. Using this method, Liu et al. (2002) found a stronger interaction between bitumen and montmorillonite than between bitumen and kaolinite when 40ppm of calcium ions was present in a de-ionized aqueous solution. This was in excellent agreement with the flotation results reported by Kasongo et al. (2000). Xu et al. (2003) conducted an electrokinetic study of clay interactions in coal flotation. Their study further demonstrated that zeta potential distribution measurements are a powerful tool for studying slime coating phenomena and are useful in diagnosing flotation systems. Therefore, this technique was used in the current study to investigate the effect of divalent cations, temperature and process aids on the interactions between bitumen and clay.

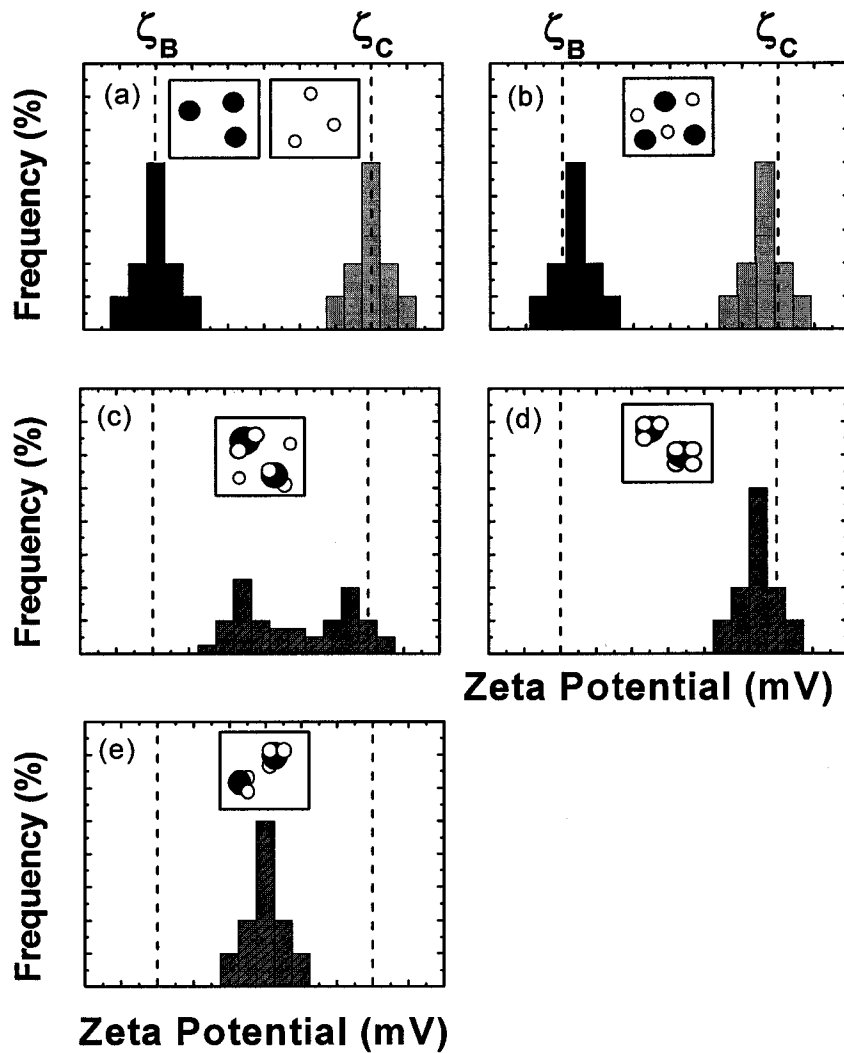


Figure 4.2. Schematic zeta potential distributions for a binary colloidal system that can be interpreted for particle interactions.

In this figure, the black and white circles represent bitumen droplets and clay particles, respectively. (a) Superimposed zeta potential distribution of the two components measured separately; (b) a binary mixture without attraction; (c) weak attraction (bitumen droplets partially covered with a substantial amount of clay particles unattached); (d) strong attraction (bitumen droplets fully covered by clay particles); (e) strong attraction (bitumen droplets partially covered with insufficient amount of clay particles).

## 4.3 Materials and Experimental Procedures

### *Materials*

Bitumen from vacuum distillate feed stock and high grade north mine esturine ore (F11B) were provided by Syncrude Canada Ltd. and used in the zeta potential measurements. Two batches of fine illite clays prepared using procedures described in Chapter 3 were used in all the measurements. Ultra-high purity KCl (>99.999%, Aldrich) was used as a supporting electrolyte while reagent grade  $\text{CaCl}_2 \cdot 2\text{H}_2\text{O}$  (Fisher) and  $\text{MgCl}_2 \cdot 6\text{H}_2\text{O}$  (BDH) were used as the source of calcium and magnesium ions. Reagent grade NaOH (Fisher) was used as pH modifier. De-ionized water as described in Chapter 3 was used in all the measurements, unless otherwise specified.

### *Sample Preparation*

For zeta potential measurements, a bitumen in water emulsion was prepared by sonication of about 1g of bitumen in 100 ml of 1mM KCl solution using a 550 Sonic Dismembrator (Fisher) for 18 min. The clay suspension was prepared using a similar procedure but with an Ultrasonic bath (Fisher) instead of the sonic dismembrator. Each sample was diluted before zeta potential distribution measurements as the instrument required relatively dilute suspension/emulsions. To prepare a bitumen-clay suspension, small amounts of prepared bitumen emulsion and clay suspension were diluted and mixed at a specified ratio and then conditioned in an ultrasonic bath (Fisher) for 18 min before the zeta potential distribution measurements.

### *Zeta Potential Measurement*

Zeta potential measurements were carried out with a Zetaphoremeter IV<sup>TM</sup> (CAD), as shown in Figure 4.4. It was equipped with an electrophoresis chamber consisting of two electrode compartments and a connecting rectangular cell, a laser illuminator, and a digital video image capture and viewing system. By alternating the polarity of the electric field, the computerized operating system can capture the image of the moving particles in the stationary plane under a known electric field and then provide a histogram of electrophoretic mobilities using a built-in image processing software. The data collected are converted to a zeta potential distribution as desired. The electrophoretic mobility,  $U_E$ , and corresponding zeta potential value,  $\zeta$ , are related through Henry's equation (4-1).

$$\zeta = \frac{3\mu}{2\varepsilon\varepsilon_0 f(\kappa a)} U_E \quad (4-1)$$

$$f(\kappa a) = \begin{cases} 1.5 & \text{if large sphere } (\kappa a \rightarrow \infty) \text{ Smoluchowski's equation} \\ 1.0 & \text{if small sphere } (\kappa a \rightarrow 0) \text{ Huckel's equation} \end{cases}$$

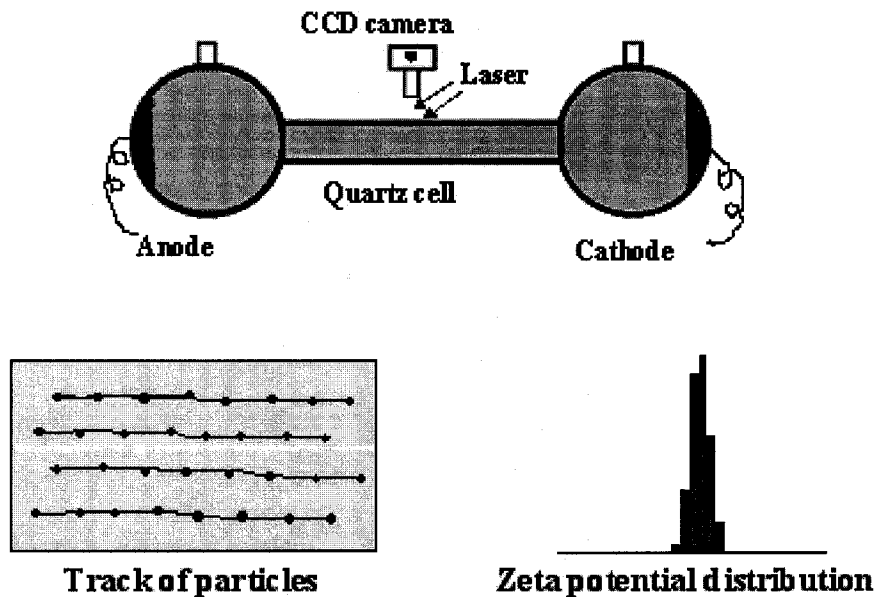


Figure 4.3. Schematic of zeta potential measurements.

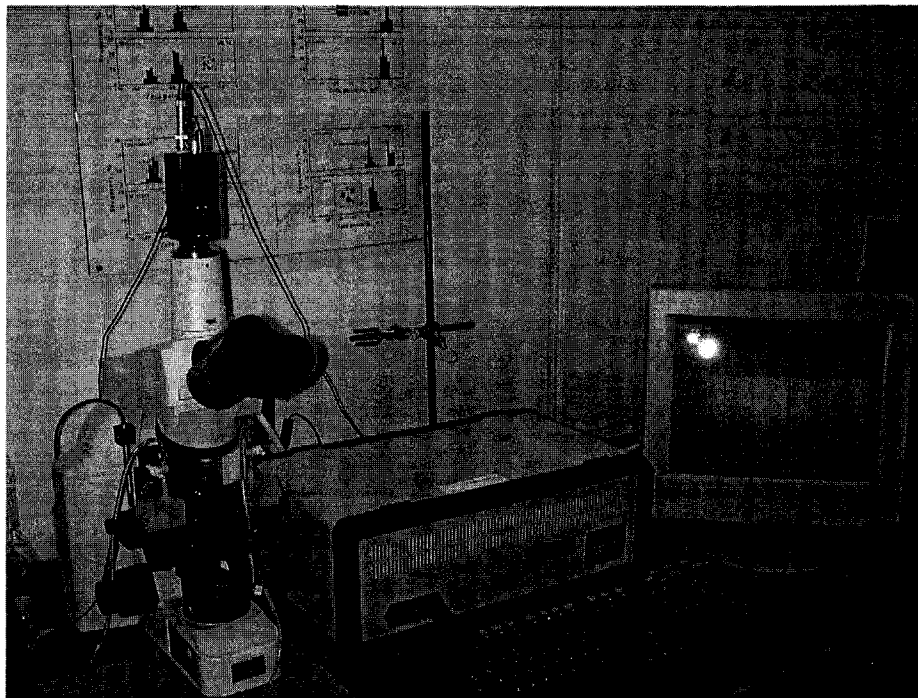


Figure 4.4. Photograph of Zetaphoremeter IV™ (CAD).

All the measurements were performed with 1mM KCl solution as the background electrolyte. When the instrument was operated at room temperature, the ambient temperature was maintained at  $25 \pm 0.1$  °C. When it was operated at 35 °C, the instrument and all the solutions were located in a thermo-stated room maintained at  $35 \pm 0.1$  °C for 24 hours prior to any measurement. This was done to avoid interference from convection currents and non-uniform expansion of the instrument. In order to ensure that the instrument was still in good condition after measurements at the higher temperature, the room was cooled slowly for 24 hours. Repeat measurements were then performed at room temperature and the results were compared with those obtained previously. Each test was repeated several times and the average was reported. The measurement error was generally less than 5%.

## 4.4 Results and discussion

### 4.4.1 Effects of divalent cations

Since the effects of 1mM calcium and 1mM magnesium were very similar for all the measurements of the zeta potentials and the zeta potential distributions, only the results for one set of data (magnesium) are reported in this chapter. The corresponding plots for calcium ions are presented in Appendix C. The effect of magnesium ions on the zeta potentials of illite clays is shown in Figure 4.5. In the absence of magnesium ions (open symbols), the average zeta potentials for both clays decreased sharply with increasing pH in the range of 2 to 7, whereas the values decreased only slightly in the range of 7 to 10. Hussain et al. (1996) reported very similar results on a Turkish illite clay. In a 1mM KCl solution containing 1mM  $MgCl_2$ , the zeta potential becomes much less negative and experiences only a slight decrease with pH as shown by solid symbols in Figure 4.6. The decrease of zeta potentials could be partially accounted for by the electrical double layer compression due to the addition of magnesium ions. Both types of the illite clays exhibited a very similar response of zeta potential values to solution pH and magnesium ions addition. The zeta potential of bitumen also decreased when magnesium ions were present in the system (Figure 4.6). Liu et al. (2002) reported similar results.

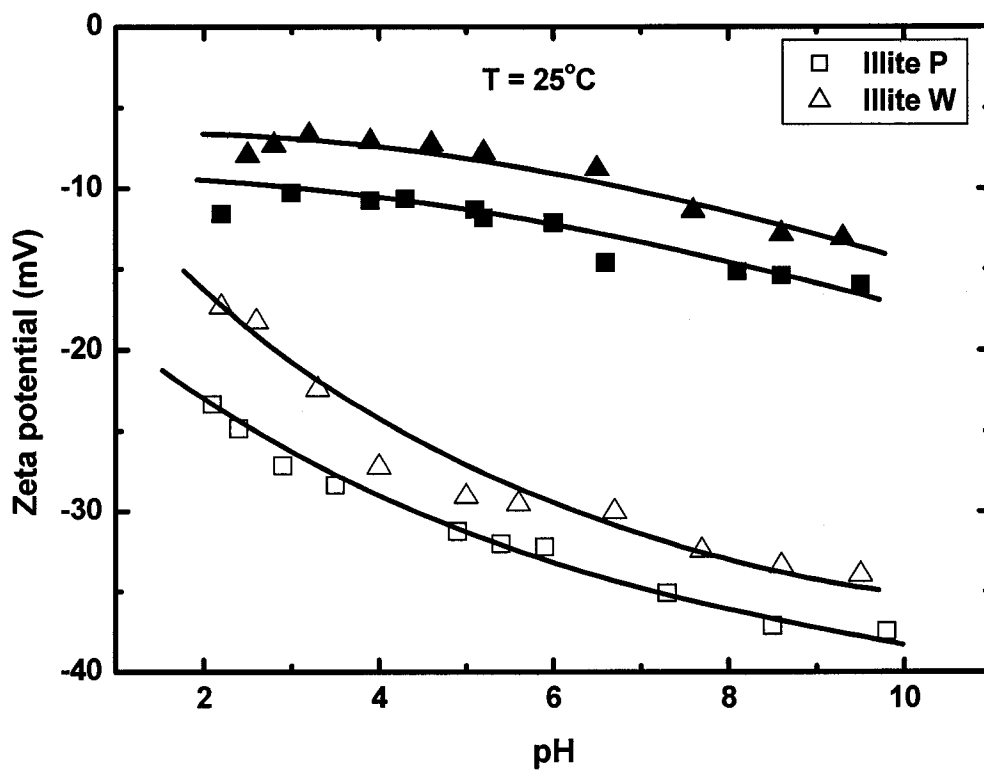


Figure 4.5. Effect of magnesium ions on the average zeta potentials of illite clays at 25°C.

Open symbols: in 1mM KCl solutions; Solid symbols: in 1mM KCl solutions containing 1mM MgCl<sub>2</sub>.

(The corresponding plot for calcium ions is included in Appendix C, see Figure C.1).

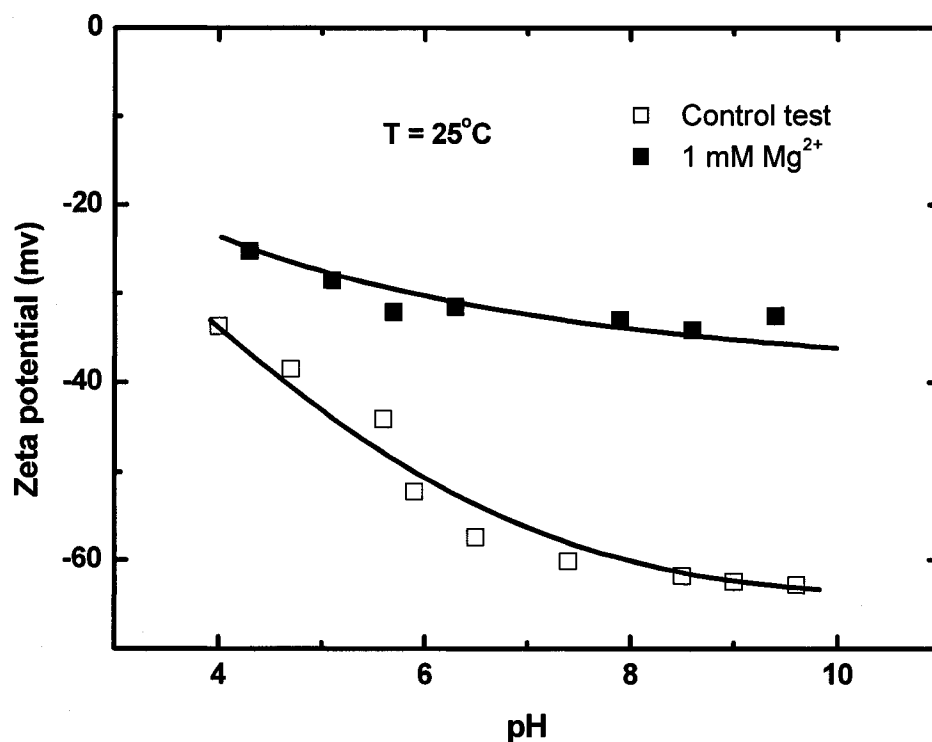


Figure 4.6. Effect of magnesium ions on the average zeta potential of bitumen in 1mM KCl solutions at 25°C. (The corresponding plot for calcium ions is included in Appendix C, see Figure C.2).

Since the pH of industrial operations is controlled around 8.5, zeta potential distribution measurements were conducted at pH 8.5 to investigate the effect of divalent cations, temperature and process aids on the interactions between bitumen and clay. The zeta potential distributions of emulsified bitumen and illite W measured individually in a 1mM KCl solutions at pH 8.5 are shown in Figure 4.7a. The peak positions for bitumen and illite W were at -62 and -33 mV, respectively. The distribution for mixtures with a clay to bitumen mass ratio of 1:1 had two peaks centered at -54 and -35 mV as shown in

Figure 4.7b. The peak at  $-35$  mV was almost the same as the value measured with illite W clay suspension alone. But the peak at  $-62$  mV previously measured for the bitumen emulsion shifted to  $-54$  mV, which was in the direction of the distribution peak of illite W clay. According to the interpretation illustrated in Figure 4.2, the observed shift suggests a weak attraction between bitumen droplets and illite W clay particles at a 1:1 mass ratio in 1mM KCl solutions at pH 8.5, as schematically shown in Figure 4.2c. For illite P clays, the same measurements were carried out and the results shown in Figure 4.8 also suggests a weak attraction between bitumen and illite P clay under the same conditions.

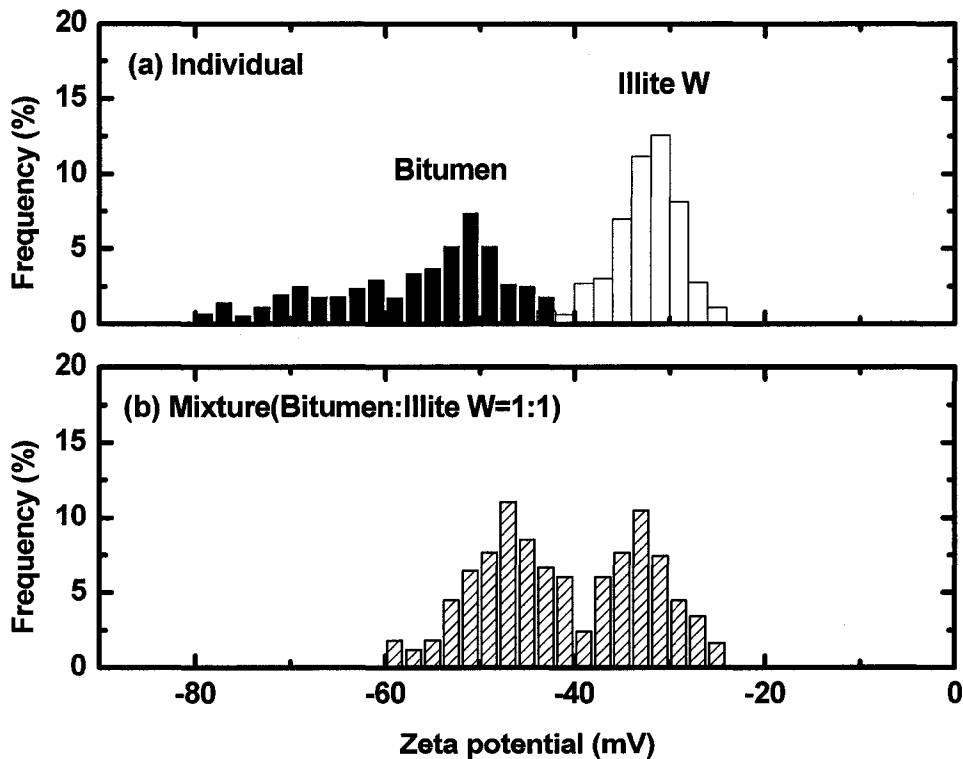


Figure 4.7. Zeta potential distributions for (a) individual bitumen emulsion and illite W suspension and (b) their mixture at pH 8.5 and  $25^{\circ}\text{C}$  in 1mM KCl solutions.

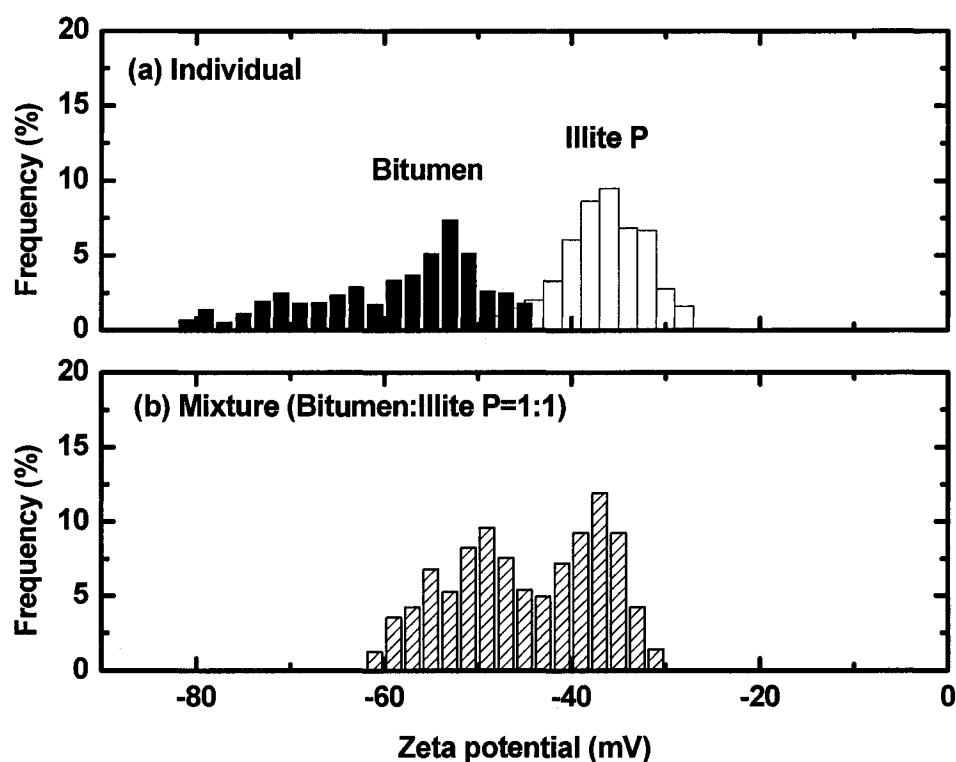


Figure 4.8. Zeta potential distributions for (a) individual bitumen emulsion and illite P suspensions and (b) their mixture at pH 8.5 and 25°C in 1mM KCl solutions.

For a 1mM KCl solution containing 1mM magnesium ions at pH 8.5, the zeta potential distributions of bitumen and illite W and their mixture at a mass ratio of 1:1 are shown in Figure 4.9. With the addition of 1mM calcium or magnesium ions, the peak positions for bitumen and illite W shifted from -62 and -37 mV to -35 and -16 mV, respectively, as shown in Figure 4.9a. The distribution of the mixture had two peaks, centered at -31 and -18 mV as shown in Figure 4.9b. The results suggest that at this pH, there was at most, a weak attraction between bitumen and illite W clays at a 1:1 mass ratio in 1mM KCl solution containing 1mM calcium or magnesium ions.

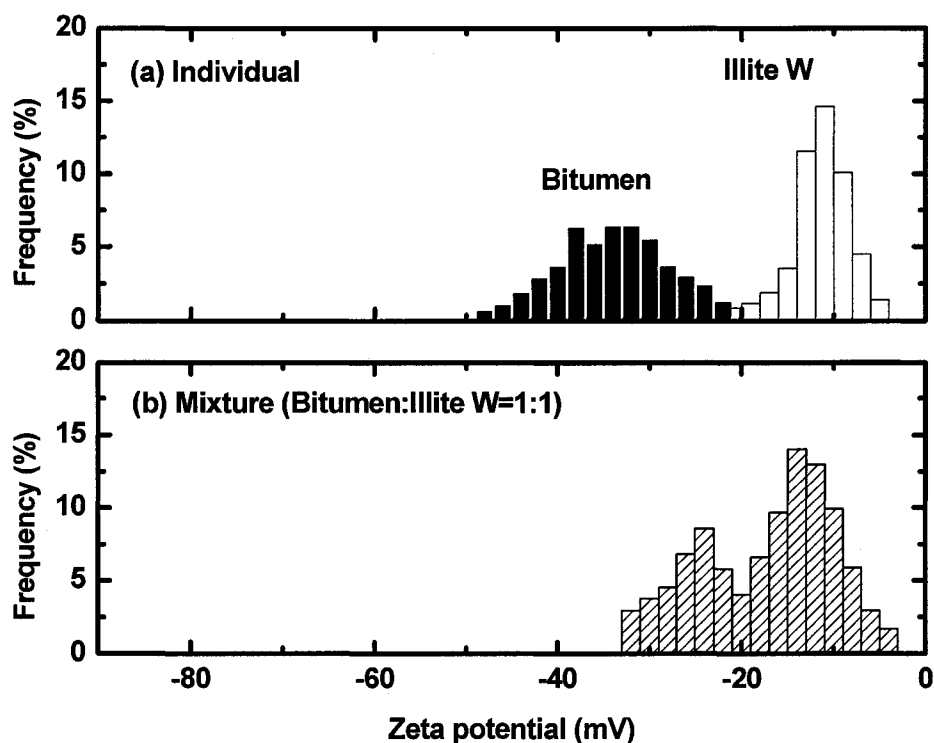


Figure 4.9. Zeta potential distributions for (a) bitumen emulsion and illite W suspensions and (b) their mixture at pH 8.5 and 25°C in 1mM KCl solutions containing 24ppm magnesium ions. (The corresponding plot for calcium ions is included in Appendix C, see Figure C.3).

In order to further confirm the weak attraction between bitumen and illite W, zeta potential distribution measurements were carried out under similar conditions but at an increased illite W to bitumen ratio. As shown in Figure 4.10, there were two peaks in each case, but the heights and positions of the peaks changed with the changing illite to bitumen ratio, as anticipated. More specifically, the height of the zeta potential distribution peak for bitumen decreased while that for the illite W increased with increasing illite to bitumen ratio. The positions of the distribution peak for bitumen

shifted towards the less negative direction and closer to the value for illite W clay particles. These distribution characteristics are representative of the system of weak attraction between the two components, which was the case illustrated in Figure 4.2c.

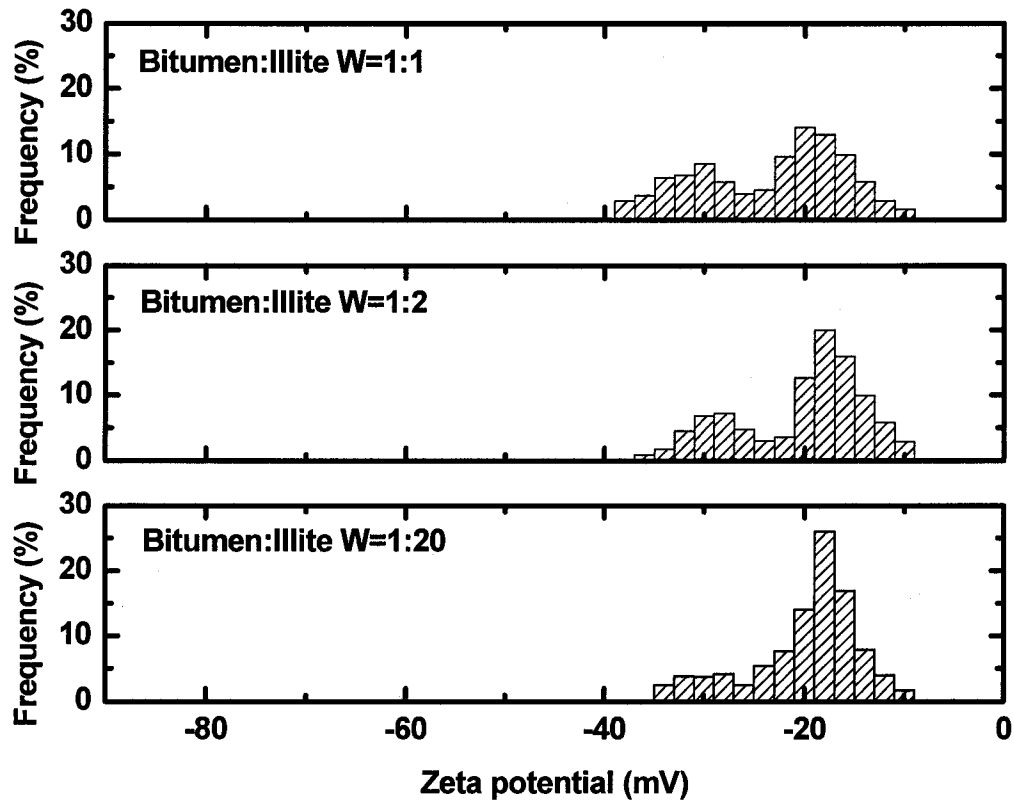


Figure 4.10. Effect of bitumen to illite W ratio on zeta potential distributions measured at pH 8.5 and 25°C in 1mM KCl solutions containing 24ppm magnesium ions.

(The corresponding plot for calcium ions is included in Appendix C, see Figure C.4).

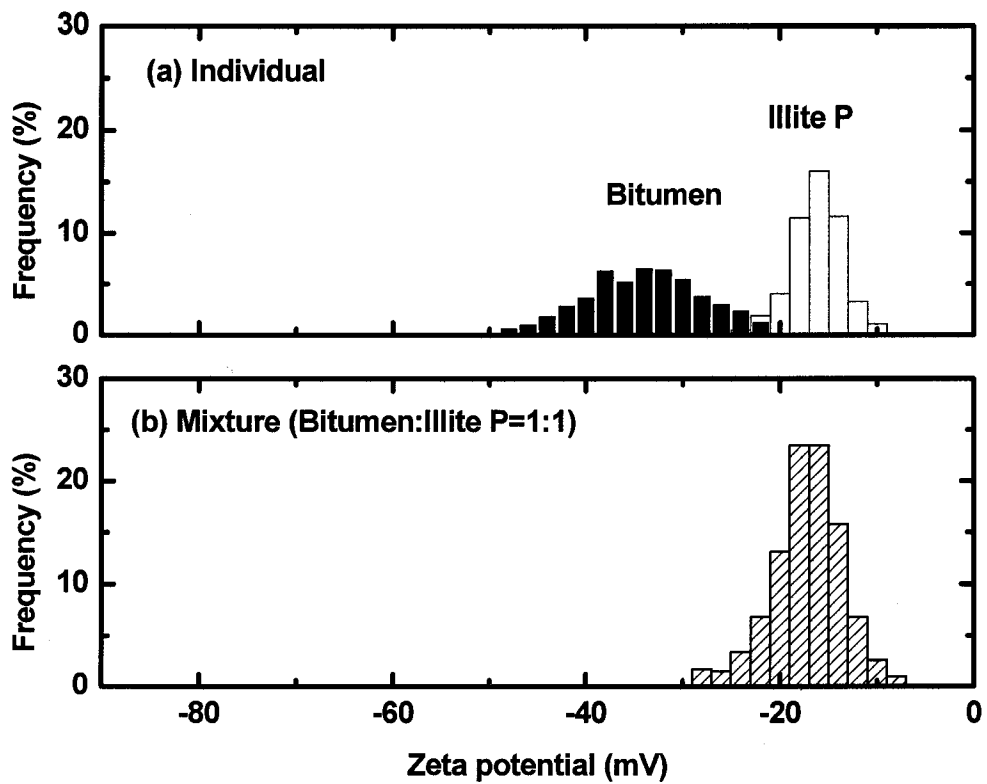


Figure 4.11. Zeta potential distributions for (a) bitumen emulsion and illite P suspensions and (b) their mixture at pH 8.5 and 25°C in 1mM KCl solutions containing 24ppm magnesium ions.

(The corresponding plot for calcium ions is included in Appendix C, see Figure C.5).

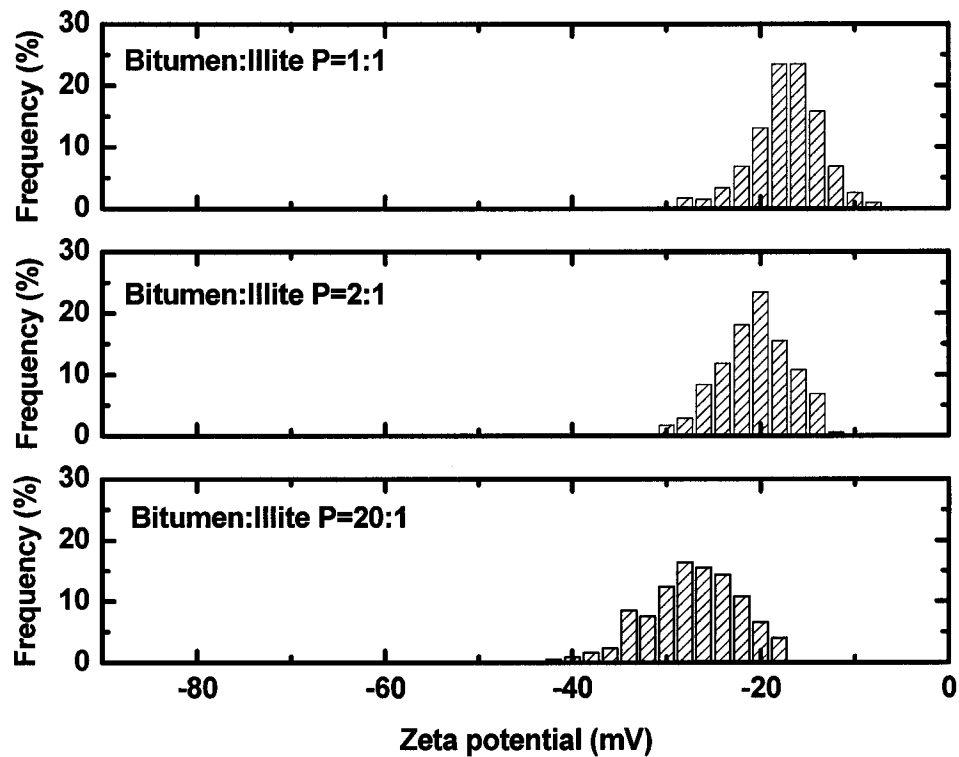


Figure 4.12. Effect of bitumen to illite P ratio on the zeta potential distributions measured at pH 8.5 and 25°C in 1mM KCl solutions containing 24ppm magnesium ions.

(The corresponding plot for calcium ions is included in Appendix C, see Figure C.6).

For illite P clay, the same measurements were performed and the results are shown in Figure 4.11. For the mixture containing a bitumen to clay mass ratio of 1:1, there was only one peak located close to the value of illite P measured alone under the same conditions. This observation suggests a strong slime coating of the bitumen surface by illite P clay. To further confirm the strong attraction between bitumen and illite P, the distribution measurements were performed at increased bitumen to illite P ratio. As shown in Figure 4.12, there was only one peak in each case, but the position of the peak

shifted from the position of illite P clay to that of bitumen. Such a distribution characteristic represents a system of strong attraction between two components with an insufficient number of coating particles, which was the case illustrated in Figure 4.2 e.

#### 4.4.2 Effect of temperature

The effect of temperature on the zeta potential of bitumen is shown in Figure 4.13. At 35°C, the zeta potential of bitumen was slightly more negative than that at 25°C. This result conformed to the work done by Dai and Chung (1995) and Long et al. (2004). One possible reason for such a decrease was the release of negatively charged surfactants at an increased temperature. For the two illite clays, little change on their zeta potentials was observed when the temperature was increased from 25 to 35°C, as shown in Figure 4.14.

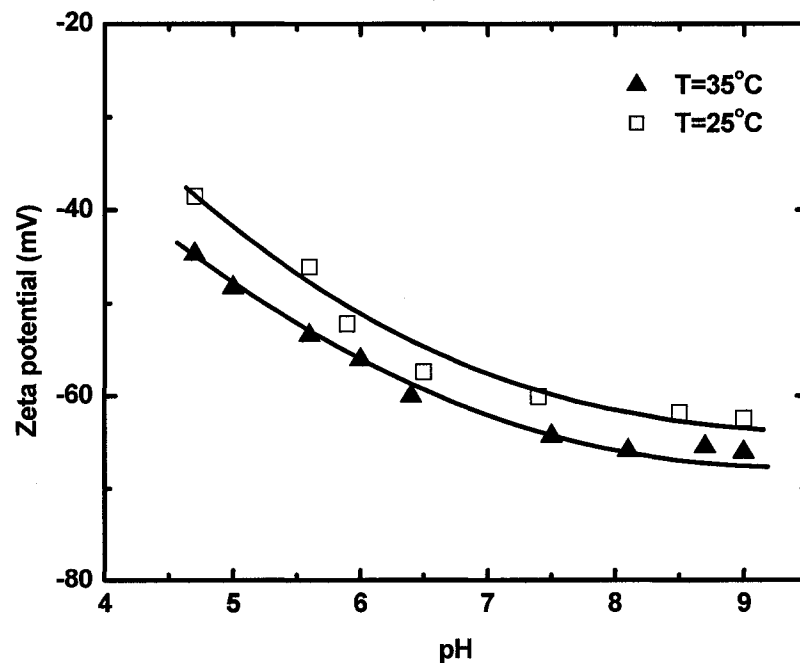


Figure 4.13. Effect of temperature on the average zeta potential of bitumen in 1mM KCl solutions.

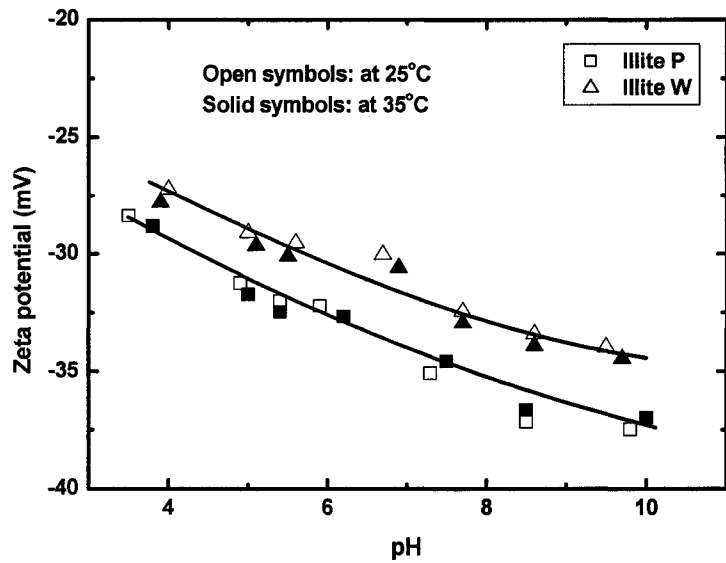


Figure 4.14. Effect of temperature on the average zeta potentials of illite clays in 1mM KCl solutions.

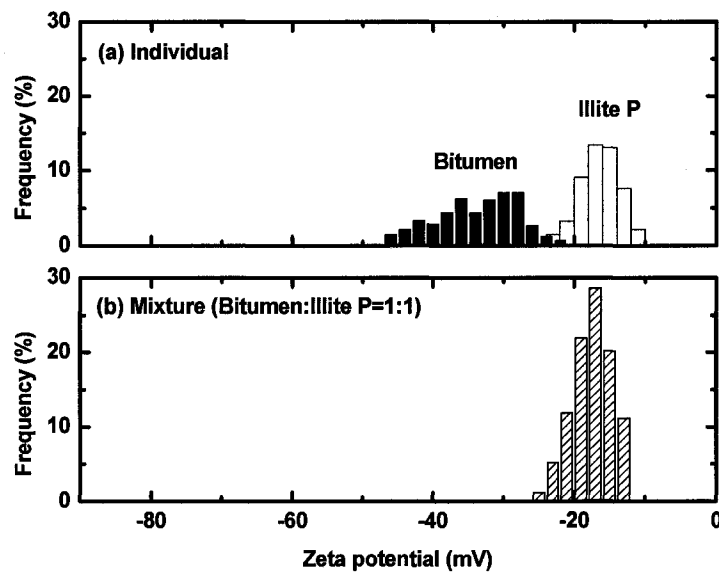


Figure 4.15. Zeta potential distributions for (a) bitumen emulsion and illite P suspensions and (b) their mixture at pH 8.5 and 35°C in 1mM KCl solutions containing 24ppm magnesium ions.

(The corresponding plot for calcium ions is included in Appendix C, see Figure C.7).

In order to investigate whether an increase in temperature can prevent illite P clay slime coating on bitumen in 1mM KCl solutions containing 24ppm magnesium ions, zeta potential distribution measurements at a 1:1 bitumen to clay mass ratio were performed at 35°C. As shown in Figure 4.15, there was still only one peak centered at the position of illite P clay, suggesting that bitumen was almost fully covered by illite P clay particles. This observation showed that temperature does not prevent slime-coating in de-ionized water. However, according to the interpretation of work of Long et al. (2004), slime coating does not occur at this temperature in process water. Therefore, water chemistry plays an important role in preventing slime coating. The effect of water chemistry will be discussed in the next section. In the flotation system with the addition of 5% clay, the bitumen to illite P ratio was around 3:1. According to the trend of the curves shown in Figure 3.6 and 3.7, a much lower bitumen recovery would be anticipated when the amount of illite P increased from a bitumen to illite ratio of 3:1. As shown in Figure 4.16, at a bitumen to clay ratio of 1:1, the bitumen surface was fully covered by clay particles and thus bitumen would not be sufficiently aerated. Low bitumen recovery is expected. When the bitumen to clay ratio was increased to 2:1, the peak started to shift away from the clay position toward that of bitumen, which would mean that the bitumen surface was only partially covered by the clay particles. A slightly higher bitumen recovery would be expected. When the ratio was increased to 20:1, the peak was very close to the bitumen distribution peak itself, which would indicate that the bitumen surface was much less covered by the clay particles. Under this condition, bitumen could easily attach to air bubbles and be floated. High bitumen recovery close to that of the baseline flotation tests would be expected.

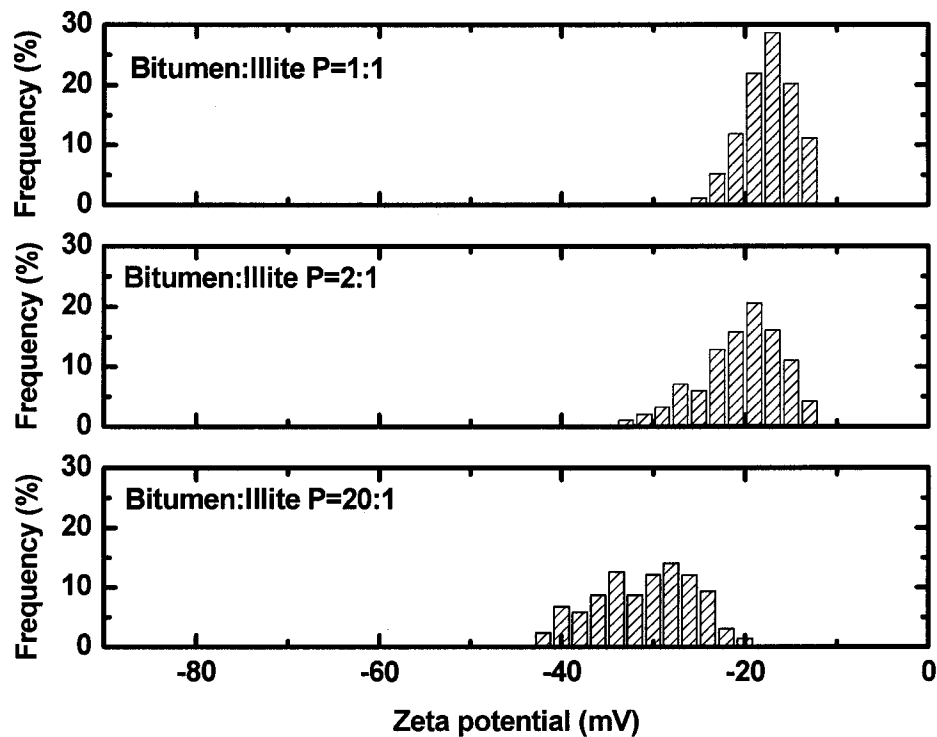


Figure 4.16. Effect of bitumen to illite P ratio on the zeta potential distributions measured at pH 8.5 and 35°C in 1mM KCl solutions containing 24ppm magnesium ions.

(The corresponding plot for calcium ions is included in Appendix C, see Figure C.8).

#### 4.4.3 Effect of process aids

As mentioned in chapter 3, pH dropped significantly (as low as 4.9) during the flotation tests under some conditions. To check whether slime coating phenomenon would occur between bitumen and illite at a low pH, zeta potential distribution measurements were conducted at a pH of 4.9. The results in Figure 4.17 and Figure 4.18 suggest a strong

slime coating between bitumen and illite P and a weak attraction between bitumen and illite W at a low pH.

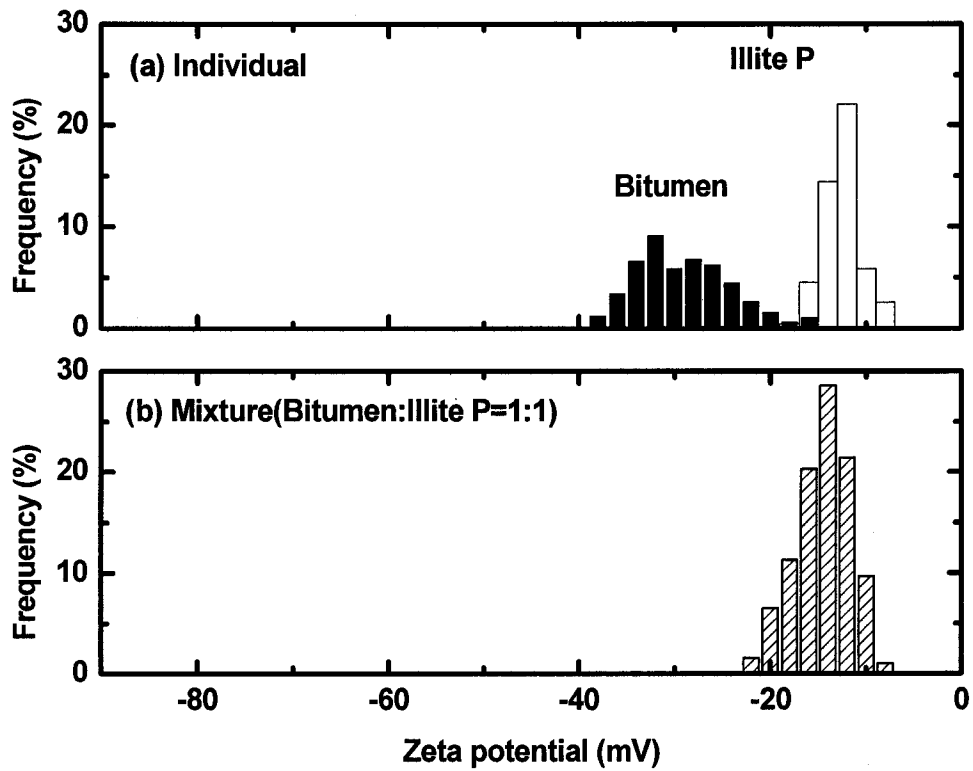


Figure 4.17. Zeta potential distributions for (a) individual bitumen emulsion and illite P suspension and (b) their mixture at pH 4.9 and 25°C in 1mM KCl solutions containing 24ppm magnesium ions. (The corresponding plot for calcium ions is included in Appendix C, see Figure C.9).

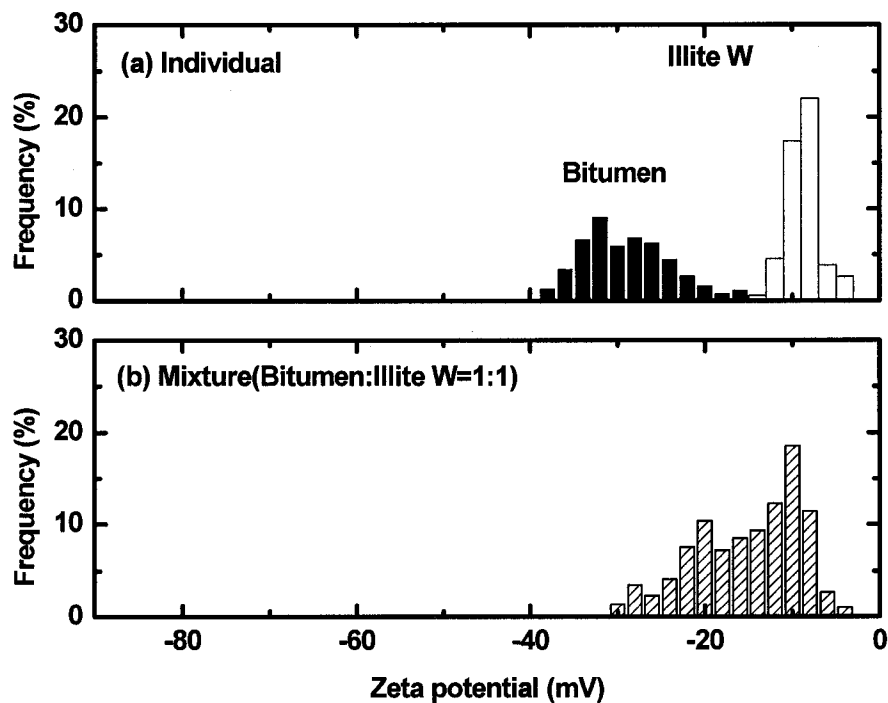


Figure 4.18. Zeta potential distributions for (a) individual bitumen emulsion and illite W suspensions and (b) their mixture at pH 4.9 and 25°C in 1mM KCl solutions containing 24ppm magnesium ions. (The corresponding plot for calcium ions is included in Appendix C, see Figure C.10).

During the flotation tests, when the pH of the slurry was controlled at 8.5 by adding NaOH, no depression of bitumen recovery due to the co-presence of divalent cations and illite clays was observed, which was contradictory to the observation from the zeta potential distribution measurements as shown in Figure 4.11. To explain this discrepancy, supernatant from the tailings water of the flotation tests was used to repeat the zeta potential distribution measurements. The results shown in Figure 4.19 suggest a weak attraction existing between bitumen and illite P clay, which correlated very well with the flotation tests. Very similar zeta potential distribution results were observed when Aurora

process water instead of the supernatant was used in the measurements. The difference in the zeta potential distributions measured between using de-ionized water and supernatant from tailing water or process water might be due to the existence of additional chemical species in the tailing water or process water. To check whether the supernatant from the flotation tests without pH control had the same effect on the interaction between bitumen and illite P, zeta potential distribution measurements were repeated using the supernatant instead of de-ionized water. The result summarized in Figure 4.20 shows that the acidic supernatant did not show the same effect as the alkaline supernatant in preventing slime coating.

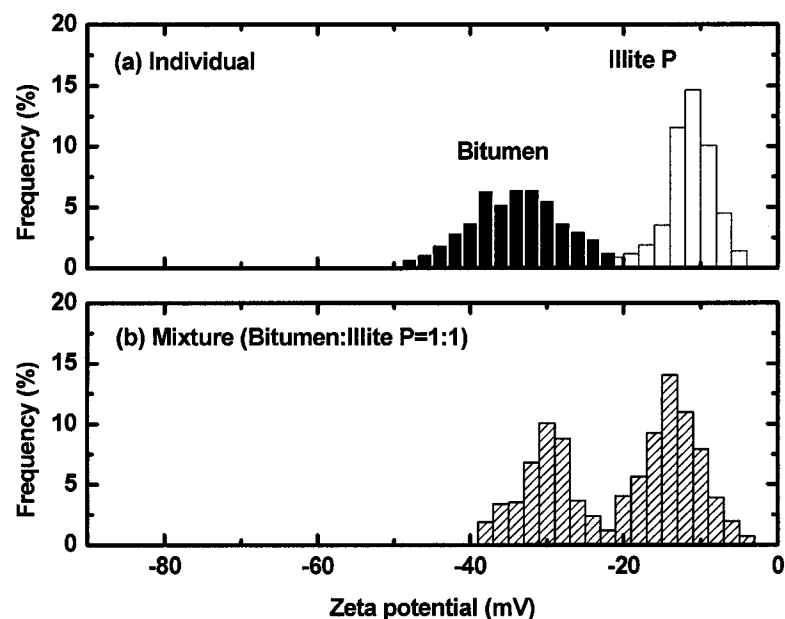


Figure 4.19. Zeta potential distributions for (a) bitumen emulsion and illite P clay suspensions and (b) their mixture at 25°C in the supernatant of the produced tailings water (pH 8.5) (from the flotation test with pH controlled at 8.5) with the addition of 24ppm magnesium ions. (The corresponding plot for calcium ions is included in Appendix C, see Figure C.11).

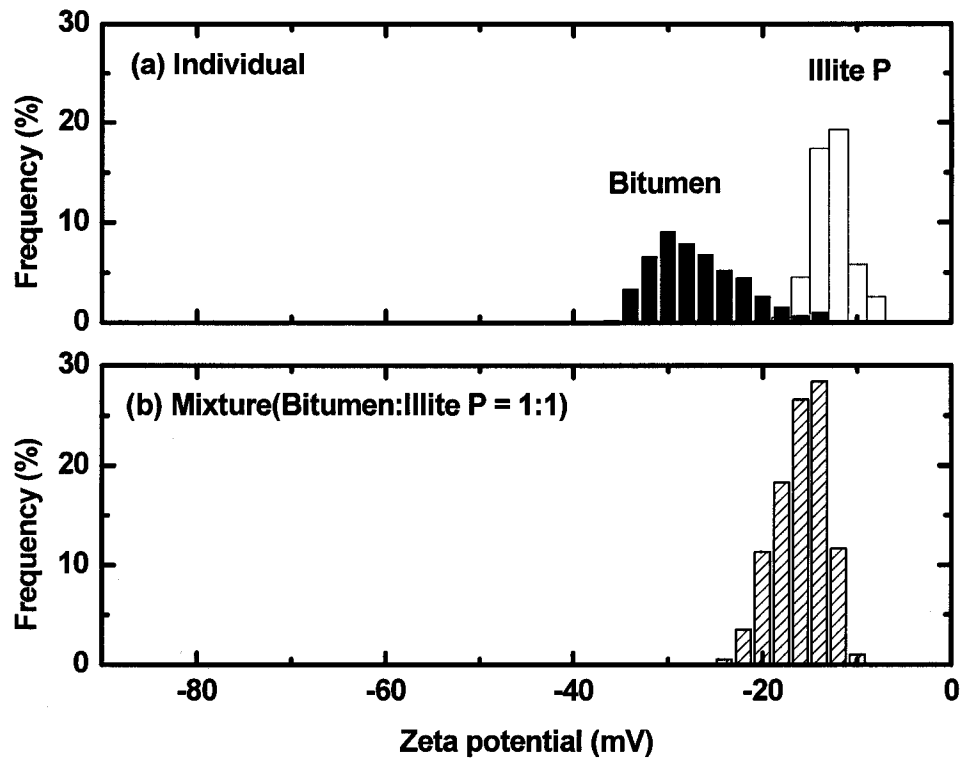


Figure 4.20. Zeta potential distributions for (a) bitumen emulsion and illite P suspensions and (b) their mixture at 25°C in the supernatant of the produced tailings water (pH 4.9) (from the flotation test without pH control) with the addition of 24ppm magnesium ions. (The corresponding plot for calcium ions is included in Appendix C, see Figure C.12).

To investigate the effect of bicarbonate on the interactions between bitumen and illite P, zeta potential distribution measurements were conducted at room temperature and 35°C. From Figures 4.21 and 4.22, we can note that the addition of bicarbonates mitigated slime coating at room temperature and completely prevented slime coating at 35°C. These observations correlated very well the flotation test results.

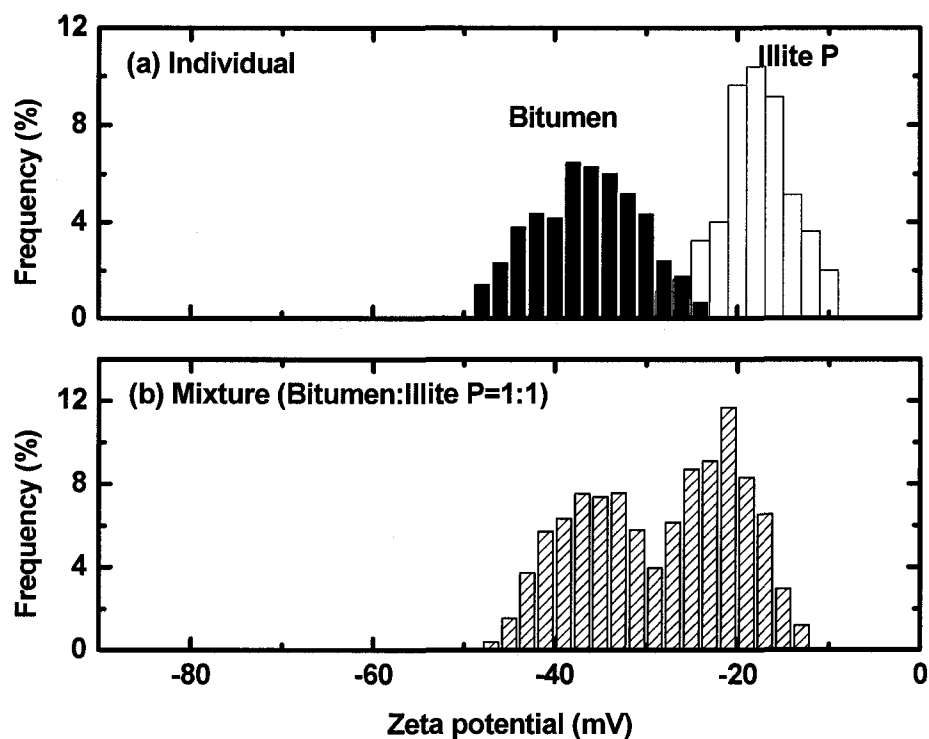


Figure 4.21. Zeta potential distributions for (a) individual bitumen emulsion and illite P suspensions and (b) their mixture at pH 8.6 and 25°C in 1mM KCl solutions with the addition of 24ppm magnesium and 1000ppm NaHCO<sub>3</sub> based on water.

(The corresponding plot for calcium ions is included in Appendix C, see Figure C.13).

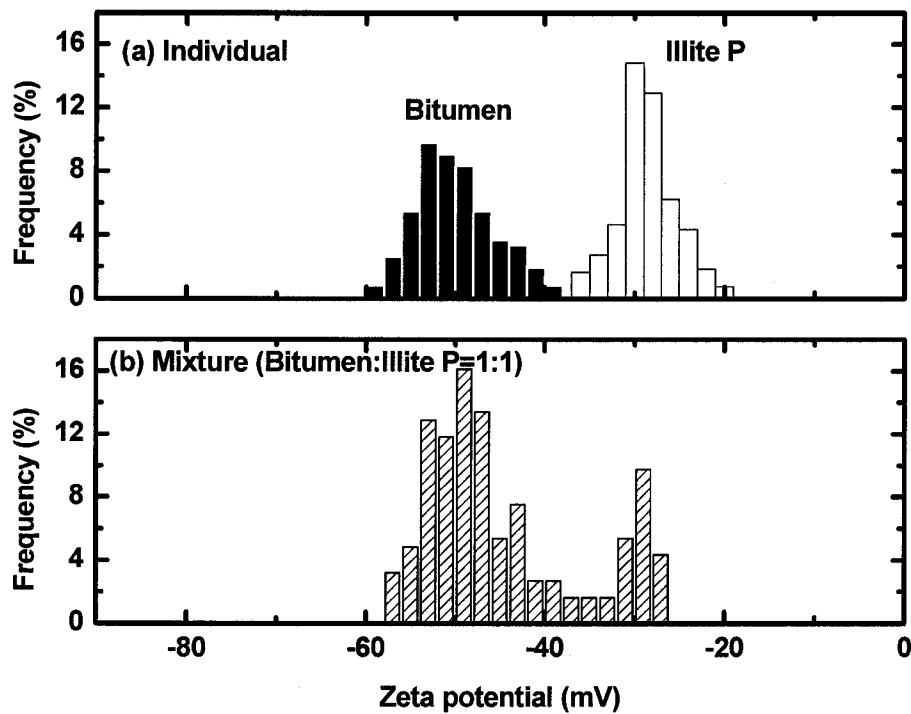


Figure 4.22. Zeta potential distributions for (a) individual bitumen emulsion and illite P suspensions and (b) their mixture at pH 8.6 and 35°C in 1mM KCl solutions with the addition of 24ppm magnesium and 1000ppm NaHCO<sub>3</sub>. (The corresponding plot for calcium ions is included in Appendix C, see Figure C.14).

From all the information gathered in this study, we have demonstrated that zeta potential distribution measurements are a powerful tool for studying slime coating phenomena and diagnosing flotation systems. The tool, however, remains qualitative in nature. From the zeta potential distribution results, temperature did not prevent slime coating. However, from the flotation test results, temperature did increase bitumen recovery. In order to better explain how temperature affects recovery, quantitative measurements of surface

forces between bitumen and clays under various chemical conditions by atomic force microscopy are suggested as a possibility for future work.

#### 4.5 Conclusions

1. Calcium and magnesium ions had the same effect on lowering the zeta potentials of bitumen and illite clays.
2. Zeta potential distributions indicated a stronger attractive interaction between bitumen and illite P than that between bitumen and illite W in the presence of magnesium or calcium ions.
3. Increasing temperature led to an increase in the absolute value of the zeta potential of bitumen but did not mitigate slime coating according to the zeta potential distribution measurement.
4. The alkaline tailings water or process water contained chemical species which were effective in preventing slime coating.
5. The presence of bicarbonates in de-ionized water prevented slime coating.

## 5.0 CHARACTERIZATION OF CLAYS

From the previous two chapters, we know that two illite clays showed different behavior in both electrokinetic studies and flotation tests. The objective of this chapter is to explore the reasons why these two illite clays had different behavior by performing a series of characterizations such as XRD, BET and CEC on these two clays.

### 5.1 Fourier transform infra-red (FTIR)

Fourier transform infrared spectroscopy is an analytical technique used to identify organic materials by measuring the absorption of infrared radiation by a material of interest. The infrared absorption bands can be used to identify specific molecular components and structures. This technique has been used to characterize fine solids from the Athabasca oil sands by Czarnecka and Gillott (1980) and Chen et al. (1999).

In this study, a Bio-Rad FTS 6000 Fourier transform IR spectrometer was used to obtain FTIR spectra. Potassium bromide powder was used as background in the middle-infrared region ( $400 - 4000 \text{ cm}^{-1}$ ). To prepare samples for measurement, 0.1 g of dried KBr and 0.005 g illite clay were mixed uniformly and ground finely. The resolution of the spectra was  $2 \text{ cm}^{-1}$ . The FTIR spectra of these two clays (Figure 5.1) show that no characteristic peak for organic functional groups, such as -OH, C=O, N-H, CH<sub>3</sub>, etc. can be found in the range  $1300\text{-}3500 \text{ cm}^{-1}$ , and that the spectra for both illite clays have the same pattern. From the FTIR spectra of the two illite clays, we can exclude the possibility that the different behaviors observed were due to possible contamination of the clays by organics.

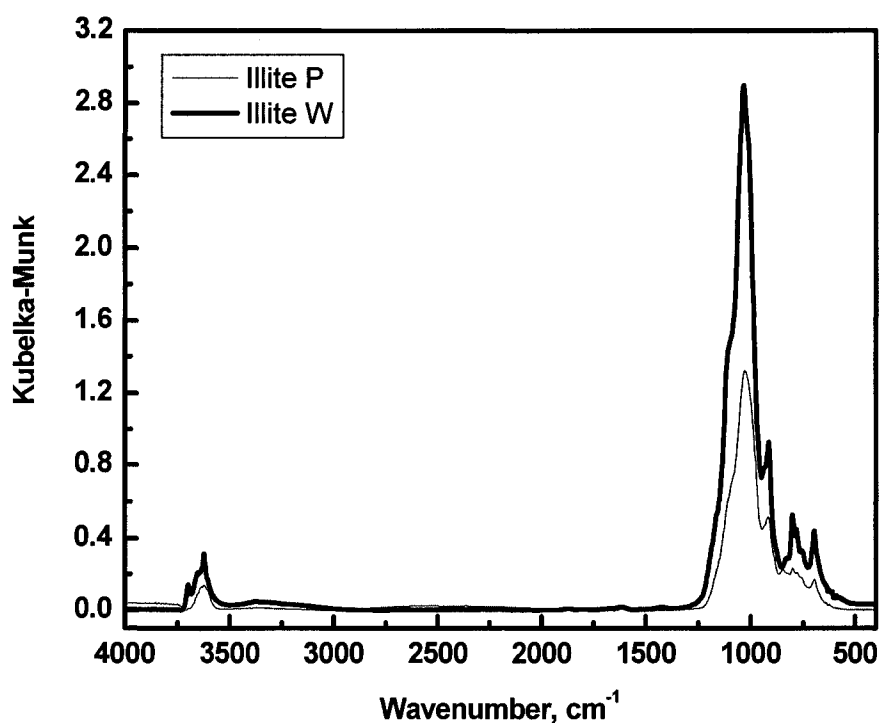


Figure 5.1. FTIR spectra of two illite clays.

## 5.2 X-ray diffraction (XRD)

### *X-ray diffraction (XRD)*

The technique of X-ray diffraction is based on the principle of interference of scattered x-rays due to the lattice periodicity of a crystallite. Bragg's Law is the most important relation for the use and understanding of XRD. Bragg's Law is expressed as:

$$2 d \sin \theta = n \lambda$$

here  $d$  is the distance between neighboring crystal planes,  $\theta$  is the scattering angle,  $n$  is the order of the diffraction and  $\lambda$  is the wavelength of the x-ray. In practice, all the diffraction peaks can be recorded by scanning the detector. The positions and the

intensities of the peaks were used to identify the structure of the material according to established database. Typically the diffracted intensity is plotted as a function of  $2\theta$ . This technique has been successfully and extensively used to identify and analyze clay minerals (Moore and Reynolds, 1997).

*Mineral analysis by X-ray diffraction (XRD)*

Table 5.1. Mineral composition by XRD

Sample	Clay Minerals (wt%) $\pm$ 10%			Non-Clay Minerals (wt %)			Total Surface Area (m <sup>2</sup> /g)*
	Illite-Smectite (70:30)	Illite	Kaolinite	Quartz	Titanium oxides	Feldspar	
Illite P	67	0	0.3	30	0	3	226
Illite W	0	63	12	24	1	0	56

\* - Only contributions from clay minerals accounted for.

Each illite sample was dispersed in de-ionized water and centrifuged at 1000 rpm for 170s to separate the clay (minus 2  $\mu$ m) fraction. Detailed mineralogical analysis was conducted on the silt (plus 2  $\mu$ m) and clay fractions using X-ray diffraction (XRD). Calcium-saturated and glycolated oriented slides of the clay fractions were prepared for mixed layer clay identification and quantification. Randomly oriented samples of the potassium saturated silt fractions were used for quantitative X-ray analysis. X-ray diffraction patterns were obtained at the Natural Resource Canada, Energy Technology Branch at Devon, with a Bruker D8  $\theta$ - $\theta$  x-ray diffractometer equipped with a parabolic CoK $\alpha$  monochromating multilayered mirror on both incident and diffracted beam sides.

The parallel beam geometry ensured that height variations in the clay slides did not result in significant d-spacing errors. The silt fractions were quantified with TOPAS<sup>TM</sup> (Bruker AXS 2003), a Rietveld refinement software. The basal diffraction pattern (001) of the illite P (from glycolated slides) was modeled with NEWMOD<sup>TM</sup> (Reynolds, 1995) and was confirmed as illite-smectite (70:30). The mineral compositions of two illite clays by XRD are shown in Table 5.1 and orientated XRD patterns are shown in Figure 5.2 and 5.3. From Table 5.1 we know that illite P consists mainly of illite-smectite whereas illite W mainly consists of illite.

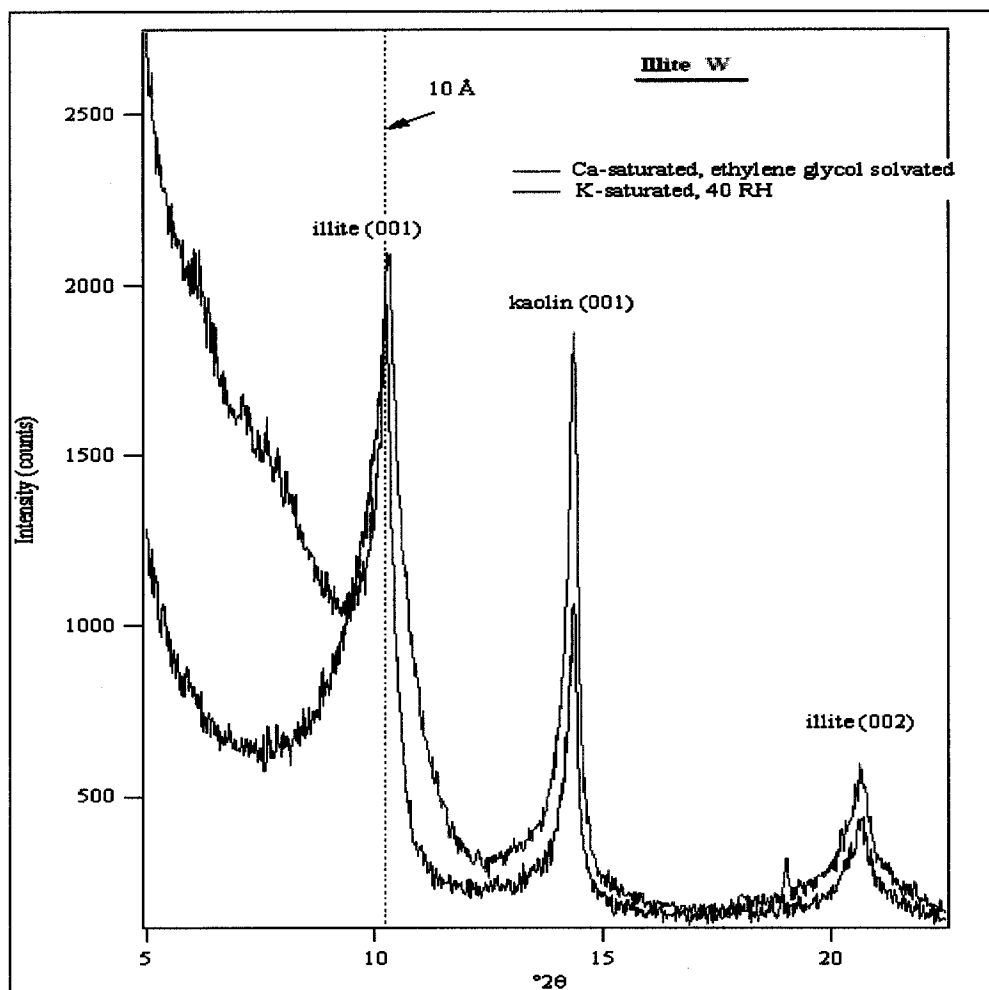


Figure 5.2. Oriented XRD Patterns of illite W.

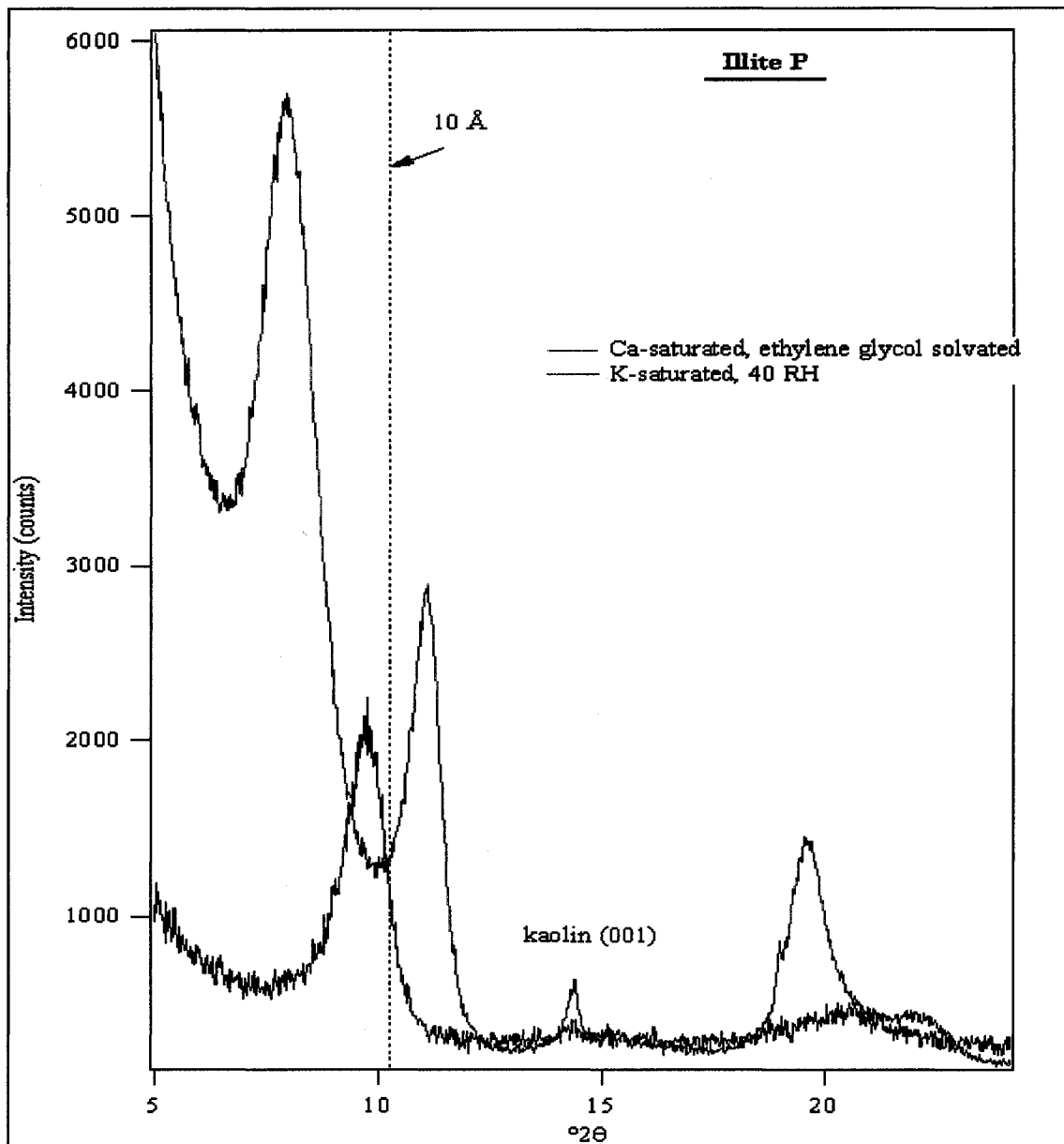


Figure 5.3. Oriented XRD Patterns of illite P

### 5.3 Cation exchange capacity (CEC)

Cation-exchange capacity is defined as the degree to which a soil or clay mineral can adsorb and exchange cations. It is related to pH dependent charges of soils and clay minerals and is usually expressed in milliequivalents per 100 grams (meq/100g) of soil or

clay. In this study, the CEC data were acquired at the Natural Resources Analytical Laboratory at the University of Alberta using a standard ammonium acetate method. Base cations were extracted by leaching 10 g of air-dried clay with successive aliquots of 1M NH<sub>4</sub>OAc at pH 7 (to a total of 250 ml) in order to saturate exchange sites with ammonium ions. Excess free ammonium ions were rinsed from the clay with isopropyl alcohol. The remaining ammonium ions held on cation exchange sites were replaced by leaching the clay with successive aliquots of 1M KCl. Ammonium was determined from the KCl leachate by colorimetry on a Technicon Auto Analyzer.

The other method used in this study was the methylene blue adsorption test. This method involves the titration of an aqueous dispersion of clay with a methylene blue compound that reacts with the clays by cation exchange. The calculations were expressed as follows:

$$\text{Methylene blue capacity or} \\ \text{cation exchange capacity} = \frac{100}{\text{sample wt, g (105}^\circ\text{C)}} \times \text{Volume titrant, ml} \times \text{Normality, meq / ml} \\ \text{meq / 100 g clay (105}^\circ\text{C)}$$

This method is often used due to its speed and simplicity. Nevins and Weintritt (1967) used the methylene blue method to determine cation exchange capacity of clays in oil well drilling fluids and the results were in good agreement with those from the standard ammonium acetate method. Kelly (1984) reviewed the correlation of many characteristics of clays, such as CEC and surface area, with the measurements of the methylene blue method. Kahr and Madsen (1995) reported that it was necessary to work with an optimum dispersion, a fixed clay to water ratio, a constant pH and a given initial amount

of methylene blue in order to achieve reproducible results by using the methylene blue method.

The CECs of the two illite clays were 15.6 and 11.2 meq/100g clay for illite P and W, respectively by the ammonium acetate method. The results from the methylene blue method were 28 and 18 meq/100g clay, respectively. Kahr and Madsen (1995) reported that the CEC of illite clay was in the range of 10 to 25 meq/100g using the methylene blue method. Although the two sets of results are different, each set of results gives illite P a relatively higher CEC than illite W.

#### 5.4 Specific surface area

Specific surface area (SA) is the surface area of the solid particles in a given quantity of clay or porous medium. It is usually expressed in square meters per gram ( $\text{m}^2/\text{g}$ ). Physical and chemical properties of a porous material may be greatly influenced by the extent of its surface area. For example, Petersen et al. (1996) investigated the relationship between SA and general soil properties such as CEC and soil texture. They found that SA was highly related to the clay fraction of the soil and CEC was highly correlated to SA. The principle used to measure the surface area is surface adsorption. The BET method developed by Brunauer, Emmett, and Teller is a direct method for the determination of the surface area of a powdered solid from the adsorption isotherm for a gas or vapor on the solid. Nitrogen is usually used in the BET method. Since the diameter of the nitrogen molecule is larger than the distance between layers in clay particles and cannot penetrate into the layers, the BET method usually gives external surface area. The ethylene glycol

monoethyl ether (EGME) method is used to determine total surface area of clay minerals including interlayer and external surface area. For clays containing smectite that has expansion properties, the total surface area is usually quite larger than the BET derived area. The EGME method for measuring surface area of clays and soils was appraised by Quirk and Murray (1999). In this study, the surface areas using the BET method were acquired at Sulzer Metco (Canada) Inc. The EGME data was obtained according to the EGME method provided by Sheldrick (1984). A detailed description of the procedures is included in Appendix D.

The BET surface areas for illite P and W were  $48.20 \pm 0.03$  and  $33.20 \pm 0.03$   $\text{m}^2/\text{g}$  (analyzed by Sulzer Metco (Canada) Inc.) and EGME surface areas were  $189 \pm 15$  and  $95 \pm 10$   $\text{m}^2/\text{g}$ , respectively. Kahr and Madsen (1995) reported that the surface area of illite clay was in the range of 78 to 196  $\text{m}^2/\text{g}$ , depending on the pretreatment of the samples using the methylene blue method. The total surface area was also estimated from the crystallite size using the double Voigt method (Balzar, 2001) implemented in TOPAS<sup>TM</sup>. The peaks were decomposed by a direct convolution of the instrument profile function to the pure profile of the specimen. The instrument function was determined experimentally from silt-sized fluorophlogopite (NIST - SRM 675). The values are listed in Table 5.1. Due to the swelling property of smectite, illite P has quite a larger surface area than illite W according to the measurements using XRD data. The EGME area for illite P correlated well with the calculated data. For illite W, the calculated area was smaller than the EGME area.

## 5.5 Cation adsorption kinetics test

The adsorption tests on the two illite clays were conducted according to the procedures provided by Liu et al. (2004). Illite clay was added to a 1mM calcium or magnesium solution at a ratio of 1 g/L (clay/solution). After conditioning for a given time, the suspension was filtered to remove the solids. The supernatant was then analyzed by the AA (atomic adsorption) method. The results show that within the first 10 minutes, the adsorption kinetics of cations on illite P are faster than those on illite W. For example, 1 g of illite P can adsorb up to 2.5 mg calcium ions in a 1mM calcium solution in 10 minutes. The amount of adsorbed calcium is two times of that 1 g illite W can adsorb under the same conditions (Figure 5.4). While in a 1mM magnesium solution, 1 g illite P can adsorb up to 1.5 mg magnesium ions in 10 minutes, which is also two times of that 1 g illite W can adsorb (Figure 5.5).

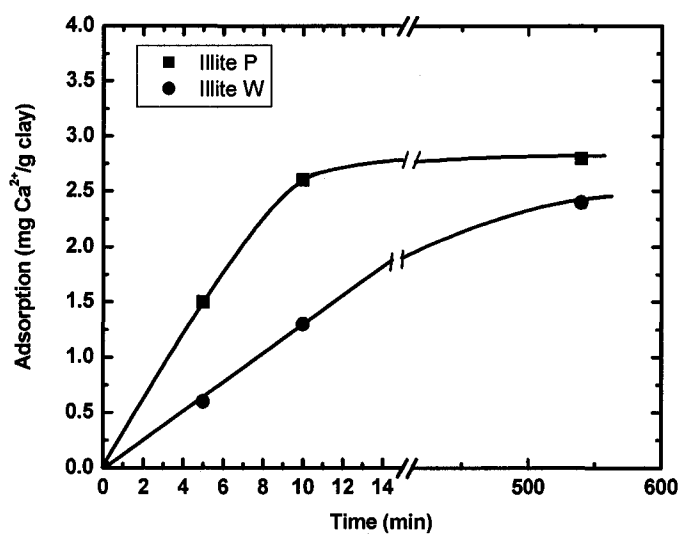


Figure 5.4. Calcium adsorption on the two illite clays as a function of time in solutions containing initially 1mM calcium ions at a solid to liquid ratio of 1 g/L.

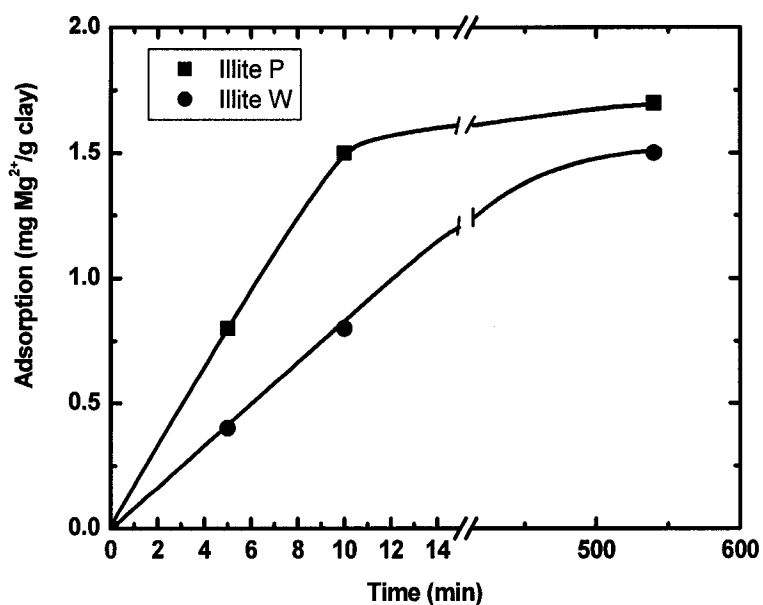


Figure 5.5. Magnesium adsorption on two illite clays as a function of time in solutions containing initially 1mM magnesium ions at a solid to liquid ratio of 1 g/L.

## 5.6 Conclusions

From the aforementioned characterization results of the two illite clays, we know that due to the presence of smectite, illite P has quite larger surface area than illite W, larger CEC and higher cation adsorption rate in the first 10 minutes than illite W. These characteristics of illite P can be the main reason for its more detrimental effect on bitumen recovery when compared with illite W.

## 6.0 CONCLUSIONS

1. The detrimental effects of illite clays on bitumen recovery using de-ionized water were due to their acidity, and the adverse effects could be reconciled by the addition of process aids such as NaOH and NaHCO<sub>3</sub>.
2. 1mM of calcium or magnesium ions alone had little effect on bitumen recovery. However, when co-added with illite P clay on molar equivalents basis, both had the same adverse effect when de-ionized water was used in the flotation tests.
3. Temperature to some extent mitigated the negative effect on bitumen recovery due to the addition of illite clays and divalent cations. However, it did not mitigate slime coating according to zeta potential distribution measurement results.
4. Alkaline tailings water or process water had a great effect on mitigating slime coating as evidenced by zeta potential distribution measurements.
5. Bitumen recovery correlates well with processing pH.
6. Zeta potential distribution measurements are a powerful tool for studying slime coating phenomena and diagnosing flotation behaviour.
7. Clay characterization results showed that the smectite nature of illite P clay in the presence of a sufficient level of divalent cations was a factor in depressing bitumen recovery.

## **7.0 RECOMMENDATIONS**

1. Surface force measurements between bitumen and illite clay under various conditions using atomic force microscopy would provide a better understanding of the effects of temperature on bitumen recovery.
2. The role of water chemistry on bitumen recovery should be investigated to understand the role of surfactants and other chemical species.
3. The distribution of divalent cations in froth, tailings water, and tailing deposits should be examined to better understand the role of divalent cations in a flotation system.

## REFERENCES

- Alberta Department of Energy (Dec. 8, 2004), Alberta's Oil Sands, <http://www.energy.gov.ab.ca/docs/oilsands/pdfs/osgenbrf.pdf> (Oct. 1, 2005).
- Balzar, D. "Voigt-function model in diffraction line-broadening analysis", in *Microstructure Analysis from Diffraction*, Snyder, R. L. et al. editors IUCR monograph (2001).
- Baptista, M.V., "Role of the Exchangeable Cations of Oil Sand Clays in Oil Sand Processing – Part 1. Batch Tests", *AOSTRA J. Res.* **5**, 237-241 (1989).
- Baptista, M.V., "Role of the Exchangeable Cations and Iron-amorphous Coatings of the Oil Sand Solids in Oil Sand Processing – Part 2. Pilot and Plant Tests", *AOSTRA J. Res.* **5**, 243-256 (1989).
- Baptista, M. V. and C.W. Bowman, "The Flotation Mechanism of Solids from the Athabasca Oil Sand" Preprint, 19th Can Chem Eng Conf Edmonton, Alberta (1969).
- Basu, S., Nandakumar, K. and Masliyah, J.H., "A Study of Oil Displacement on Model Surfaces", *J. Colloid Interf. Sci.* **182**, 82–94 (1996)
- Basu, S., Nandakumar, K., Lawrence, S. and Masliyah, J.H., "Effect of calcium ion and montmorillonite clay on bitumen displacement by water on a glass surface", *Fuel*, **83**, 17-22 (2004).
- Bichard, J.A., "Oil Sands Composition and Behavior Research", *The Research Papers of John A. Bichard 1957-1965*, AOSTRA, Edmonton, AB (1987).
- Budziak, C. J., Vargha-Butler, E.I., Hancock, R. G. V. and Wilhelm Neumann, A. "Study of fines in bitumen extracted from oil sands by heat-centrifugation", *Fuel*, **67**(12), 1633-8 (1988).
- Bulmer, J. T. and Star, J., "Syn crude analytical methods for oil sand and bitumen processing", Alberta Oil Sands Information Centre, Edmonton, AB, pp. 46–51 (1979).

- Chen, F., Finch, J.A., Xu, Z. and Czarnecki, J., "Wettability of fine solids extracted from bitumen froth", *J. Adhesion Sci. Technol.*, **13(10)**, 1209-1224 (1999).
- Chong, J., Ng, S., Chung, K., Sparks, L. and Kotlyar, L., "Impact of fines content on a warm slurry extraction process using model oilsands", *Fuel*, **82**, 425-438(2003).
- Clark, K.A., "The Separation of the Bitumen from Alberta Bituminous Sand", *Annual Western Meeting, Edmonton, Alberta*, October(1929).
- Clark, K.A. and D.S. Pasternack, "Hot water Separation of Bitumen from Alberta Bituminous Sand", *Ind Eng Chem*, **24**, 1410-1416(1932).
- Clark, K.A., "Hot Water Separation of Alberta Bituminous Sand", *Tran Can Inst Min Met*, **47**, 257-274 (1944).
- Clark, K.A. and Pasternack, D.S., "The Role of Very Fine Mineral Matter in the Hot Water Separation Process as Applied to Athabasca Bitumenous Sand", *Research Council of Alberta, Report NO. 53* (1949).
- Cox, D., "Suncor experiences: sinking bitumen, high chloride concentration, type X ore, high fines ore, oxidized ore, and hard ore", in "Problem Ores. 1<sup>st</sup> Extraction Fundamentals Seminar", CONRAD, Ft. McMurray (2000).
- Cuddy, G., "Empirical studies on the relationship between process water chemistry and oil sands processability (Syncrude Canada Ltd.)", in "Problem Ores.1st Extraction Fundamentals Seminar", CONRAD, Ft. McMurray (2000).
- Czarnecka, E. and Gillott, J.E., "Formation and Characterization of Clay Complexes with Bitumen from Athabasca Oil Sand", *Clays and Clays Minerals*, **28**, 197-203 (1980).
- Dai, Q. and Chung, K.H., "Bitumen-sand interaction in oil sand processing", *Fuel*, **74(12)**, p1858-1864 (1995).
- Dai, Q. and Chung, K.H., "Trona (Mineral Grade Sodium Carbonate) as a Process Aid for the Hot Water Process", *J. Can. Petro. Tech.* **35(1)** (1996a).
- Dai, Q. and Chung, K.H., "Hot water extraction process mechanism using model oil sand", *Fuel*, **75(2)**, p220-226 (1996b).

- Dai, Q., Chung, K.H. and Czarnecki, J., "Formation of Calcium Carbaonate in the Bitumen/Aqueous Solution Hydroxide System", *AOSTRA Journal of Research*, **8**, p95 (1992).
- Ding, X., Xu, Z. and Masliyah, J., "Effects of Divalent Ions, Illite Clays and Temperature on Bitumen Recovery", **54<sup>th</sup>** Canadian Chemical Engineering Conference, Calgary, Canada, October 3-6 (2004).
- Du, Q., Sun, Z., Forsling, W., and Tang, H., "Acid-Base Properties of Aqueous Illite Surfaces", *J. Colloid Interface Sci.*, **187**, 221-231 (1997).
- Fong, N., Ng, S., Chung, K.H., Tu, Y., Li, Z., Sparks, B.D., and Kotlyar, L.S., "Bitumen recovery from model systems using a warm slurry extraction process: effects of oilsands components and process water chemistry", *Fuel*, **83(14-15)**, 1865-1880 (2004).
- Hepler, L.G., and Hsi, C., *AOSTRA Technical Handbook on oil sands, Bitumen and Heavy Oils*, AOSTRA technical publication series **6**. Alberta Oil Sands Technology and Research Authority, Edmonton, (1989).
- Hepler, L.G., and Smith, R.G., *The Alberta Oil Sands: Industrial Procedures for Extraction and Some Recent Fundamental Research*, AOSTRA technical publication series **14**. Alberta Oil Sands Technology and Research Authority, Edmonton, (1994).
- Hunter, Robert J., "Foundations of Colloid Science", Second edition, Oxford, New York: Oxford University Press (2001).
- Hussain, S.A., Demirci, Ş. and Özbayoğlu, G., "Zeta Potential Measurements on Three Clays from Turkish and Effects of Clays on Coal Flotation", *J. Colloid Interface Sci.*, **184**, 535-541(1996).
- Kahr, G. and Madsen, F.T., "Determination of the cation exchange capacity and the surface area of bentonite, illite and kaolinite by methylene blue adsorption", *Applied Clay Science*, **9**, 327-336 (1995).
- Kasongo, T., Zhou, Z., Xu, Z., and Masliyah, J.H., "Effect of Clays and Calcium Ions on Bitumen Extraction from Athabasca Oil Sands Using Flotation", *Can. J. Chem. Eng.* **78**, 674-681 (2000).

- Kasperski, K.L., "Review of Research on Aqueous Extraction of Bitumen from Mined Oil Sads", *CETC-Devon* 01-17 (2001).
- Kelly, W.J., "Review of the methylene blue test", *Ceram. Eng. Sci. Proc.*, **5**(11-12), 886-894 (1984).
- Liu, J., Zhou, Z., Xu, Z., and Masliyah, J.H., "Bitumen-Clay Interaction in Aqueous Media Studied by Zeta Potential Distribution Measurement", *J. Colloid Interface Sci.*, **252**(2), 409 (2002).
- Liu, J., Xu, Z., and Masliyah, J.H., "Role of Fine Clays in Bitumen Extraction from Oil Sands", *AIChE J.*, **50**(8), 1917 (2004).
- Liu, J., Zhou, Z., Xu, Z., and Masliyah, J.H., "Colloidal forces between bitumen surfaces in aqueous solutions measured with atomic force microscope", *Colloid andsurfaces A: Physicochem. Eng. Aspects*, **260**, 217-228 (2005).
- Long, Jun, Xu, Z., and Masliyah, J.H., "On the Role of Temperature in Oil Sands Processing", submitted to *Energy & Fuels*, (2004).
- Luthra, M., Lopetinsky, R., Sanders, R.S., Nandakumar, K. and Masliyah, J.H., "A New Device to Determine Bitumen Extraction from Oil Sands", *Can. J. Chem. Eng.* **82**, 752-762 (2004).
- Masliyah, J.H., "Electrokinetic Transport Phenomena", AOSTRA technical publication series **12**, Alberta Oil Sands Technology and Research Authority, Edmonton, (1994).
- Masliyah, J.H., Zhou, Z., Xu, Z., Czarnecki, J. and Hamza, H., "Understanding Water-Based Bitumen Extraction from Athabasca Oil Sands", *Can. J. Chem. Eng.* **82**, 674-681 (2004).
- Mathieson, D. and Stenason, D., "Investing in Oil Sands", Scotia Capital, *The Drill Bit.*, (May, 2001).
- Mikula, R.J., Omotoso, O., Munoz V. Bjornson B. and Cox D. *54<sup>th</sup> Canadian Chemical Engineering Conference* (2004), Calgary, Alberta, Canada.

- Moore, D.M. and Reynolds, R.C., X-Ray Diffraction and the Identification and Analysis of Clay Minerals, Oxford University Press, Oxford, New York (1997).
- Munoz, V.A. and Mikula, R.J., "Characterization of Petroleum Industry Emulsions and Suspensions Using Microscopy", *J. Can. Petro. Tech.* **46(10)** (1997).
- National Energy Board (Sept. 2004), Canada's Oil Sands: Opportunities and Challenges to 2015: <http://www.neb.gc.ca>. (Oct.1, 2005)
- Nevins, M.J. and Weintritt, D.J., "Determination of Cation Exchange Capacity by Methylene Blue Adsorption", *Ceramic Bulletin*, **46(6)**, 587-592 (1967).
- Omotoso, O.E. and Mikula, R.J., "High surface areas caused by smectitic interstratification of kaolinite and illite in Athabasca oil sands", *Applied Clay Scienc*, **25**, 37- 47(2004).
- Petersen, L.W., Moldrup, P., Jacobsen, O.H., Rolston, D.E., "Relations between Specific Surface Area and Soil Physical and Chemical Properties" *Soil Science*. **161(1)**, 9-21(1996).
- Quirk, J. P. and Murray, R. S., "Appraisal of the Ethylene Glycol Monoethyl Ether Method for Measuring Hydratable Surface Area of Clays and Soils", *Soil Sci. Soc. Am. J.*, **63**: 839-849 (1999).
- Reynolds, R., NEWMOD™ Clay modeling software (1995).
- Sanford, E.C. and Seyer, F.A., "Processibility of Athabasca Tar Sand Using a Batch Extraction Unit: The Role of NaOH", *CIM Bullitin* 164-169 (March 1979).
- Sanford, E.C., "Processibility of Athabasca Oil Sand: Interrelationship between Oil Sand Fine Solids, Process Aids, Mechanical Energy and Oil Sand Age after Mining", *Can. J. Chem. Eng.* **61**, 554-567 (1983).
- Schramm, L.L., Smith, R.G. and Stone, J.A., "The Influence of Natural Surfactant Concentration on The Hot Water Process for Recovering Bitumen from the Athabasca Oil Sands", *AOSTRA J. Res.* **1**, 5-13 (1984).
- Schramm, L.L., Smith, R.G. and Stone, J.A., "On the Processibility of Mixtures of Oil Sands", *AOSTRA J. Res.* **1(3)**, 147-161 (1985).

- Schramm, L.L. and Smith, R.G., "Two Classes of Anionic Surfactants and their Significance in Hot Water Processing of Oil Sands", *Can. J. Chem. Eng.* **65**, 799-811 (1987).
- Schramm, L.L. and Smith, R.G., "Some parametric studies of oil sand conditioning in the hot water flotation process", *AOSTRA J. Res.* **5**, 87-107 (1989).
- Schramm, L.L., Stasiuk, E.N. and Turner, D., "The Influence of Interfacial Tension in the Hot-Water Process for Recovering Bitumen from the Athabasca Oil Sands", *The Petroleum Society's Canadian International Petroleum Conference*, Calgary, Alberta, Canada (2001).
- Schramm, L.L., Stasiuk, E.N., Yarranton, H., Maini, B.B. and Shelfantook, B., "Temperature Effects From the Conditioning and Flotation of Bitumen From Oil Sands in Terms of Oil Recovery and Physical Properties", *J. Can. Petro. Tech.* **42(8)**, (2003).
- Sheldrick, B.H., Analytical methods manual 1984, 84-042, Specific Surface Area, Agriculture Canada.
- Smith, R.G. and Schramm, L.L., "The Influence of Mineral Components on the Generation of Natural Surfactants from Athabasca Oil Sands in the Alkaline Hot Water Process", *Fuel Pro. Tech.* **30**, 1-14 (1992).
- Takamura, K., and Wallace, D., "The physical chemistry of the hot water process", *J. Can. Petrol. Technol.* **27(6)**, 98 (1988).
- Tipman, R., "Muskeg River pilot plant: experience with poorly processing ores", in "Problem Ores. 1<sup>st</sup> Extraction Fundamentals Seminar", CONRAD, Ft. McMurray (2000).
- Wallace, D., R. Tipman, B. Komishke, V. Wallwork and E. Perkins, "Fines/Water Interactions and Consequences of the Presence of Degraded Illite on Oil Sands Extractability", *Can. J. Chem. Eng.* **82**, 667-677 (2004).
- Xu, Z., Liu, J., Choung, J.W. and Zhou, Z., "Electrokinetic study of clay interactions with coal in flotation", *Int. J. Miner. Process.* **68**, 183-196 (2003).

Zhou, Z.; Kasongo, T.; Xu, Z.; Masliyah, J.H., "Assessment of bitumen recovery from the athabasca oil sands using a laboratory Denver flotation cell". *Can. J. Chem. Eng.* **82(4)**, 696-703 (2004).

Zhou, Z., Xu, Z., Masliyah, J.H., and Czarnecki, J., "Coagulation of bitumen with fine silica in model systems", *Colloids Surf. A*, **148**, 199 (1999).

## APPENDIX A

### Dean Stark Method

The Dean Stark method was used to analyze the compositions of the oil sand ore and flotation froth. The following procedures were used.

1. Label and weigh glass jars with desiccant-dried thimbles inside. Record the total weight,  $W_{J,i}$ .
2. For the analysis of oil sand ores, place a given set amount of ore into a thimble in a jar. Record the total weight of the jar and the ore,  $W_{J+O,i}$ . The weight of the ore equals  $W_{J+O,i} - W_{J,i}$ . For froth analysis, place the froth into the thimble and weigh the jar and thimble together. Record the total weight of the jar and the froth  $W_{J+F,i}$ . The weight of the froth equals  $W_{J+F,i} - W_{J,i}$ .
3. Add about 200 ml of toluene to each Dean Stark flask to be used.
4. Transfer the thimbles to the flasks using the baskets and hang on the adapters. Cover the top of each thimble with the small screen before inserting the thimble into the flask.
5. Attach a water trap and a condenser to each adapter. Be sure that each trap stopcock is closed.
6. Turn on the heating mantles to level 9 to begin boiling and refluxing.
7. Turn on the condenser water and readjust to a good flow rate, ensuring that there is no leak and the toluene reflux in the last one of the serial flasks is almost the same as that in the others.

8. Label and weigh plastic water bottles. Each bottle is for a given Dean Stark flask.  
Record each weight,  $W_{B,i}$ .
9. As water accumulates in the water trap, the water may rise to the top of the trap.  
Drain some water into the water bottle until an interface between the toluene and the water can be seen in the trap.
10. Continue refluxing for about two hours until the toluene dripping from the thimble is colorless and the reflux to the trap is very clear. During the course of refluxing, periodically check the level of the liquid in the flask. If it is too low, add some more toluene.
11. Weigh filter papers and record the weights,  $W_{P,i}$ .
12. Turn off the mantles and keep the condenser water running until the apparatus is cool for at least one hour.
13. Transfer all the water in each trap to a corresponding water bottle by draining water until the interface disappears.
14. Weigh each plastic water bottle and record each weight  $W_{B+W,i}$ .
15. Empty the traps into the toluene waste container.
16. Transfer the thimbles back into the corresponding glass jars and place in a vacuum oven maintained at around  $50^{\circ}\text{C}$  to dry over night.
17. Transfer the liquid in the Dean Stark flask to a 250 mL flask, wash the Dean Stark flask with toluene and transfer all the liquid into the 250 mL flask. Be sure not to overfill the flask past the 250 mL mark.
18. Allow the 250 mL flask to cool to room temperature and add toluene to the 250 mL mark.

19. Shake the 250 mL flask to homogenize the liquid. Transfer about 50 mL liquid into a labeled plastic centrifuge tube. Place all the tubes in a low speed centrifuge (IEC HN-SII) and run at 3000 rpm for half an hour to settle the solids from the liquid.
20. Pipette 5 mL of supernatant liquid from the centrifuged sample and spread uniformly onto the weighed filter paper that is horizontally placed on a watch glass, leaving a small area dry on the top of the filter.
21. Hang the saturated filter paper in the fume hood by attaching the paper clip to the dry area of the filter and start the stop-watch.
22. After 20 minutes, weigh the filter paper and recorder the weight,  $W_{P+B, i}$ .
23. Empty the 250 ml flasks into the waste toluene container and clean all the apparatus.
24. The next day, weigh the dried jars with the thimble and solids content. Record the total weight,  $W_{J+S, i}$ .
25. Do the calculation according to the following formula:

For froth analysis,

$$\% \text{ bitumen} = \frac{\text{bitumen collected}}{\text{sample weight}} \times 100 = \frac{(W_{P+B, i} - W_{P, i}) \times 50}{W_{J+F, i} - W_{J, i}} \times 100$$

$$\% \text{ water} = \frac{\text{water collected}}{\text{sample weight}} \times 100 = \frac{W_{B+W, i} - W_{B, i}}{W_{J+F, i} - W_{J, i}} \times 100$$

$$\% \text{ solids} = \frac{\text{solids collected}}{\text{sample weight}} \times 100 = \frac{W_{J+S, i} - W_{J, i}}{W_{J+F, i} - W_{J, i}} \times 100$$

For the oil sand ore analysis, just replace the term  $W_{J+F, i}$  with  $W_{J+O, i}$ .

To check the validity of the compositions, add the above compositions together and compare with 100%. In theory, the summation should be equal to 100%. Actually, the normal value of the summation is around 99%, due to the loss of the fine solids into the liquid in the Dean Stark flasks.

## APPENDIX B

### Effect of Calcium Ions on Bitumen Flotation Tests

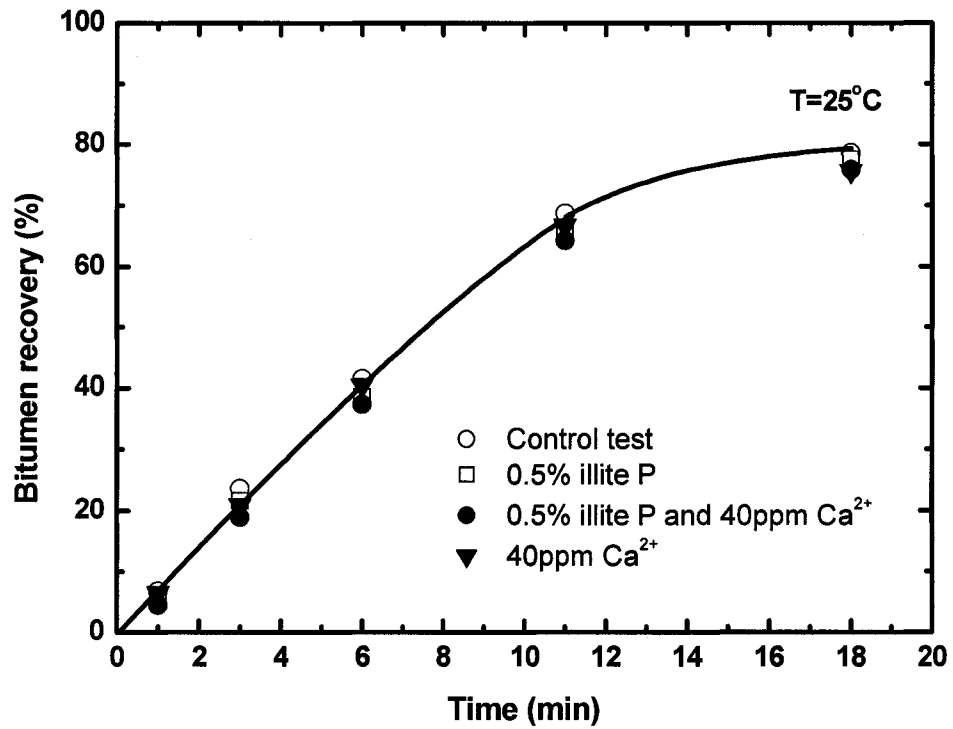


Figure B.1. Effect of calcium ions and illite P on bitumen flotation kinetics at 25°C using de-ionized water initially adjusted to pH 8.5.

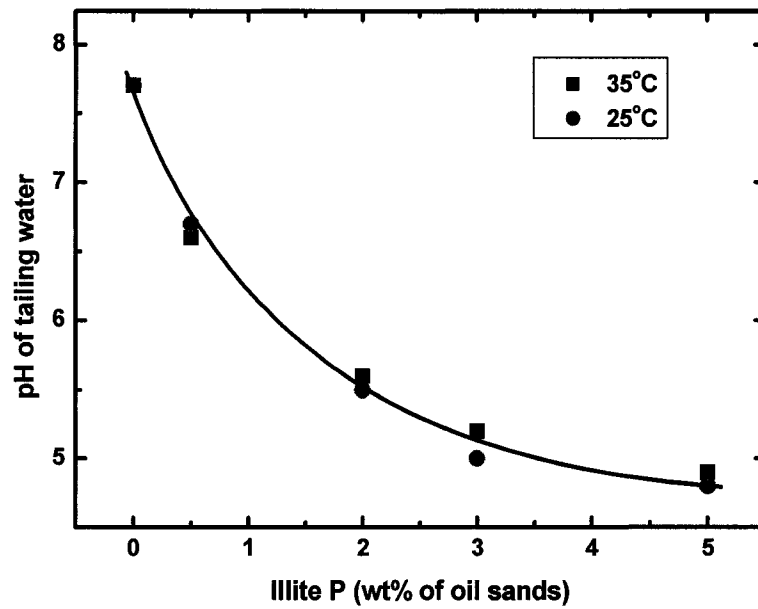


Figure B.2. Effect of illite P on pH of the tailings water from the flotation systems with the addition of 1 mM calcium ions.

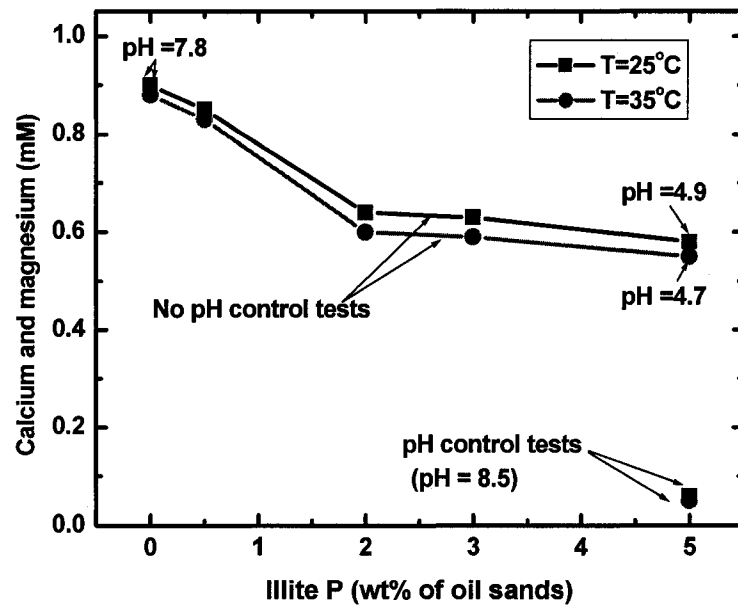


Figure B.3. Divalent cation concentrations of tailing water as a function of the amount of illite P addition in the flotation systems with the co-addition of 1mM  $\text{CaCl}_2$ .

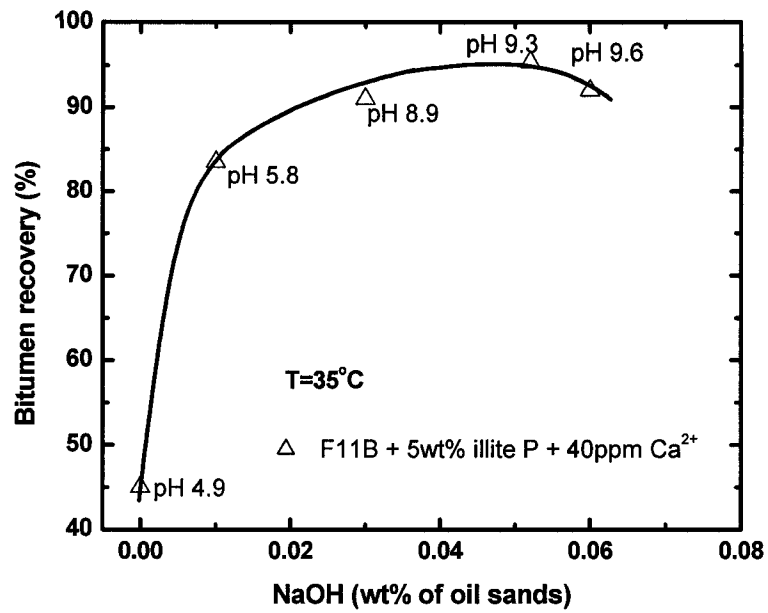


Figure B.4. Effect of NaOH addition on bitumen recovery P for the flotation systems with the co-addition of 40ppm calcium ions and 5 wt% illite P at 35°C.

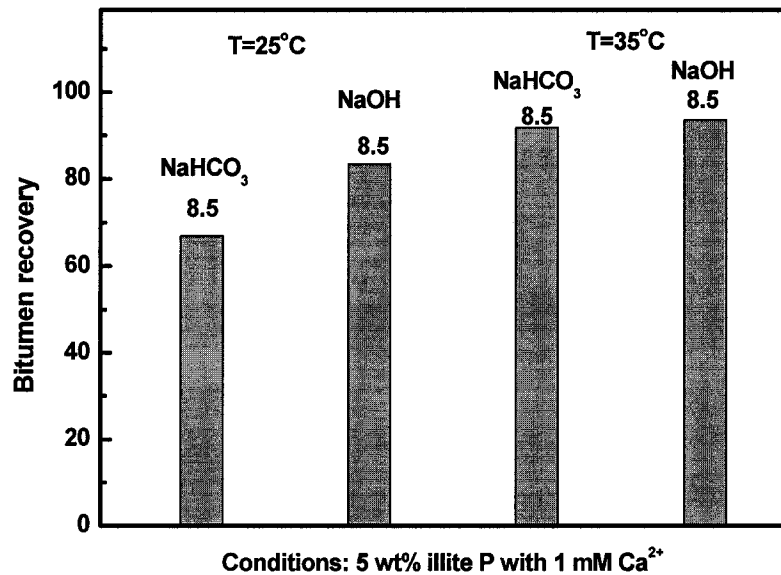
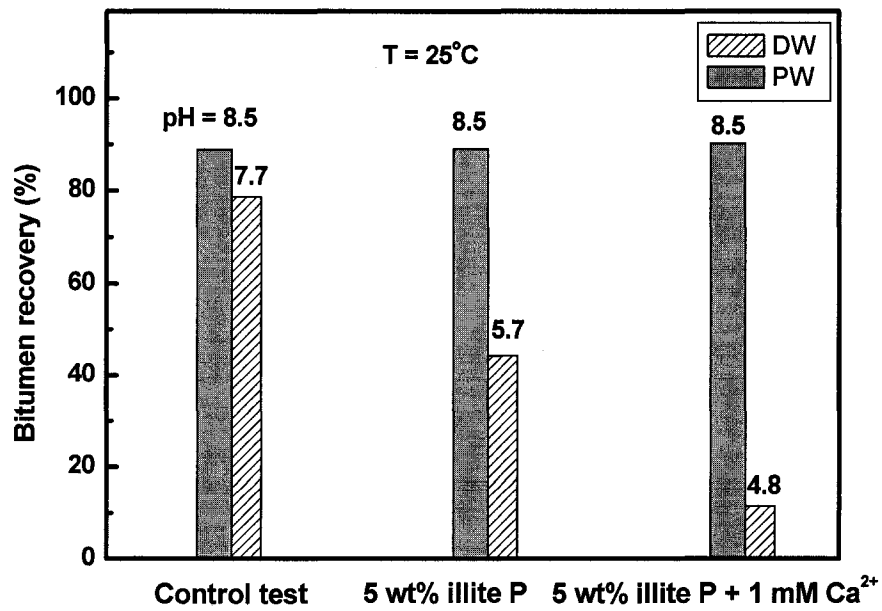


Figure B.5. Effect of NaOH (0.03wt% of oil sands) and NaHCO<sub>3</sub> (0.33wt% of oil sands or 1000ppm based on water) addition on bitumen recovery for the flotation systems with the co-addition of 1mM CaCl<sub>2</sub> and 5 wt% illite P using de-ionized water.



Baseline test: F11B oil sands only; DW: de-ionized water; PW: process water

Figure B.6. Effect on bitumen recovery of Aurora process water compared with de-ionized water.

## APPENDIX C

### Effect of Calcium Ions on Zeta Potential Measurements

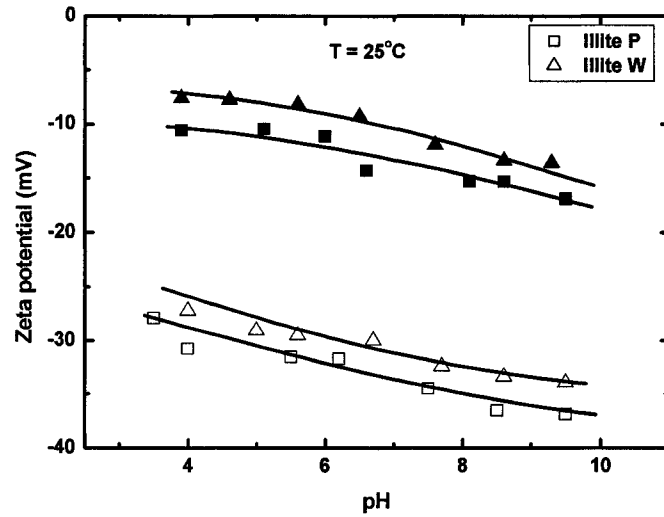


Figure C.1. Effect of calcium ions on the zeta potentials of illite clays in 1 mM KCl solution at 25°C.

Open symbols: in 1mM KCl solution; Solid symbols: in 1mM KCl solution containing 40ppm calcium ions.

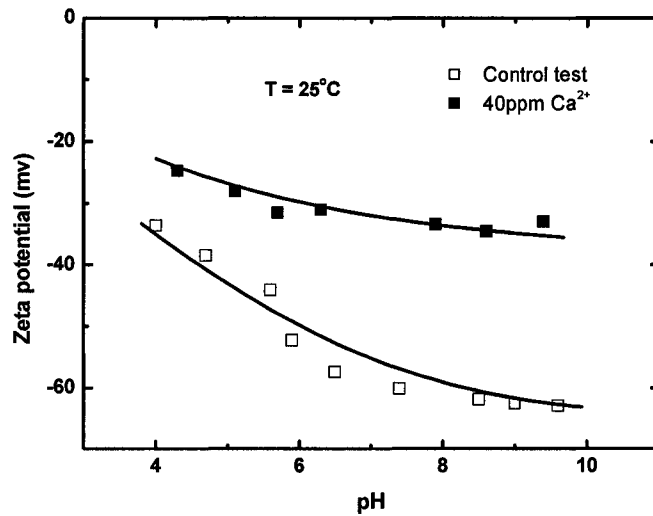


Figure C.2. Effect of calcium ions on zeta potential of bitumen in 1 mM KCl solution at 25°C.

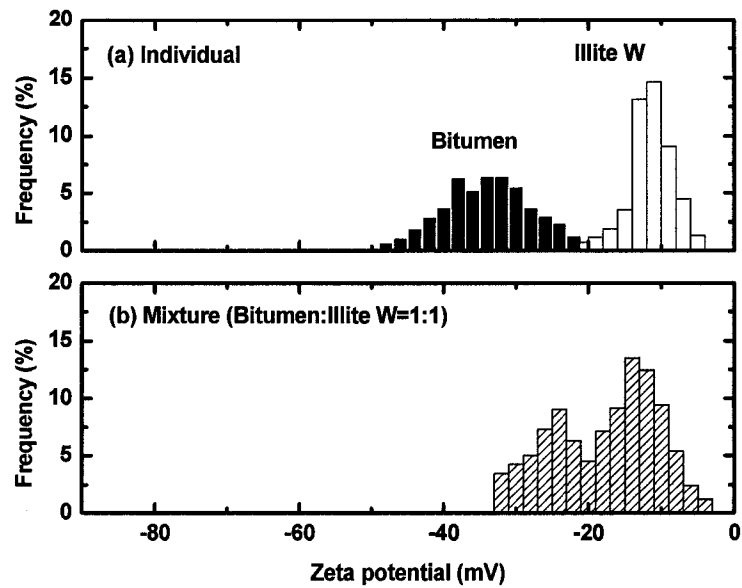


Figure C.3. Zeta potential distributions for (a) bitumen emulsion and illite W suspensions and (b) their mixture at pH 8.5 and 25°C in 1mM KCl solutions containing 40ppm calcium ions.

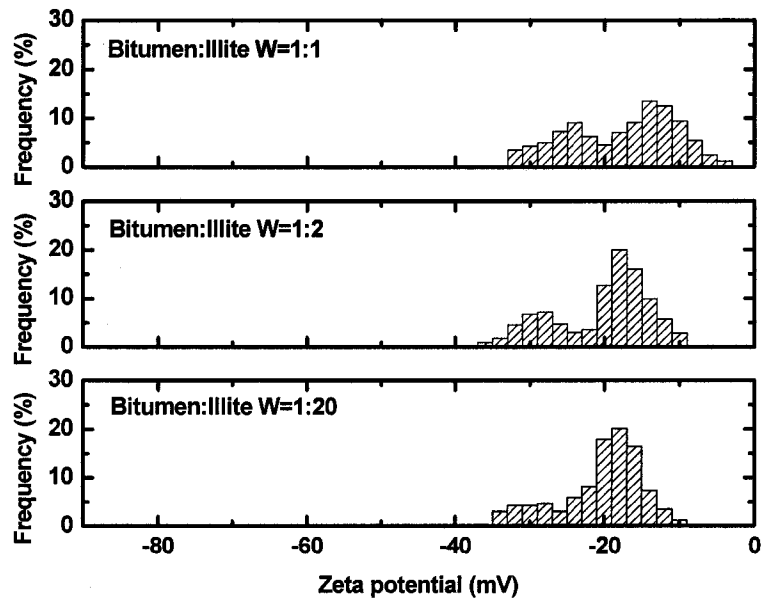


Figure C.4. Effect of bitumen to illite W ratio on the zeta potential distributions measured at pH 8.5 and 25°C in 1mM KCl solutions containing 40ppm calcium ions.

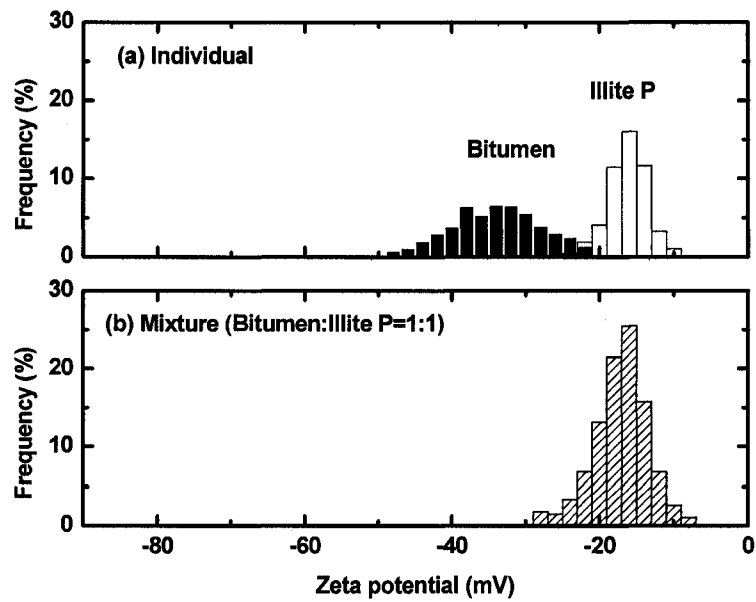


Figure C.5. Zeta potential distributions for (a) bitumen emulsion and illite P suspensions and (b) their mixture at pH 8.5 and 25°C in 1mM KCl solutions containing 40ppm calcium ions.

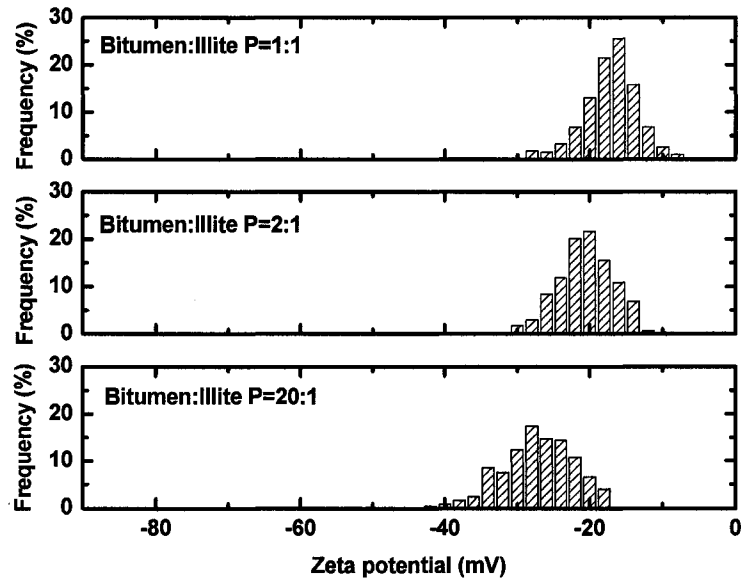


Figure C.6. Effect of bitumen to illite P ratio on the zeta potential distributions measured at pH 8.5 and 25°C in 1mM KCl solutions containing 40ppm calcium ions.

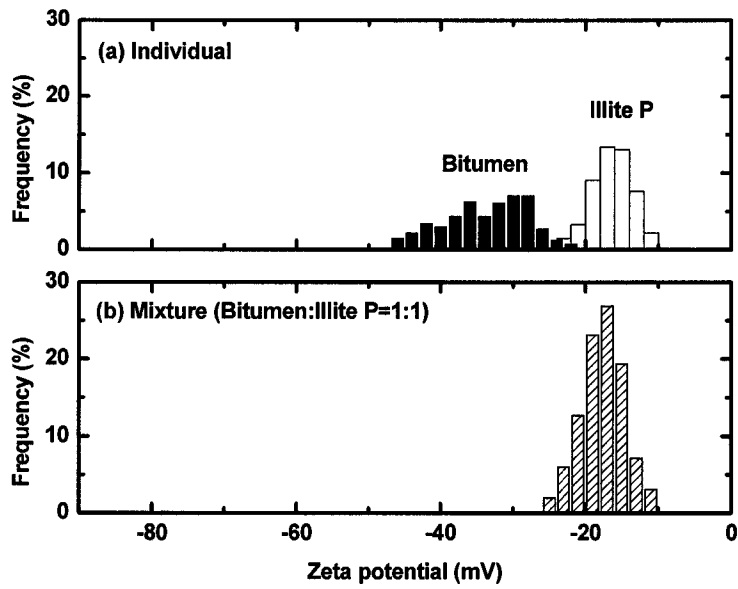


Figure C.7. Zeta potential distributions for (a) bitumen emulsion and illite P suspensions and (b) their mixture at pH 8.5 and 35°C in 1mM KCl solutions containing 40ppm calcium ions.

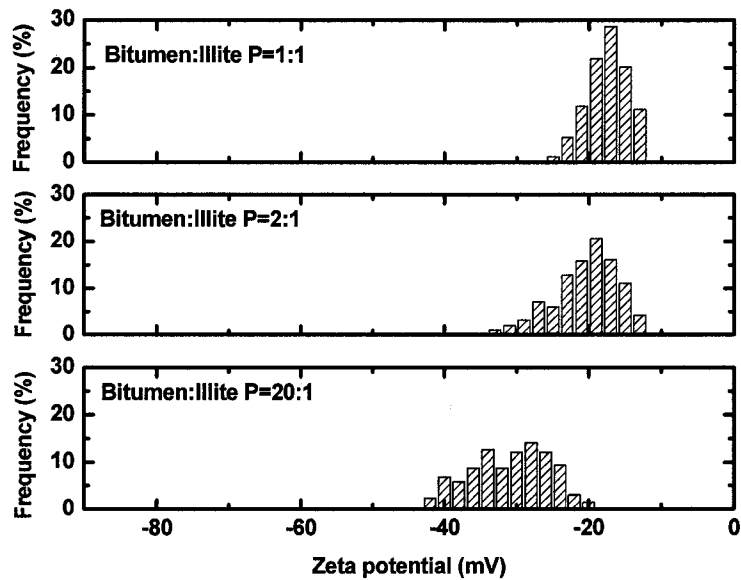


Figure C.8. Effect of bitumen to illite P ratio on the zeta potential distributions measured at pH 8.5 and 35°C in 1mM KCl solutions containing 40ppm calcium ions.

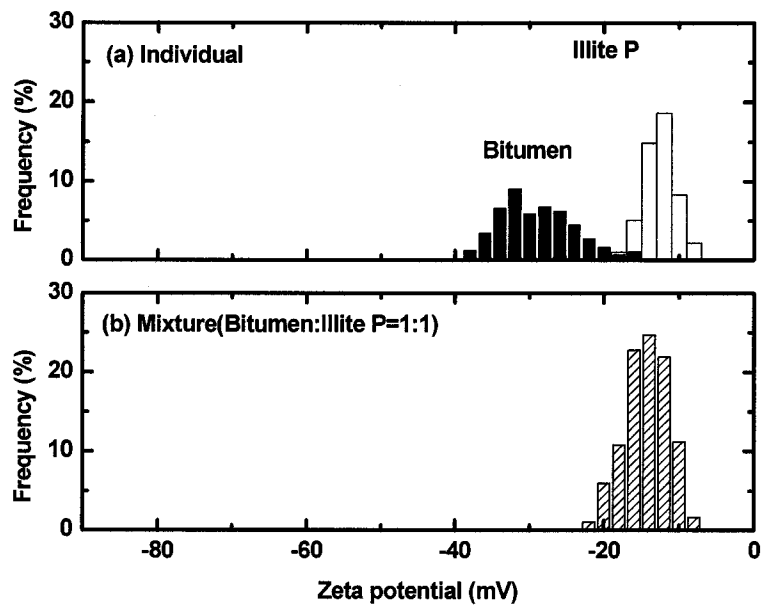


Figure C.9. Zeta potential distributions for (a) individual bitumen emulsion and illite P suspension and (b) their mixture at pH 4.9 and 25°C in 1mM KCl solutions containing 40ppm calcium ions.

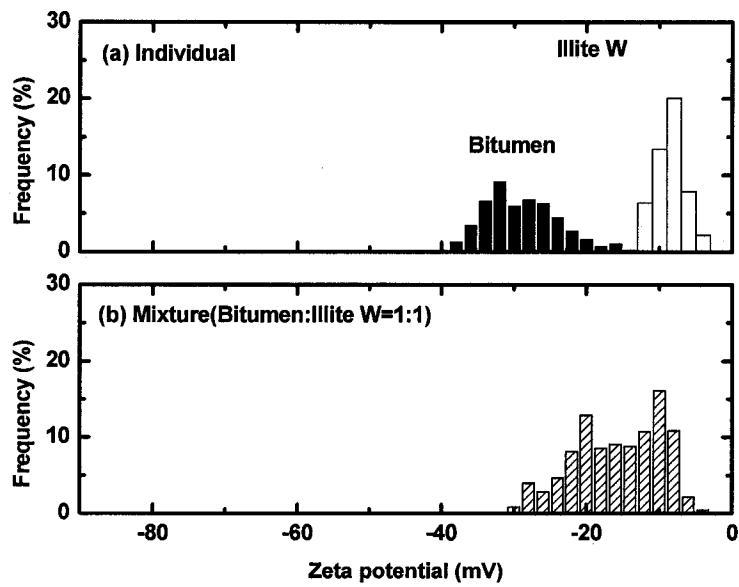


Figure C.10. Zeta potential distributions for (a) individual bitumen emulsion and illite W suspensions and (b) their mixture at pH 4.9 and 25°C in 1mM KCl solutions containing 40ppm calcium ions.

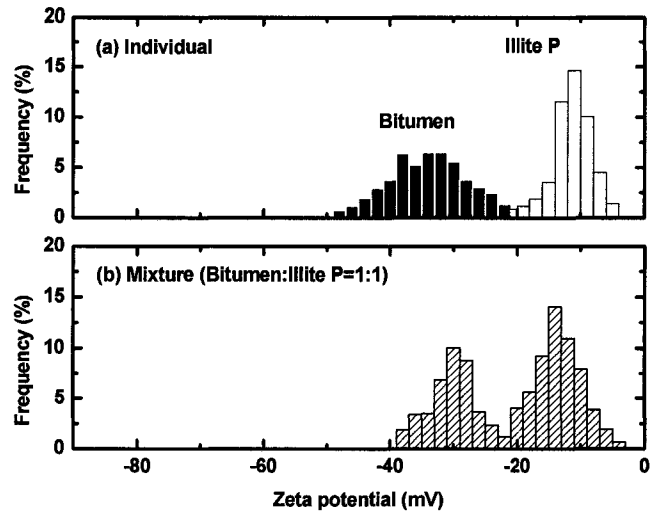


Figure C.11. Zeta potential distributions for (a) bitumen emulsion and illite P suspensions and (b) their mixture at 25°C in the supernatant of the produced tailings water (pH 8.5) (from the flotation test with pH controlled at 8.5) with the addition of 40ppm calcium ions.

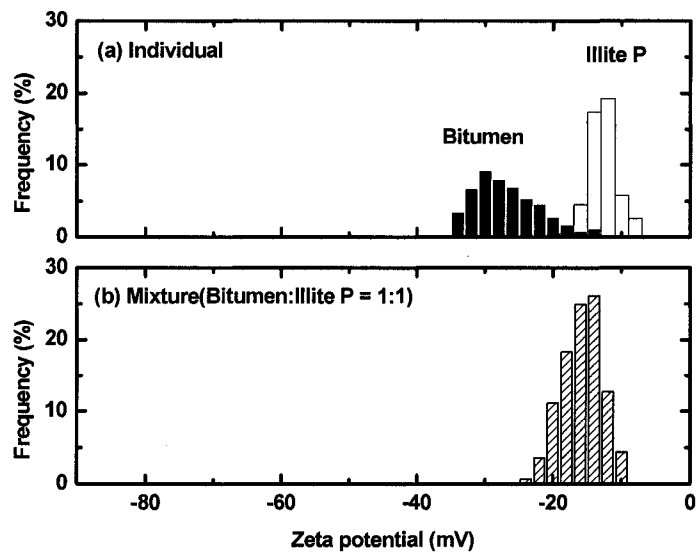


Figure C.12. Zeta potential distributions for (a) bitumen emulsion and illite P suspensions and (b) their mixture at 25°C in the supernatant of the produced tailings water (pH 4.9) (from the flotation test without pH control) with the addition of 40ppm calcium ions.

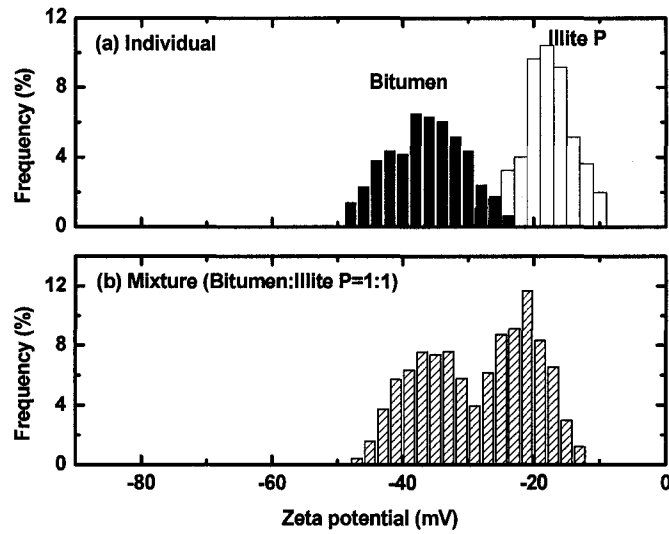


Figure C.13. Zeta potential distributions for (a) individual bitumen emulsion and illite P suspensions and (b) their mixture at pH 8.6 and 25°C in 1mM KCl solutions with addition of 40ppm calcium ions and 1000ppm NaHCO<sub>3</sub>.

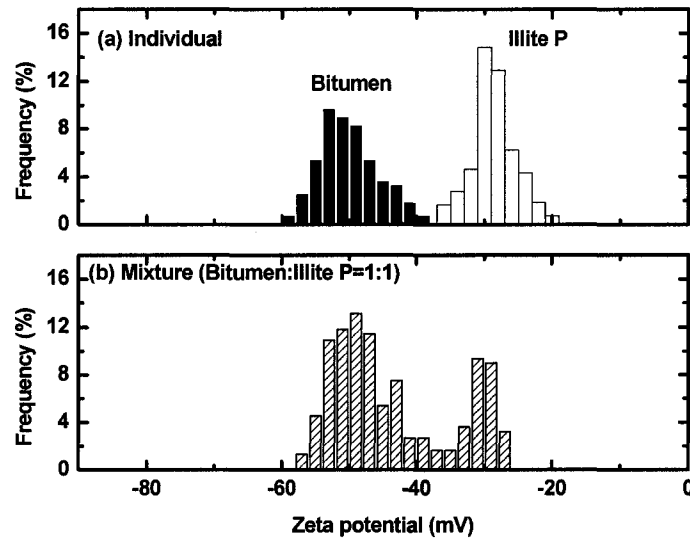


Figure C.14. Zeta potential distributions for (a) individual bitumen emulsion and illite P suspensions and (b) their mixture at pH 8.6 and 35°C in 1mM KCl solutions with the addition of 40ppm calcium ions and 1000ppm NaHCO<sub>3</sub>.

## APPENDIX D

### **Ethylene Glycol Monoethyl Ether (EGME) Method for Specific Surface Area (SA)**

The EGME method was developed by Sheldrick (1984). The method is based on the principle that solid materials will absorb a monomolecular layer of a polar liquid - ethylene glycol monoethyl ether (EGME). Under this condition, the surface area per gram of EGME is already known. If the total amount of EGME adsorbed by the material is known, it is easy to calculate the total surface area of the material. The detailed procedure is outlined as following.

1. Place oven dried aluminum moisture dishes (50 mm diameter x 23 mm high) in an evacuated desiccator (40 cm. I.D.) over fresh anhydrous  $P_2O_5$  for a few hours. Use fresh  $P_2O_5$  for every other run for increased accuracy and speed.
2. Weigh the dishes ( $W_{D, i}$ ) and weigh about 1.1 g. of 35 mesh air-dried illite clay samples in the dishes ( $W_{D+C, i}^0$ ). Place dishes in the desiccator, evacuate for 45 minutes with vacuum and let stand overnight. Precision is increased and time saved by placing a maximum of 6 samples per 40 cm. I.D. desiccator. 35 mesh samples are used because it is a standard grind in this laboratory and surface area values are not greatly affected by different mesh sizes.
3. After 12 hours, release the vacuum using a drying trap containing anhydrous calcium sulphate, and weigh to the nearest 0.1 mg. Record the weight ( $W_{D+C, i}^1$ ). Always use a drying trap while releasing vacuum to prevent adsorption of water which is also a polar liquid.

4. Re-evacuate for 45 minutes and weigh again after almost 3 hours. Record the weight ( $W_{D+C,i}^2$ ).
5. Repeat again after 2 hours. The weights should be constant (within 1 mg), but if not repeat until constant. Record the constant weight ( $W_{D+C,i}^c$ ).
6. As soon as a constant weight is attained add just enough EGME (1-2ml) to form a soil-EGME slurry, cover the samples about 80% with the lids, place in a desiccator over anhydrous granular  $\text{CaCl}_2$  and allow to equilibrate for 30 minutes. Add the EGME as soon as a constant weight is attained to prevent adsorption of water. Adding just enough EGME and covering the samples prevents loss of sample if and when the EGME boils under high vacuum and spattering occurs.
7. Evacuate the desiccator for 45 minutes and let it stand overnight.
8. In the morning weigh the samples ( $W_{D+C+EGME,i}^0$ ) and re-evacuate for 45 minutes.
9. Repeat before noon and again in early afternoon. A constant weight (within 1 mg.) should be attained but if not repeat until constant. Record the constant weight ( $W_{D+C+EGME,i}^c$ ). Note that prolonged and repeated high evacuations of the EGME treated samples will give lower results because parts of the monomolecular layer will be removed.
10. The total surface area for each sample is calculated by dividing the grams of adsorbate per gram of soil by  $2.86 \text{ g/m}^2$ , i.e.

$$SA = \frac{\text{amount of EGME absorbed by clay}}{\text{amount of clay}} \times 3496.5(m^2 / g)$$

$$= \frac{W_{D+C+EGME,i}^c - W_{D+C,i}^c}{W_{D+C,i}^c - W_{D,i}^c} \times 3496.5(m^2 / g)$$

Surface area values range from less than  $10 \text{ m}^2/\text{g}$  for sandy soils to greater than  $300 \text{ m}^2/\text{g}$  for clay soils. Since 1 mg of adsorbate approximately represents a surface area of  $3 \text{ m}^2/\text{g}$ , variability of surface area values in the range of  $20 \pm 5$ ,  $100 \pm 10$ , and  $200 \pm 20 \text{ m}^2/\text{g}$  are considered very good.